CHAPTER ONE

INTRODUCTION

Today's political considerations to move the world's energy consumption away from fossil fuels such as oil, coal and gas has increased the focus on renewable energy. This should be seen in relation to the environmental concerns, e.g. cutting carbon dioxide emissions and supply concerns, which can have a large economic and political influence. Renewable energy is perceived as a sustainable solution to ensure future energy supply as well as being carbon dioxide emissions free or neutral.

Solar energy is by far the renewable energy source with the greatest potential (table 1.1) [31]. It has the ability to cover the world's energy demand several thousand times over and, unlike fossil fuels, solar energy is readily available world-wide [40].

Table 1.1 Energy available for harvesting from different sources compared to the global energy demand

Global consumption	Hydro	Gerthermal	Wind	Solar
15 TW	7.2 TW	32 TW	870 TW	86,000 TW

Unfortunately, utilization of solar energy is very expensive; something that particular goes for the conversion into electricity. Solar cells are therefore not widely used for commercial electricity production since they cannot compete with fossil fuels or other renewable energy sources [36] as seen in figure 1.1

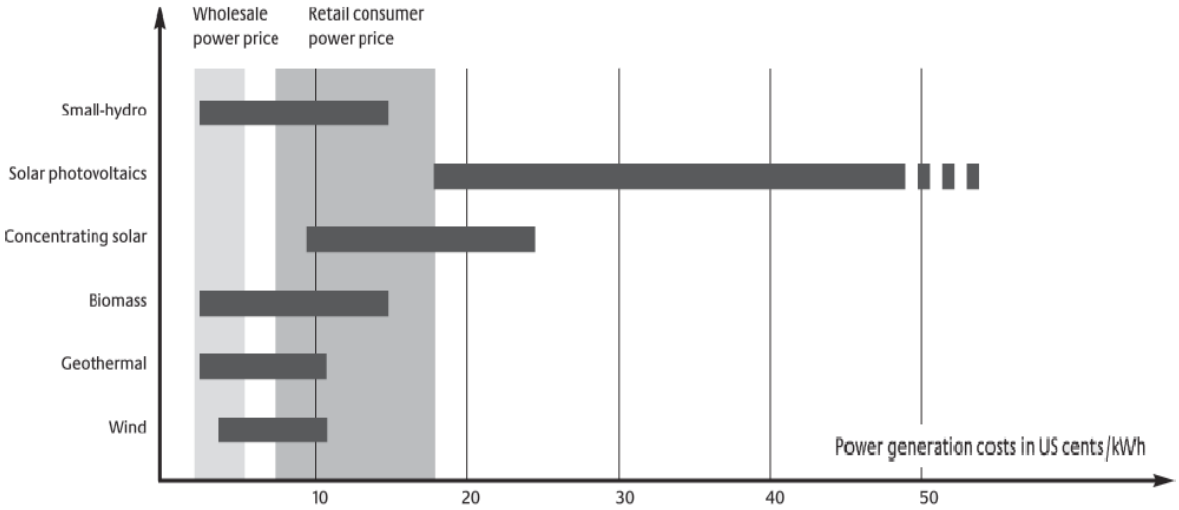

Figure1.1: Prices of electricity produced from different renewable energy sources.

For this reason, solar cells are commonly used in remote regions with no access to the power grid or in private homes as a green alternative to fossil fuels. As a result a mere 0.04 % of the world's energy supply came from solar photovoltaics in 2006.[79]

To understand why electricity from solar cells is so expensive one needs to look closer at the solar cells used to produce it. A typical solar cell is made out of silicon wafers similar to those used in the production of micro chips.[95] The production of these wafers is outlined in figure 1.2.

The process is long and very energy intensive due to the elevated temperatures needed in most steps. Solar cells are as a result relatively expensive.[95]

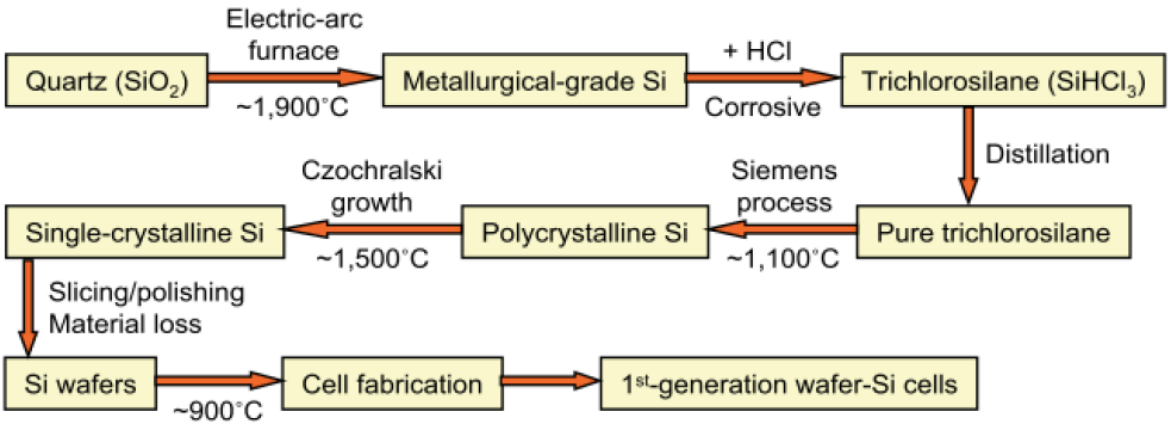

Figure1.2: The manufacturing process of the first generation silicon solar cells from silica.

In order to earn back the production cost within a reasonable timeframe the electricity needs to be more expensive than other types of electricity.[95]

A polymer solar cell (PSC) is one of the possible replacements. These solar cells add some very interesting properties to the solar cell as well as reducing the price considerably. Krebs[55] have demonstrated that the production of large area PSC ($1m^2$) can be done at a cost 100 times lower than that of monocrystalline silicon solar cells in terms of material cost.

Another area where the (PSC) has advantages over silicon cells is in flexibility. Whereas silicon crystal is rigid a polymer layer is very flexible yielding the possibility of a very flexible thin film solar cell. This is a property that can enable a variety of new applications, solar cell coated clothes has been demonstrated on [Krebs][56].

However there are still challenges to overcome. Firstly the service life of a PSC is very short, only a few hours for a simple metal/polymer/metal solar cell. Secondly the efficiency of the PSC is not high compared to the SSCs. [91]

1.1 Definition of solar cells:-

Solar cells are optical volt adapters that convert sunlight directly into electricity. They are mainly fabricated from semi-conductor material and optically sensitive membrane and surrounded by front and rear conductor of electricity. For the manufacture of solar cells was developed various materials of the semiconductor elements in the form of silicon crystals, gallium arsenic, cadmium carbide, indium phosphide, sulphide copper and other materials promising for the manufacture of solar cells.[9]

1.2 Formulation of the problem

Semiconductors which are used in solar cells are very expensive and have low efficiency which cannot meet the requirements for which are manufactured.

1.3 Aim of the work

The aim of this work is to search for highly efficient solar cells and reduce the cost of manufacturing solar cells. This can be done by manufacturing solar cells using conjugate Polymer coating by Solder (Sn/Pb).

1.4 Research Methodology

The material utilized in this work:

1- Titanium Dioxide glass and conjugate polymer beside different organic dyes (Rhodamine 6G- Coumarin 500 – Dibenzocyanin 45).

2- The coating will done by the Spin Coating Machine.

3-The concentration of different organic dyes (Rhodamine 6G- Coumarin 500 – Dibenzocyanin 45) was changes and the corresponding output current voltage, power and efficiency are recorded.

4- The empirical relations are compared with previous studies or theoretical relations.

1.5 Research Framework

Research Framework applied to know steps which will be done in research

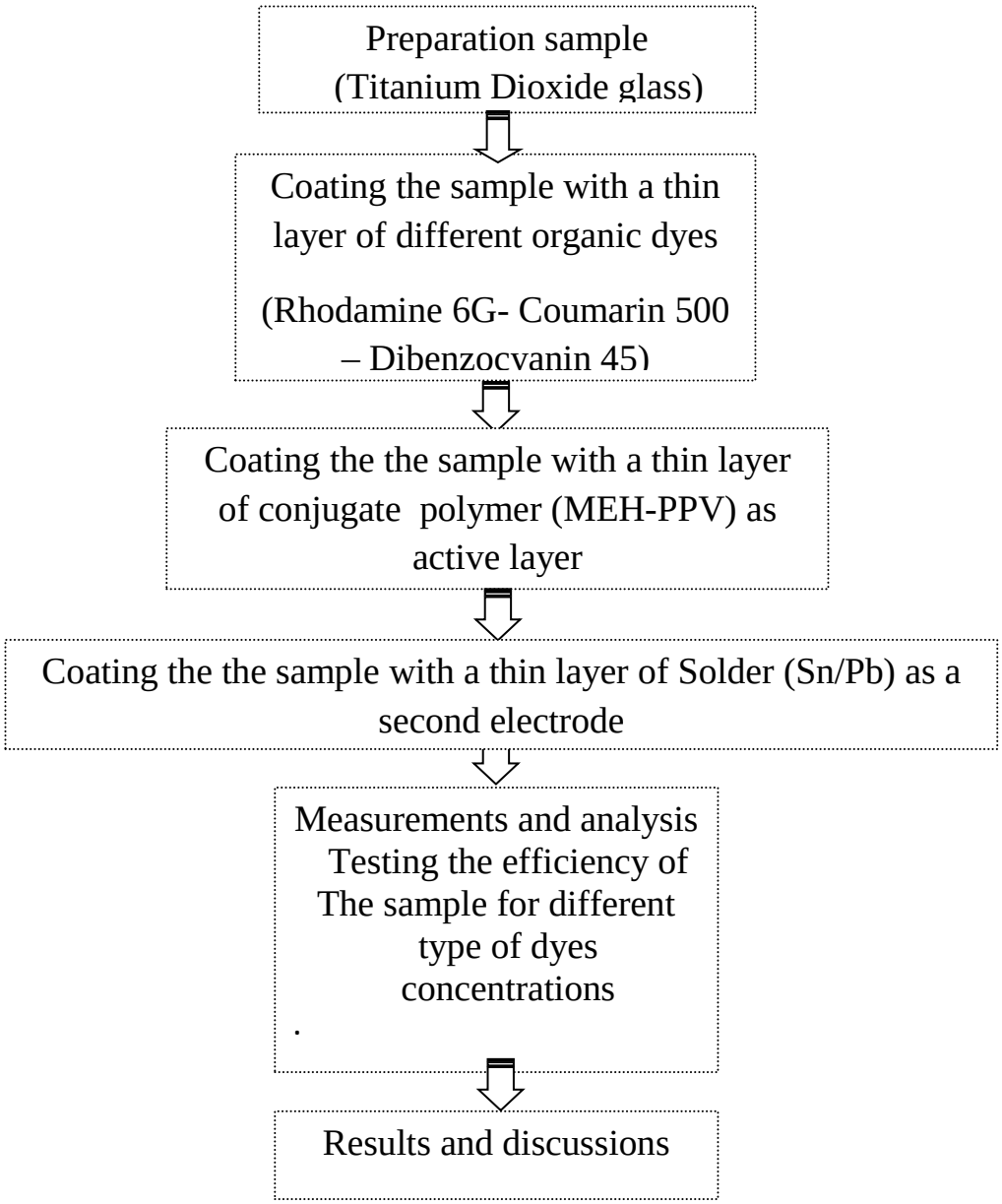

1.6 Structure of thesis

The thesis is organized into six chapters. The first chapter gives an introduction to the solar energy and the definition of solar cells. Also it is includes a formulation of the problem of the thesis, the aim of the work, research methodology

and research framework and finally describes how the thesis is structured. The second chapter is concerned with the definition of polymers. It is also pays attention to their atomic structure, types and production. The third chapter deals with review of literature on history of solar cells. The chapter also looks at the efficiency, the cost and the materials of manufacturing the solar cells. The fourth chapter is divided into two sections. One presents the previous studies in polymer solar cells and the second one presenting the mechanism of polymer cells and the way of comparing them. Methodology and materials used in carrying out this research are presented in the fifth chapter, whiles the sixth chapter deals with results in graphical format and in-depth discussion of results and closed it with conclusions. Lastly, references cited in this thesis and appendices are presented.

CHAPTER TWO

POLYMERS

2.1 Introduction:

Polymers play an important role in civilization. They are widely used in industry in manufacturing the interior bodies of cars and in furniture's beside roofs and buildings. Recently polymers are utilized in the solar cells. Due to these wide applications of polymers, this chapter is concerned with the definition of polymers. It is also pays attention to their atomic structure, types and production.

2.2 What is Polymer?

Polymer is a large molecule consisting of (at least five) repeated chemical units (`**mers**') joined together, like beads on a string. Polymers usually contain many more than five monomers, and some may contain hundreds or thousands of monomers in each chain.

There are both naturally occurring and synthetic polymers. Among naturally occurring polymers are proteins, starches, DNA, cellulose, and latex. Synthetic polymers are produced commercially on a very large scale and have a wide range of properties and uses such as nylon or polyethylene. The materials commonly called plastics are all synthetic polymers. The importance of both natural and synthetic polymers in our lives cannot be overestimated. The desirable properties of these **macromolecules**, such as tensile strength and flexibility, make them extremely useful both in nature and in the manufacture of products that we use every day. Most polymers are organic and formed from hydrocarbon molecules [29].

2.3 Hydrocarbon molecules structure:

In hydrocarbon molecules structure each C atom has four e^- that participate in bonds, each H atom has one bonding e^-.

Examples of **saturated** (all bonds are single ones) hydrocarbon molecules:

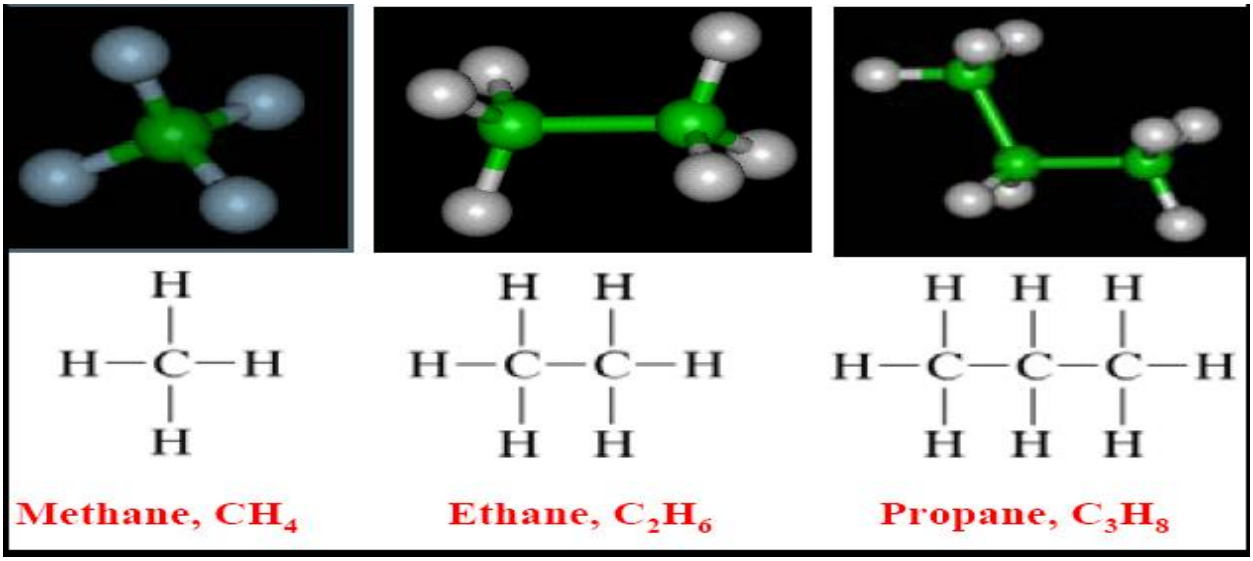

Figure 2.1: Shows the structure of Methane, CH_4 , Ethane, C_2H_6 , Propane, C_3H_8

Double and triple bonds can exist between C atoms (sharing of two or three electron pairs). These bonds are called **unsaturated bonds**. Unsaturated molecules are more reactive [29]

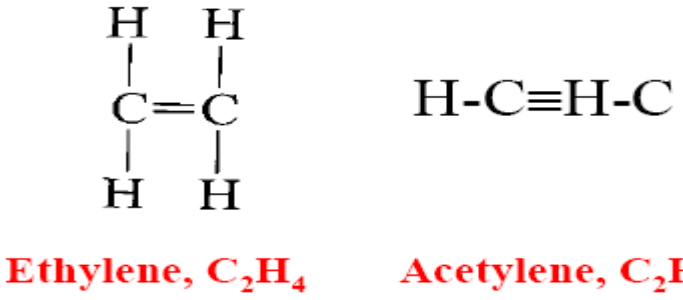

Figure 2.2: Shows the unsaturated bonds of Ethane C_2H_4 and Acetylene C_2H_2

Isomers: are molecules that contain the same atoms but in a different arrangement. An example is butane and Isobutane:

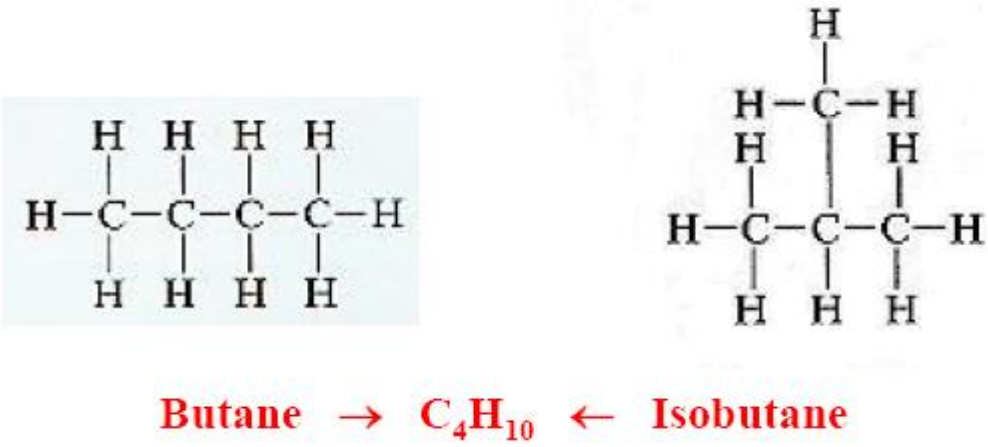

Figure 2.3: Shows the different arrangement of molecules (Isomers).[29]

2.4 Polymer molecules:-

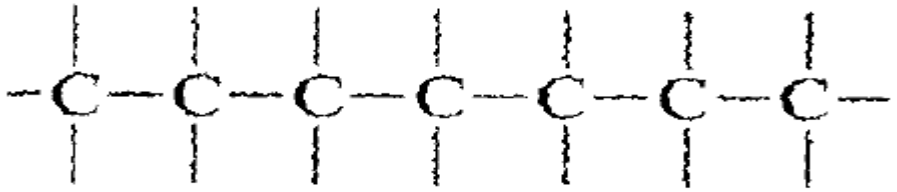

Figure 2.4: Shows the chains of C atoms as a backbone.

Polymer molecules are very large macromolecules and most polymers consist of long and flexible chains with a string of C atoms as a backbone. Side-bonding of C atoms can be connected to H atoms or radicals.

Radical: an organic group of atoms that remain as a unit and maintain their identity during chemical reactions (e.g. CH_3, C_2H_5, C_6H_5).

Double bonds are possible in both chain and side bonds and a repeat unit in a polymer chain ("unit cell") is a **mer** the single **mer** is called a **monomer**.

Polymers are formed by chemical reactions in which a large number of molecules called monomers are joined sequentially, forming a chain. In many polymers, only one monomer is used. In others, two or three different monomers may be combined. Polymers are classified by the characteristics of the reactions by which they are formed.[29]

2.5 Polymerization:

The polymerization processes by which polymers are synthesized fall into two categories. It has three steps initiation, propagation and termination of polymerization.

If all atoms in the monomers are incorporated into the polymer, the polymer is called an ***addition polymer***. If some of the atoms of the monomers are released into small molecules, such as water, the polymer is called a ***condensation polymer***. Most addition polymers are made from monomers containing a double bond between carbon atoms. Such monomers are called olefins, and most commercial addition polymers are polyolefin.[29]

2.5.1 Polymerization steps:

1. Initiation reaction:

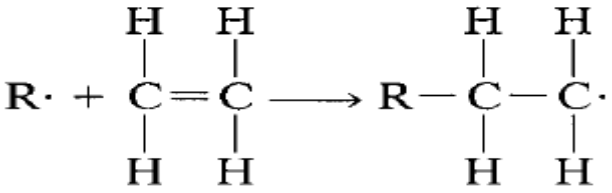

Figure 2.5: Shows the first step of polymerization.

2. Rapid propagation ~1000 mer units in 1-10 ms:

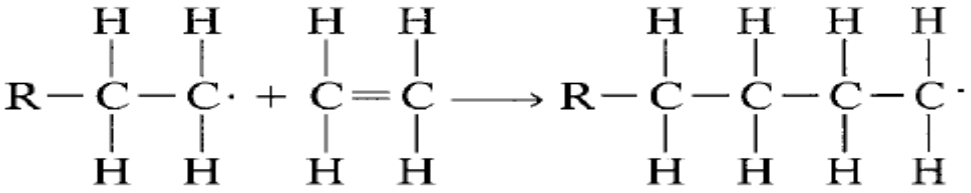

Figure 2.6: Shows the second step of polymerization.

3. Termination: When two active chain ends meet each other or active chain ends meet with initiator or other species with single active bond:

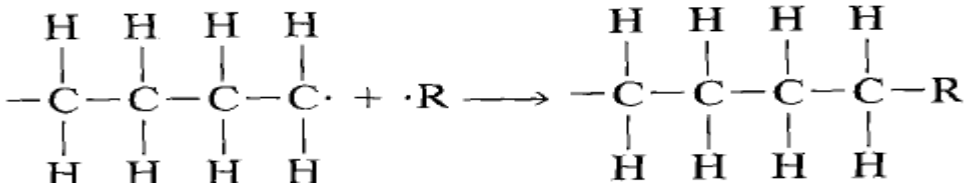

Figure 2.7: Shows the third step of polymerization.

(·) Denotes unpaired electron (active site)[29]

2.5.2 Polyethylene:

Example for addition polymer is Ethylene (C_2H_4) is a gas at room temp and pressure and it will transforms to polyethylene (solid) by forming active mers through reactions with an initiator or catalytic radical (R**.**)

The properties of polyethylene depend on the manner in which ethylene is polymerized. When catalyzed by organometallic compounds at moderate pressure (15 to 30 atm), the product is high density polyethylene, HDPE. Under these conditions, the polymer chains grow to very great length, and molar masses average many hundred thousand. HDPE is hard, tough, and resilient. Most HDPE is used in the manufacture of containers, such as milk bottles and laundry detergent jugs. When ethylene is polymerized at high pressure (1000–2000 atm), elevated

temperatures (190–210^{0}C), and catalyzed by peroxides, the product is low density polyethylene, LDPE. This form of polyethylene has molar masses of 20,000 to 40,000 grams. LDPE is relatively soft, and most of it is used in the production of plastic films, such as those used in sandwich bags.[17]

2.5.3 Polypropylene:

This polymer is produced by the addition polymerization of propylene, CH_2=$CHCH_3$ (propene). Its molecular structure is similar to that of polyethylene, but has a methyl group (CH_3) on alternate carbon atoms of the chain. Its molar masses fall in the range 50,000 to 200,000 grams. Polypropylene (PP) is slightly more brittle than polyethylene, but softens at a temperature about 40^{0}C higher. Polypropylene is used extensively in the automotive industry for interior trim, such as instrument panels, and in food packaging, such as yogurt containers. It is formed into fibers of very low absorbance and high stain resistance, used in clothing and home furnishings, especially carpeting.[17]

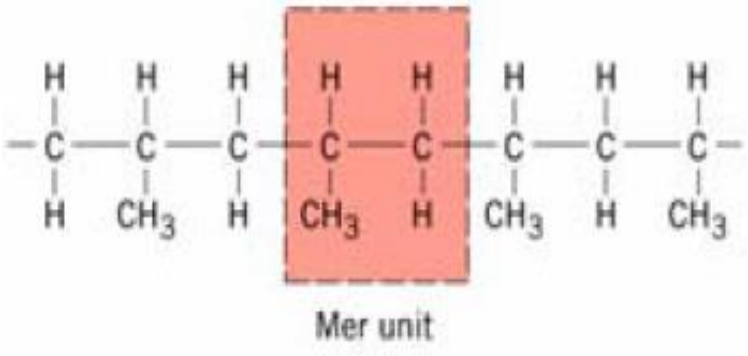

Figure 2.8: Shows the structure of polypropylene.[29]

2.5.4 Polyvinyl chloride

Polymerization of vinyl chloride, CH_2=CHCl (chloroethene), produces a polymer similar to polyethylene, but having chlorine atoms at alternate carbon atoms on the chain. Polyvinyl chloride (PVC) is rigid and somewhat brittle. About two-thirds of the PVC produced annually is used in the manufacture of pipe. It is also used in the production of "vinyl" siding for houses and clear plastic bottles. When it is blended with a plasticizer such as a phthalate ester, PVC becomes pliable and is used to form flexible articles such as raincoats and shower curtains.[17]

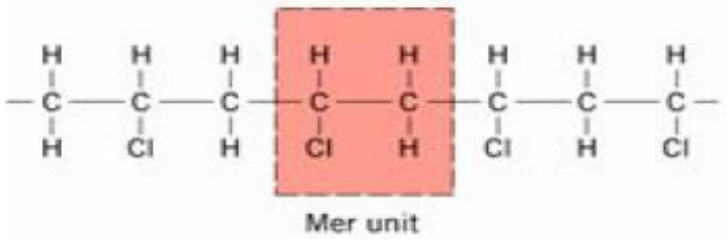

Figure 2.9: Shows the structure of polyvinyl chloride.[29]

2.5.5 Polytetraflouroethylene:

Teflon is a trade name of polytetraflouroethylene, PTFE. It is formed by the addition polymerization of tetrafluoroethylene by replace hydrogen atoms in polyethylene with Fluorine atoms make polytetraflouroethylene, $CF_2=CF_2$. PTFE is distinguished by its complete resistance to attack by virtually all chemicals and by its slippery surface. It maintains its physical properties over a large temperature range, -270^0C to 385^0C. These properties make it especially useful for components that must operate under harsh chemical conditions and at temperature extremes. It's most familiar household use is as a coating on cooking utensils [17].

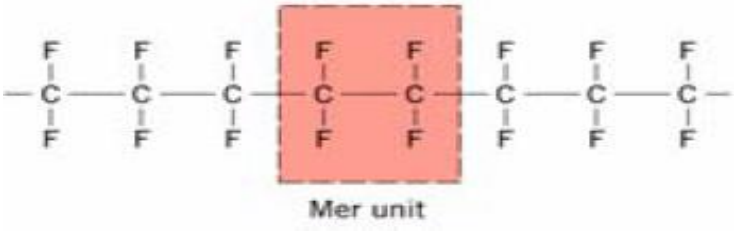

Figure 2.10: Shows the structure of polytetraflouroethylene[29].

2.5.6 Polystyrene:

Styrene, $CH_2=CH–C_6H_5$, polymerizes readily to form polystyrene (PS), a hard, highly transparent polymer. The molecular structure is similar to that of polypropylene, but with the methyl groups of polypropylene replaced by phenyl groups (C_6H_5). A large portion of production goes into packaging. The thin, rigid, transparent containers in which fresh foods, such as salads, are packaged are made from polystyrene. Polystyrene is readily foamed or formed into beads. These foams and beads are excellent thermal insulators and are used to produce home insulation and containers for hot foods. Styrofoam is a trade name for foamed polystyrene. When rubber is dissolved in styrene before it is polymerized, the polystyrene produced is much more impact resistant. This type of polystyrene is used

extensively in home appliances, such as the interior of refrigerators and air conditioner housing.[17]

2.5.7 Polyethylene Terephthalate:

Polyethylene terephthalate (PET), or polyethylene terephthalic ester (PETE), is a condensation polymer produced from the monomers ethylene glycol, $HOCH_2CH_2OH$, a dialcohol, and dimethyl terephthalate, $CH_3O_2C–C_6H_4–CO_2CH_3$, a diester. By the process of transesterification, these monomers form ester linkages between them, yielding a polyester. PETE fibers are manufactured under the trade names of Dacron and Fortrel. Pleats and creases can be permanently heat set in fabrics containing polyester fibers, so-called permanent press fabrics. PETE can also be formed into transparent sheets and castings. Mylar is a trade name for a PETE film. Transparent 2-liter carbonated beverage bottles are made from PETE. (The opaque base on some bottles is generally made of HDPE.) One form of PETE is the hardest known polymer and is used in eyeglass lenses.[17]

2.5.8 Polyurethane:

This important class of condensation polymers is formed by the polymerization of a diisocyanate (whose molecules contain two –NCO groups) and a dialcohol (two –OH groups). The polymer chain is linked by urethane groups (–O–CO–NH–). The –NH– portion of the urethane group can react similarly to an –OH group, producing cross-linking between polymer chains. Polyurethane is spun into elastic fibers, called spandex, and sold under the trade name Lycra. Polyurethane can also be foamed. Soft polyurethane foams are used in upholstery, and hard foams are used structurally in light aircraft wings and sail boards. The formation of some polyurethane (and polystyrene) foams exploits the exothermic nature of the polymerization reaction. A liquid with a low boiling point, called a blowing agent, is added to the monomers before the polymerization starts. As the polymerization proceeds, it releases enough heat to boil the liquid. The boiling liquid produces bubbles that create foam. In the past, the most commonly used low-boiling liquids were chlorofluorocarbons. However, the damaging effect of chlorofluorocarbons on the stratospheric ozone layer has eliminated their use. Other low-boiling liquids have other disadvantages, such as flammability. Therefore, most

polyurethane and polystyrene foams are manufactured by forcing a pressurized gas, such as nitrogen or carbon dioxide, into the polymerizing mixture.[17]

2.5.9 Polyamide:

Polyamides are a group of condensation polymers commonly known as nylon. Nylon is made from two monomers, one a dichloride and the other a diamine. One particular nylon is made from 1,6-diaminohexane, $NH_2(CH_2)_6NH_2$ and sebacoyl chloride, $ClCO(CH_2)_8COCl$. When these polymerize, the resulting molecules contain repeating units of $–NH(CH_2)_6NH–CO(CH_2)_8CO–$. Molecules of HCl are released during the polymerization. This particular polymer is called nylon 6-10 because it contains alternating chains of 6 and 10 carbon atoms between nitrogen atoms. Nylon can be readily formed into fibers that are strong and long wearing, making them well suited for use in carpeting, upholstery fabric, tire cords, brushes, and turf for athletic fields. Nylon is also formed into rods, bars, and sheets that are easily formed and machined. In this form, nylon is used for gears and for automobile fuel tanks.[17]

2.5.10 Polyacrylamide:

Polyacrylamide is a condensation polymer with an unusual and useful property. The structure of polyacrylamide is similar to that of polyethylene, but having a hydrogen on every other carbon replace by an amide group, $–CONH_2$. The molecule is composed of repeating $–CH_2–CH(CONH_2)–$ units. The amide groups allow for linking between polymer strands. The $–CONH_2$ group from one molecule can react with the same group of another molecule, forming a link between them with the structure –CONHCO–. This produces a network of polymer chains, rather like a tiny sponge. The free, unlinked amide groups, because they contain $–NH_2$ groups, can form hydrogen bonds with water. This gives the tiny cross linked sponges a great affinity for water. Polyacrylamide can absorb many times its mass in water. This property is useful in a variety of applications, such as in diapers and in potting soil. The polyacrylamide will release the absorbed water if a substance that interferes with hydrogen bonding is added. Ionic substances, such as salt, cause polyacrylamide to release its absorbed water.[17]

2.5.11 Other type of Polymers:

When all the mers are the same, the molecule is called a *homopolymer* and if there is more than one type of mer present, the molecule is a *copolymer* **(conjugate polymer)** and that is the material which we will use in this study**.**

Mer units that have 2 active bonds to connect with other mers are called *bifunctional* and those mer units that have 3 active bonds to connect with other mers are called *trifunctional***.** They form three dimensional molecular network structures.

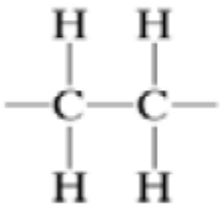

Polyethylene (bifunctional)

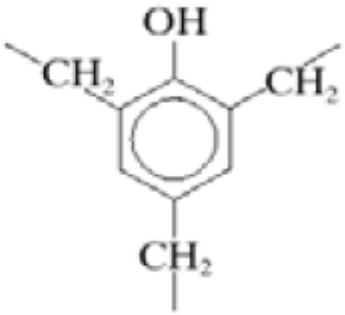

Phenol-formaldehyde (trifunctional)

Figure 2.11: Shows the structure of trifunctional polymer.[29]

2.6 Molecular shape of polymers:

In polymers molecule the angle between the singly bonded carbon atoms is ~109^{o} and the carbon atoms form a zigzag pattern. Moreover, while maintaining the 109^{o} angle between bonds polymers chains can rotate around single C-C bonds making random kinks and coils lead to entanglement, like in the spaghetti structure (double and triple bonds are very rigid).

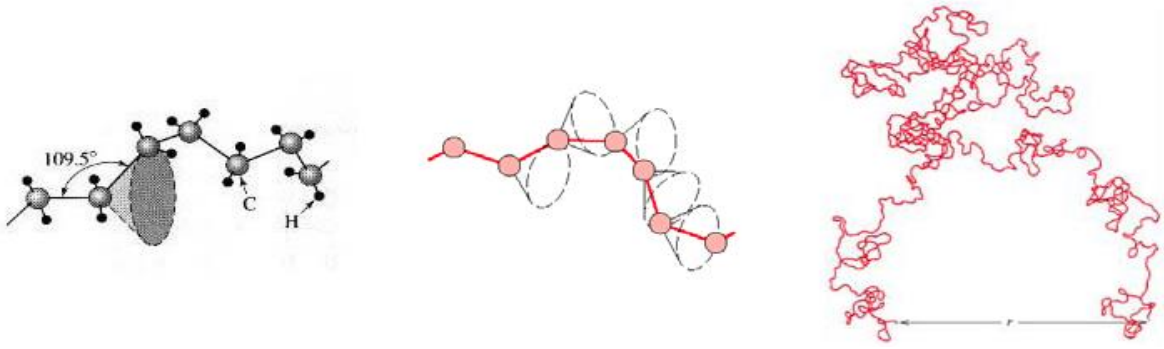

Figure 2.12: Shows the spaghetti structure of polymers.

The large elastic extensions of rubbers, mechanical and thermal characteristics of polymers material depend on the ability of chain segments to rotate.[29]

2.7 Molecular structure of polymers:

The physical characteristics of polymer material depend not only on molecular weight and shape, but also on molecular structure. There are four types of polymers structure:

1- Linear polymers: Van der Waals bonding is existed between chains. Examples: polyethylene, nylon.

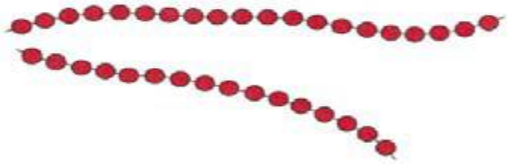

Figure 2.13: Shows the linear polymers structure.

2- Branched polymers: Chain packing efficiency is reduced compared to linear polymers and it has lower density.

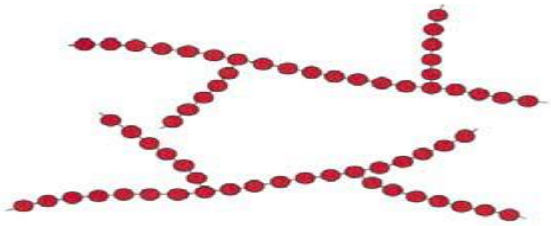

Figure 2.14: Shows the branched polymers structure.

3- Cross-linked polymers: Often achieved by adding atoms or molecules that form covalent links between chains. Many rubbers have this structure.

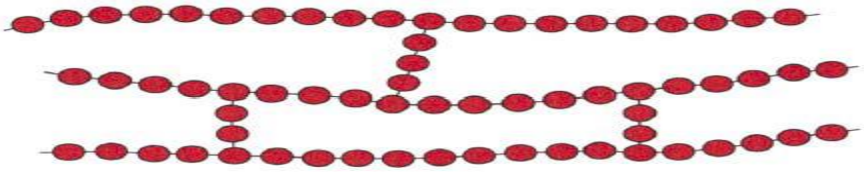

Figure 2.15: Shows the cross-linked polymers structure.

4- Network polymers: 3D networks made from trifunctional mers. Examples: epoxies, phenol formaldehyde.

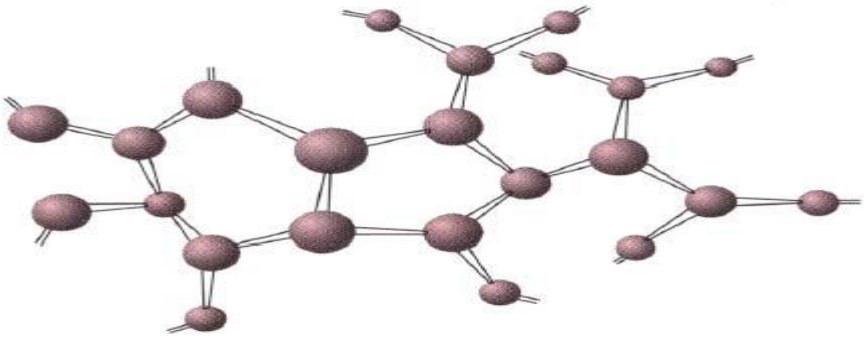

Figure 2.16: Shows the network polymers structure.

Isomerism: Hydrocarbon compounds with same composition may have different atomic compositions. Physical properties may also depend on isomeric state (e.g. boiling temperature of normal butane is -0.5 ºC, of isobutene - 12.3 ºC)

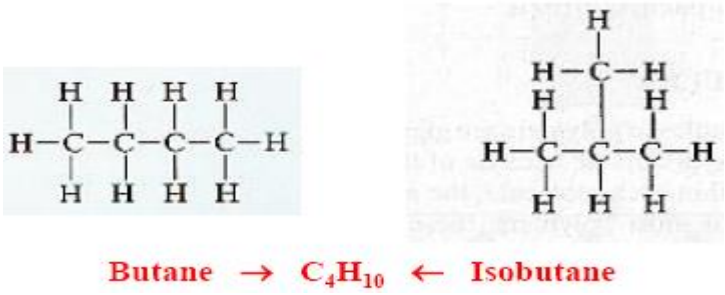

Figure 2.17: Shows the Isomerism structure.

There are two types of isomerism stereoisomerism and geometrical isomerism.

(1) Stereoisomerism: atoms are linked together in the same order, but can have different spatial arrangement

1- Isotactic configurations: all side of R groups is on the same side of the chain.

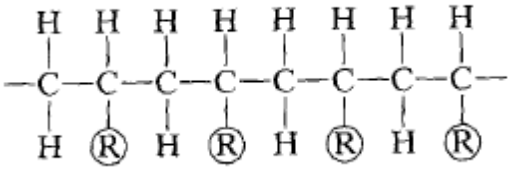

Figure 2.18: Shows the Isotactic structure (Stereoisomerism).

2- Syndiotactic configurations: side groups R alternate sides of the chain.

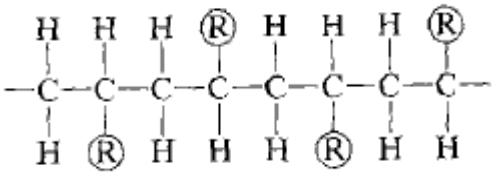

Figure 2.19: Shows the syndiotactic structure (Stereoisomerism).

3- Atactic configurations: random orientations of groups R along the chain.

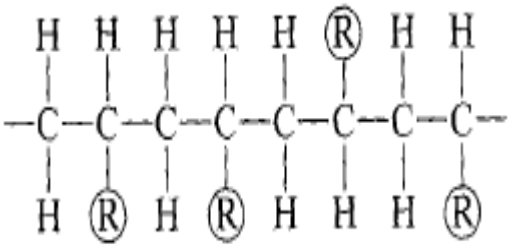

Figure 2.20: Shows the Atactic structure (Stereoisomerism).

(2) Geometrical isomerism: consider two carbon atoms bonded by a double bond in a chain. H atom or radical R bonded to these two atoms can be on the same side of the chain (**cis** structure) or on opposite sides of the chain (**Trans** structure).

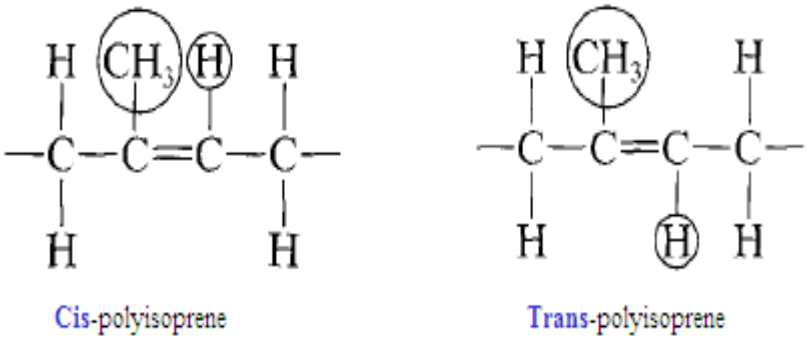

Figure 2.21: Shows the geometrical isomerism structure (Geometrical isomerism).[29]

2.8 Polymers Classifications

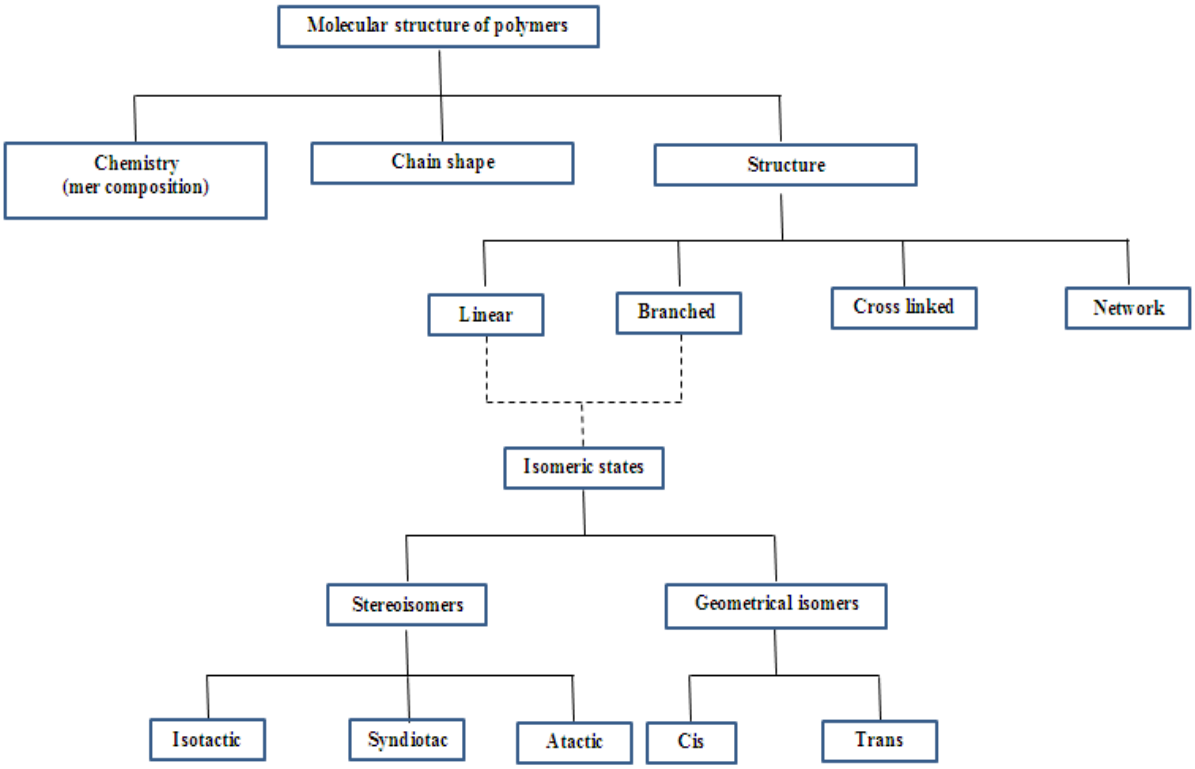

Figure 2.22: Shows a diagram of polymers classifications.[29]

2.9 Copolymers (conjugate polymers):

Copolymers, is a polymer with at least two different types of mers, can differ in the way that the mers are arranged.

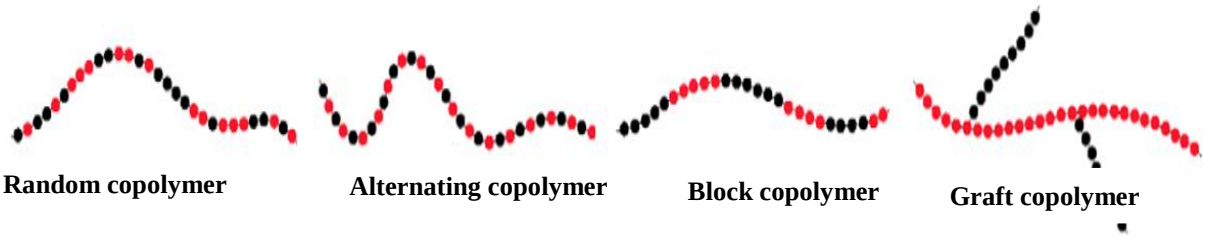

Figure 2.23: Shows a different arrangement of copolymers.

2.10 Polymer Crystallinity:

Atomic arrangement in polymer crystals is more complex than in metals or ceramics (unit cells are typically large and complex). Polymer molecules are often partially crystalline (semi-crystalline), with crystalline regions dispersed within amorphous material.

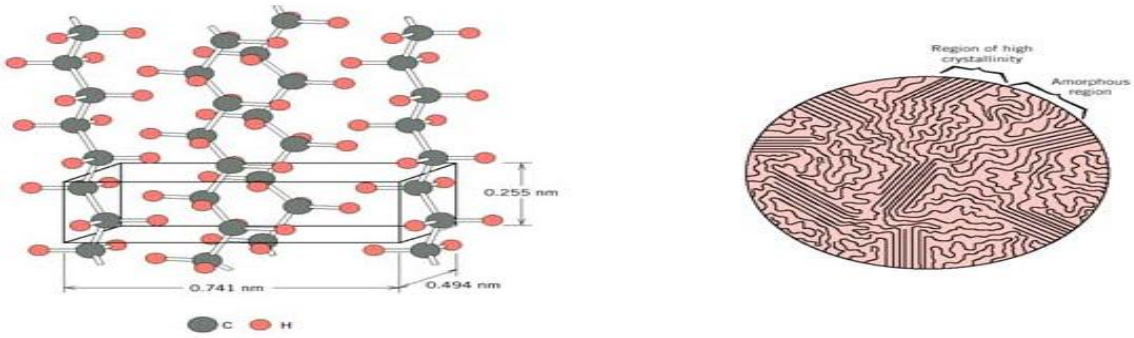

Figure 2.24: Shows the atomic arrangement of polymers crystal.

The degree of crystallinity is determined by:

1- Rate of cooling during solidification: Time is necessary for chains to move and align into a crystal structure.

2- **Mer complexity**: Crystallization less likely in complex structures, simple polymers, such as polyethylene, crystallizes relatively easily.

3- **Chain configuration**: Linear polymers crystallize relatively easily, branches inhibit crystallization, and network polymers almost completely amorphous, cross linked polymers can be both crystalline and amorphous.

4- **Isomerism**: Isotactic, syndiotactic polymers crystallize relatively and easily geometrical regularity allows chains to fit together, atactic difficult to crystallize.

5- **Copolymerism**: Easier to crystallize if mer arrangements are more regular. Alternating, block can crystallize more easily compared to random and graft polymers.

More crystallinity: higher density, more strength, higher resistance to dissolution and softening by heating. Crystalline polymers are denser than amorphous polymers, so the degree of crystallinity can be obtained from the measurement of density:

$$\text{crystallinity} = \frac{\rho_C(\rho_s - \rho_a)}{\rho_s(\rho_c - \rho_a)} \times 100\%$$

Where ρ_c: Density of perfect crystalline polymer, ρ_a: Density of completely amorphous polymer, ρ_s: Density of partially crystalline polymer that we are analyzing.

Thin crystalline platelets grown from solution - chains fold back and forth: chain-folded model and the average chain length are much greater than the thickness of the crystallite.[29]

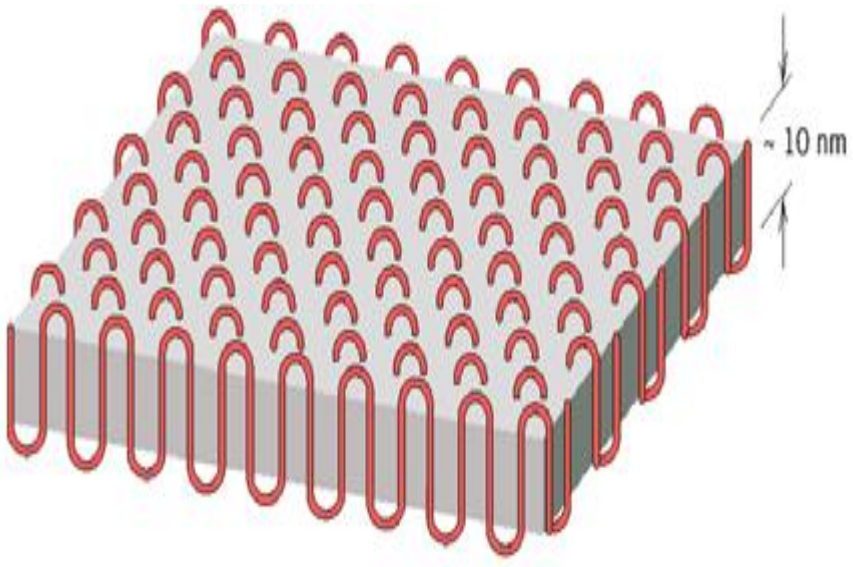

Figure 2.25: Shows the chains fold and the thickness of polymers crystal.

2.10.1 Other type of Polymer Crystals:

1- **Spherulites:** Aggregates of lamellar crystallites ~ 10 nm thick, separated by amorphous material it has approximately spherical in shape.

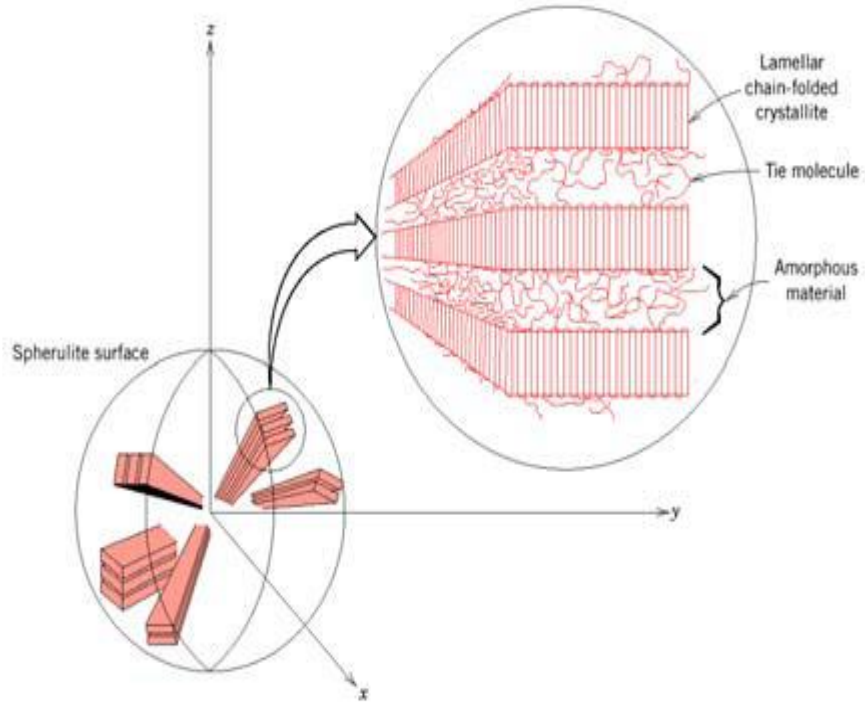

Figure 2.26: Shows the Spherulites surface of polymers crystal.

2- **Five Bakers Dancing:** Phosphatidyl choline[29]

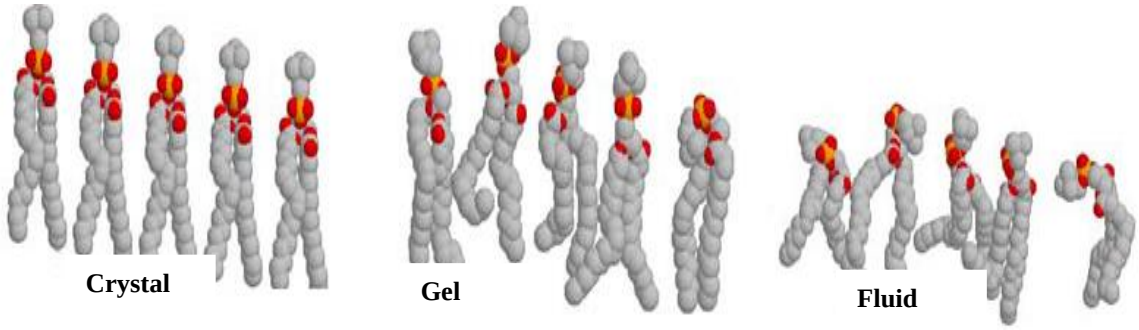

Figure 2.27: Shows the structure of Phosphatidyl Choline (Five Bakers Dancing).

3- **Number Eighty Eight:** Human a polipoprtein A-I. Biopolymers can be complex… and nice.

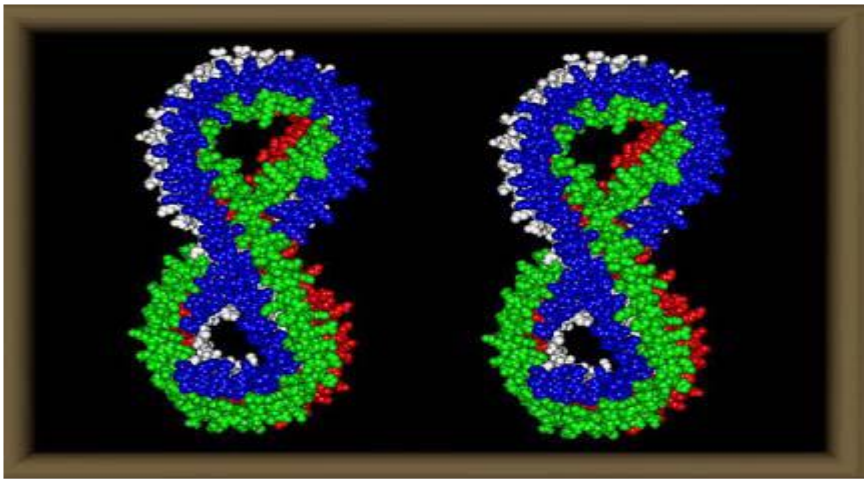

Figure 2.28: Shows the structure of Biopolymers (Number Eighty Eight)[29].

Finally we will discuss about the material which we will used in this study (conjugate polymer).

Polymers as reviewed are a carbon based long compounds that are made of a repeating unit - a monomer. Π-conjugated polymers (***conjugated polymers*** in short) can be defined as organic polymers with π and π* molecular orbitals delocalized over the whole polymer chain. In the language of chemical structural formulae, these orbitals are represented as an alternation of single and double carbon bonds along the chain as in Figure below. Another characteristic feature of these formulae is that it is possible to swap the positions of the single and double bonds and end up with a structure that still satisfies the chemical-bonding requirements for carbon [24].

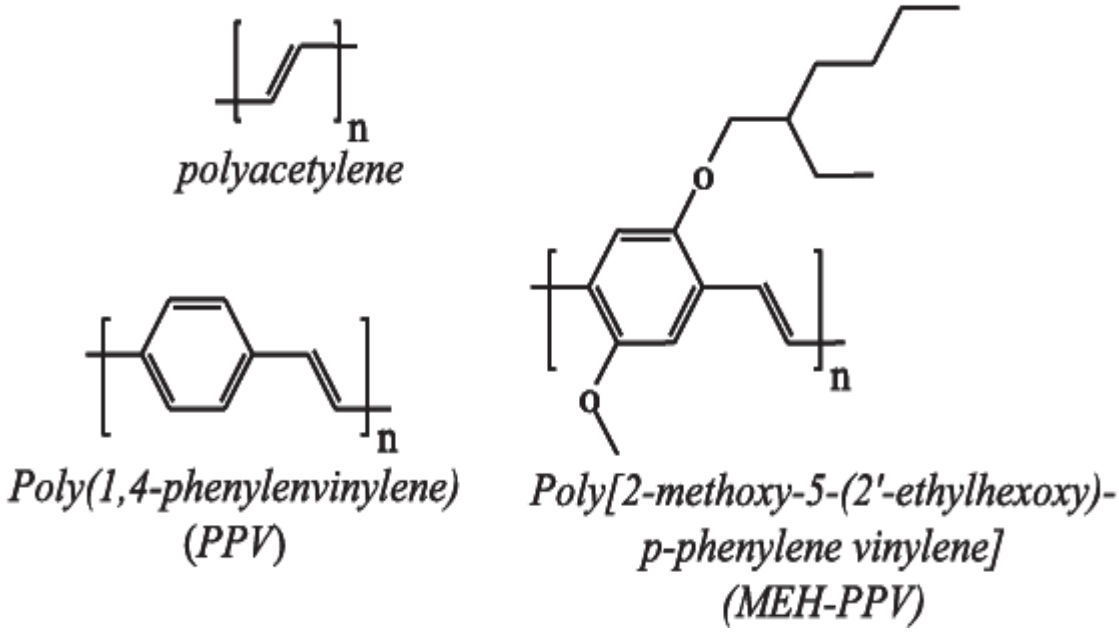

Figure 2.29: Shows the structural formulae of some π-conjugated polymers.

A lot of research effort has been concentrated on these polymers since the discovery of high conductance in doped polyacetylene[24]by A.J. Heeger, A.G. MacDiarmid, H. Shirakawa, *et. al.* in 1977. In the year 2000 these researchers have been awarded a Nobel Prize in chemistry for this discovery [39]. The reason for such strong interest in π-conjugated polymers is rooted in a unique combination of properties these materials possess. To get an insight into these properties, it is helpful to consider how π and π* molecular orbitals are formed from the point of view of the linear combination of atomic orbitals technique as show in Figure 2.30 below. Two of the three 2p orbitals on each carbon atom combine with the 2s

orbital to form three sp^2 "hybrid" orbitals. These orbitals lie in a plane, directed at 120° to one another, and form three σ molecular orbitals with neighboring atoms, including one with hydrogen.

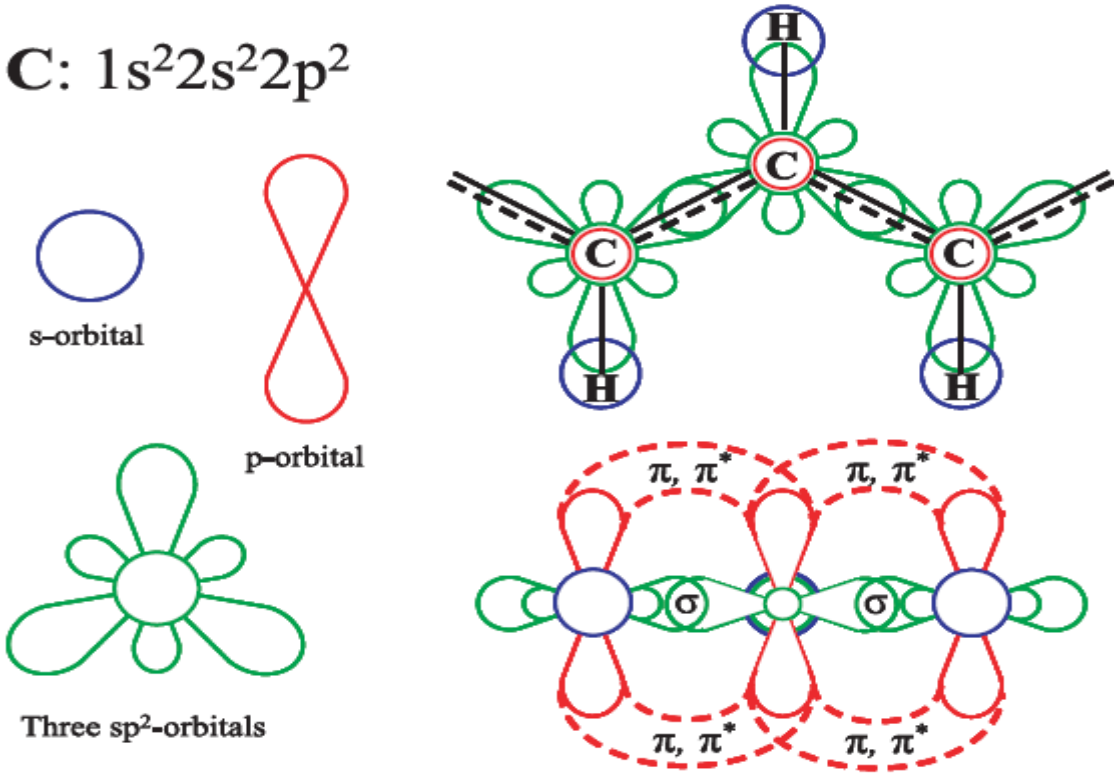

Figure 2.30: Shows a scheme of molecular orbital formation in π-conjugated polymers.

The third p-orbital on the carbon atom points perpendicular to the sp^2-orbital plane. It overlaps with the other non-hybrid p-orbitals on neighboring carbon atoms to form a pair of molecular orbitals: π (bonding) and π* (anti-bonding). Since electrons can have two different spin states, the lower-energy bonding π-orbital gets occupied, and the higher energy anti-bonding π*-orbital is left unoccupied. The resulting electronic structure of π-conjugated polymers is similar to that of semiconductors as show in Figure below. Indeed, the highest occupied molecular orbital (HOMO) is analogous to the valence band edge in semiconductors, the lowest unoccupied molecular orbital (LUMO) is analogous to the conduction band edge, and the gap between them is analogous to the semiconductor band gap. Most conjugated polymers have semiconductor band gaps of 1.5-3 eV, which means that they are suitable for optoelectronic devices that emit visible light. It is the combination of fluorescence and semiconducting properties together with process ability of plastics that makes these materials so attractive for applications.

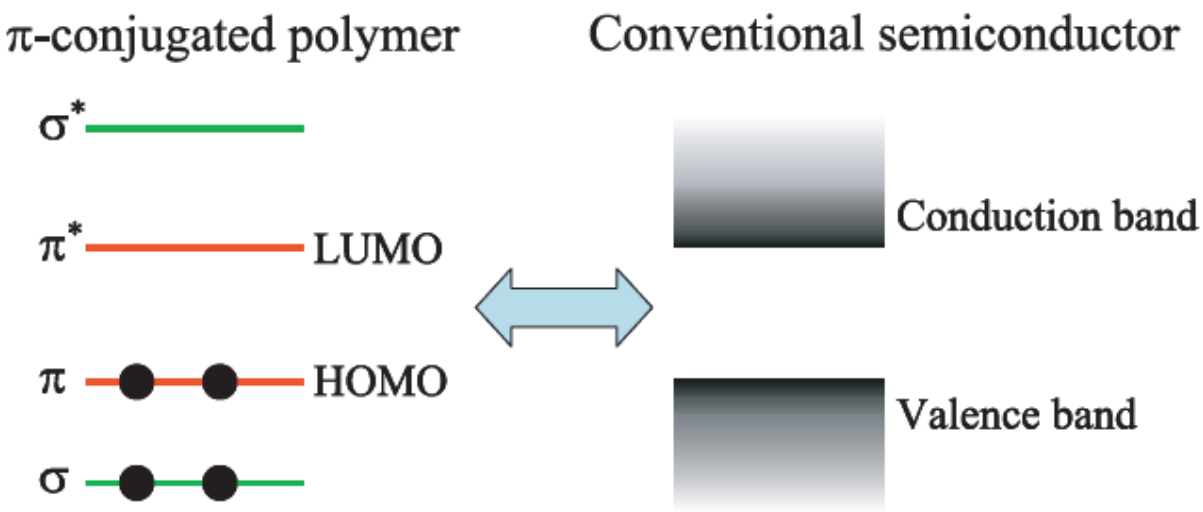

Figure 2.31: Shows the analogy between π-conjugated polymers and semiconductors.

However, the above picture holds only in the ideal case of perfectly straight polymer chains and absence of chemical defects. In reality such imperfections break the conjugation and "chop" the π-orbitals into "pieces" called spectroscopic units [76] as show in Figure 2.32 below. The typical length of a spectroscopic unit is ~ 5 monomer units for MEH-PPV [22].

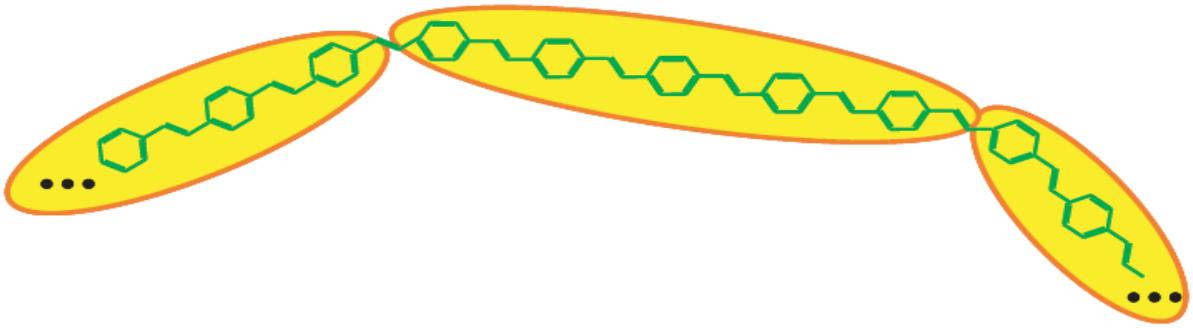

Figure2.32: Spectroscopic units.

Such a polymer chain is no longer a single semiconductor "crystal" but a series of chemically connected oligomers with semiconductor like electronic structure. It was found to be more appropriate to describe electronic excited states in this system in terms of the exciton (correlated electron-hole pair) [20],[36].

CHAPTER THREE

SOLAR CELLS AND POLYMER SOLAR CELLS

3.1 Introduction:

Today's political considerations to move the world's energy consumption away from fossil fuels such as oil, coal and gas has increased the focus on renewable energy. Renewable energy is perceived as a sustainable solution to ensure future energy supply as well as being carbon dioxide emissions free or neutral. Solar energy is by far the renewable energy source with the greatest potential. It has the ability to cover the world's energy demand several thousand times over and, unlike fossil fuels, solar energy is readily available world-wide.

3.2 Solar Cells:

A **solar cell** (also called a **photovoltaic cell**) is an electrical device that converts the energy of light directly into electricity by the photovoltaic effect. It is a form of **photoelectric cell** which, when exposed to light, can generate and support an electric current without being attached to any external voltage source. The term "photovoltaic" comes from the Greek meaning "light", and from "Volt", the unit of electro-motive force. The term "photo-voltaic" has been in use in English since 1849.[9]

Photovoltaic's is the field of technology and research related to the practical application of photovoltaic cells in producing electricity from light, though it is often used specifically to refer to the generation of electricity from sunlight. Cells can be described as photovoltaic even when the light source is not necessarily sunlight (lamplight, artificial light, etc.). In such cases the cell is sometimes used as a photo detector (for example infrared detectors), detecting light or other electromagnetic radiation near the visible range, or measuring light intensity.

The operation of a photovoltaic (PV) cell requires three basic attributes:

(1) Photons in sunlight hit the solar panel and are absorbed by semiconducting materials, generating either electron-hole pairs or excitons.

(2) Electrons (negatively charged) are knocked loose from their atoms, causing an electric potential difference. Current starts flowing through the material to cancel the potential and this electricity is captured. Due to the special composition of solar cells, the electrons are only allowed to move in a single direction.

(3) An array of solar cells converts solar energy into a usable amount of direct current (DC) electricity.

In contrast, a solar thermal collector collects heat by absorbing sunlight, for the purpose of either direct heating or indirect electrical power generation. "Photo electrolytic cell" (photo electrochemical cell), on the other hand, refers either a type of photovoltaic cell (like that developed by A.E. Becquerel and modern dye-sensitized solar cells) or a device that splits water directly into hydrogen and oxygen using only solar illumination.

3.3 History of solar cells

The photovoltaic effect was first experimentally demonstrated by French physicist A. E. Becquerel in 1839, at age 19, experimenting in his father's laboratory, he built the world's first photovoltaic cell. However, it was not until 1883 that the first solid state photovoltaic cell was built, by Charles Fritts, who coated the semiconductor selenium with an extremely thin layer of gold to form the junctions. The device was only around 1% efficient. In 1888 Russian physicist Aleksandr Stoletov built the first photoelectric cell based on the outer photoelectric effect discovered by Heinrich Hertz earlier in 1887.[73]

Albert Einstein explained the underlying mechanism of light instigated carrier excitation--the photoelectric effect in 1905, for which he received the Nobel Prize in Physics in 1921.[99] Russell Ohl patented the modern junction semiconductor solar cell in 1946,[59] which was discovered while working on the series of advances that would lead to the transistor.

The first practical photovoltaic cell was developed in 1954 at Bell Laboratories [51] by Daryl Chapin, Calvin Souther Fuller and Gerald Pearson. They used a diffused silicon p-n junction that reached 6% efficiency, compared to the selenium cells that found it difficult to reach 0.5%.[72] At first, cells were developed for toys and other minor uses, as the cost of the electricity they produced was very high, in relative terms, a cell that produced 1 watt of electrical power in bright sunlight cost about $250, comparing to $2 to $3 per watt for a coal plant.

Solar cells were brought from obscurity by the suggestion to add them to the Vanguard I satellite, launched in 1958. In the original plans, the satellite would be powered only by battery, and last a short time while this ran down. By adding cells to the outside of the body, the mission time could be extended with no major changes to the spacecraft or its power systems. There was some skepticism at first, but in practice the cells proved to be a huge success, and solar cells were quickly designed into many new satellites, notably Bell's own Telstar.

Improvements were slow over the next two decades, and the only widespread use was in space applications where their power-to-weight ratio was higher than any competing technology. However, this success was also the reason for slow progress, space users were willing to pay anything for the best possible cells, and there was no reason to invest in lower-cost solutions if this would reduce efficiency. Instead, the price of cells was determined largely by the semiconductor industry; their move to integrated circuits in the 1960 led to the availability of larger boules at lower relative prices. As their price fell, the price of the resulting cells did as well. However these effects were limited, and by 1971 cell costs were estimated to be $100 per watt.[72]

3.3.1 Berman's price reductions:

In the late 1960, Elliot Berman was investigating a new method for producing the silicon feedstock in a ribbon process. However, he found little interest in the project and was unable to gain the funding needed to develop it. In a chance encounter, he was later introduced to a team at Exxon who were looking for projects 30 years in the future. The group had concluded that electrical power would

be much more expensive by 2000, and felt that this increase in price would make new alternative energy sources more attractive, and solar was the most interesting among these. In 1969, Berman joined the Linden, New Jersey Exxon lab, Solar Power Corporation (SPC).[72]

His first major effort was to canvass the potential market to see what possible uses for a new product were, and they quickly found that if the price per watt were reduced from then-current $100/watt to about $20/watt there would be significant demand. Knowing that his ribbon concept would take years to develop, the team started looking for ways to hit the $20 price point using existing materials.[72]

The first improvement was the realization that the existing cells were based on standard semiconductor manufacturing process, even though that was not ideal. This started with the boule, cutting it into disks called wafers, polishing the wafers, and then, for cell use, coating them with an anti-reflective layer. Berman noted that the rough-sawn wafers already had a perfectly suitable anti-reflective front surface, and by printing the electrodes directly on this surface, two major steps in the cell processing were eliminated. The team also explored ways to improve the mounting of the cells into arrays, eliminating the expensive materials and hand wiring used in space applications. Their solution was to use a printed circuit board on the back, acrylic plastic on the front, and silicone glue between the two, potting the cells. The largest improvement in price point was Berman's realization that existing silicon was effectively "too good" for solar cell use; the minor imperfections that would ruin a boule (or individual wafer) for electronics would have little effect in the solar application.[72] Solar cells could be made using cast-off material from the electronics market.

Putting all of these changes into practice, the company started buying up "reject" silicon from existing manufacturers at very low cost. By using the largest wafers available, thereby reducing the amount of wiring for a given panel area, and packaging them into panels using their new methods, by 1973 SPC was producing panels at $10 per watt and selling them at $20 per watt, a fivefold decrease in prices in two years.

3.3.2 Further improvements:

In the time since Berman's work, improvements have brought production costs down under $1 a watt, with wholesale costs well under $2. "Balance of system" costs are now more than the panels themselves. Large commercial arrays can be built at below $3.40 a watt,[75][89] fully commissioned.

As the semiconductor industry moved to ever-larger boules, older equipment became available at fire-sale prices. Cells have grown in size as older equipment became available on the surplus market. Panels in the 1990s and early 2000s generally used 5 inch (125 mm) wafers, and since 2008 almost all new panels use 6 inch (150 mm) cells. This material has less efficiency, but is less expensive to produce in bulk. The widespread introduction of flat screen televisions in the late 1990s and early 2000s led to the wide availability of large sheets of high-quality glass, used on the front of the panels.

In terms of the cells themselves, there has been only one major change. During the 1990s, polysilicon cells became increasingly popular. These cells offer less efficiency than their monosilicon counterparts, but they are grown in large vats that greatly reduce the cost of production. By the mid-2000s, poly was dominant in the low-cost panel market, but more recently a variety of factors has pushed the higher performance mono back into widespread use.

3.3.3 Current events:

Other technologies have tried to enter the market. First Solar was briefly the largest panel manufacturer in 2009, in terms of yearly power produced, using a thin-film cell sandwiched between two layers of glass. Since then silicon panels reasserted their dominant position both in terms of lower prices and the rapid rise of Chinese manufacturing, resulting in the top producers being Chinese. By late 2011, efficient production in China, coupled with a drop in European demand due to budgetary turmoil had dropped prices for crystalline solar-based modules further, to about $1.09[89] per watt in October 2011, down sharply from the price per watt in 2010.

A more modern process, mono-like-multi, aims to offer the performance of mono at the cost of poly, and is in the process of being introduced in 2012.

3.4 Solar cell efficiency:

The efficiency of a solar cell may be broken down into reflectance efficiency, thermodynamic efficiency, charge carrier separation efficiency and conductive efficiency. The overall efficiency is the product of each of these individual efficiencies.

Due to the difficulty in measuring these parameters directly, other parameters are measured instead: thermodynamic efficiency, quantum efficiency, integrated quantum efficiency, V_{OC} ratio, and fill factor. Reflectance losses are a portion of the quantum efficiency under "external quantum efficiency". Recombination losses make up a portion of the quantum efficiency, V_{OC} ratio, and fill factor. Resistive losses are predominantly categorized under fill factor, but also make up minor portions of the quantum efficiency, V_{OC} ratio.

The **fill factor** is defined as the ratio of the actual maximum obtainable power to the product of the open circuit voltage and short circuit current. This is a key parameter in evaluating the performance of solar cells. Typical commercial solar cells have a fill factor > 0.70. Grade B cells have a fill factor usually between 0.4 to 0.7.[96] Cells with a high fill factor have a low equivalent series resistance and a high equivalent shunt resistance, so less of the current produced by the cell is dissipated in internal losses.

Single p-n junction crystalline silicon devices are now approaching the theoretical limiting power efficiency of 33.7%, noted as the Shockley–Queisser limit in 1961. In the extreme, with an infinite number of layers, the corresponding limit is 86% using concentrated sunlight.[1]

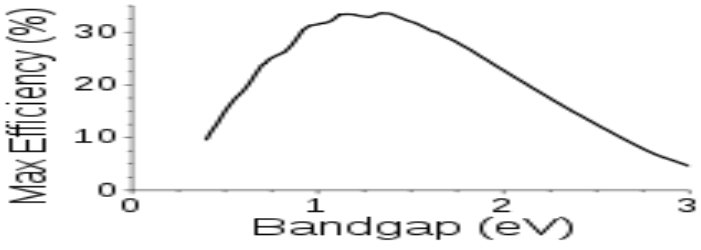

Figure 3.1: Shows the relations between the band gap the efficiency for semiconductors.

Semiconductors with band gap between 1 and 1.5eV, or near-infrared light, have the greatest potential to form an efficient cell.

Solar panels on the International Space Station absorb light from both sides. These Bifacial cells are more efficient and operate at lower temperature than single sided equivalents.

3.5 Solar cell Materials:

Various materials display varying efficiencies and have varying costs. Materials for efficient solar cells must have characteristics matched to the spectrum of available light. Some cells are designed to efficiently convert wavelengths of solar light that reach the Earth surface. However, some solar cells are optimized for light absorption beyond Earth's atmosphere as well. Light absorbing materials can often be used in **multiple physical configurations** to take advantage of different light absorption and charge separation mechanisms.

Materials presently used for photovoltaic solar cells include monocrystalline silicon, polycrystalline silicon, amorphous silicon, cadmium telluride, and copper indium selenide/sulfide.[62]

Many currently available solar cells are made from bulk materials that are cut into wafers between 180 to 240 micrometers thick that are then processed like other semiconductors.

Other materials are made as thin-films layers, organic dyes, and organic polymers that are deposited on supporting substrates. A third group are made from nanocrystals and used as quantum dots (electron-confined nanoparticles). Silicon remains the only material that is well-researched in both **bulk** and **thin-film** forms.

3.5.1 Crystalline Silicon:

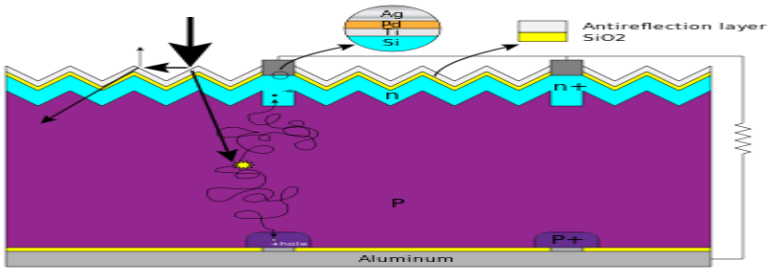

Figure 3.2: Shows the basic structure of a silicon based solar cell and its working mechanism.

By far, the most prevalent bulk material for solar cells is crystalline silicon (abbreviated as a group as c-Si), also known as "solar grade silicon". Bulk silicon is separated into multiple categories according to crystallinity and crystal size in the resulting ingot, ribbon, or wafer.

1- Monocrystalline silicon (c-Si): often made using the Czochralski process. Single-crystal wafer cells tend to be expensive, and because they are cut from cylindrical ingots, do not completely cover a square solar cell module without a substantial waste of refined silicon. Hence most c-Si panels have uncovered gaps at the four corners of the cells.

2- Polycrystalline silicon, or multicrystalline silicon, (poly-Si or mc-Si): made from cast square ingots — large blocks of molten silicon carefully cooled and solidified. Poly-Si cells are less expensive to produce than single crystal silicon cells, but are less efficient. United States Department of Energy data show that there were a higher number of polycrystalline sales than monocrystalline silicon sales.

3- Ribbon silicon [30] is a type of polycrystalline silicon: it is formed by drawing flat thin films from molten silicon and results in a polycrystalline structure. These cells have lower efficiencies than poly-Si, but save on production costs due to a great reduction in silicon waste, as this approach does not require sawing from ingots.

4- Mono-like-multi silicon: Developed in the 2000s and introduced commercially around 2009, mono-like-multi, or cast-mono, uses existing polycrystalline casting chambers with small "seeds" of mono material. The result is a bulk mono-like material with poly around the outsides. When sawn apart for processing, the inner sections are high-efficiency mono-like cells (but square instead of "clipped"), while the outer edges are sold off as conventional poly. The result is line that produces mono-like cells at poly-like prices.[105]

Analysts have predicted that prices of polycrystalline silicon will drop as companies build additional polysilicon capacity quicker than the industry's projected demand. On the other hand, the cost of producing upgraded metallurgical-grade silicon, also known as UMG Si, can potentially be one-sixth that of making polysilicon.[23]

3.5.2 Thin films:

In 2010 the market share of thin film declined by 30% as thin film technology was displaced by more efficient crystalline silicon solar panels.

Thin-film technologies reduce the amount of material required in creating the active material of solar cell. Most thin film solar cells are sandwiched between two panes of glass to make a module. Since silicon solar panels only use one pane of glass, thin film panels are approximately twice as heavy as crystalline silicon panels. The majority of film panels have significantly lower conversion efficiencies. Thin-film solar technologies have enjoyed large investment due to the success of first Solar and the largely unfulfilled promise of lower cost and flexibility compared to wafer silicon cells, but they have not become mainstream solar products due to their lower efficiency and corresponding larger area consumption per watt production. Cadmium telluride (CdTe), copper indium gallium selenide (CIGS) and amorphous silicon (A-Si) are three thin-film technologies often used as outdoor photovoltaic solar power production. CdTe technology is most cost competitive among them.[100] CdTe technology costs about 30% less than CIGS technology and 40% less than A-Si technology in 2011. Copper indium gallium selenide (CIGS) is a direct band gap material. It has the highest efficiency (~20%) among thin film materials.

3.5.3 Amorphous Silicon thin films:

Silicon thin-film cells are mainly deposited by chemical vapor deposition (typically plasma-enhanced, PE-CVD) from silane gas and hydrogen gas. Depending on the deposition parameters, this can yield:[59]

1. Amorphous silicon (a-Si or a-Si:H).
2. Proto-crystalline silicon.
3. Nanocrystalline silicon (nc-Si or nc-Si:H), also called microcrystalline silicon.

It has been found that proto-crystalline silicon with a low volume fraction of nanocrystalline silicon is optimal for high open circuit voltage.[62] These types of silicon present dangling and twisted bonds, which results in deep defects (energy levels in the band gap) as well as deformation of the valence and conduction bands (band tails). The solar cells made from these materials tend to have lower *energy*

conversion efficiency than *bulk* silicon, but are also less expensive to produce. The quantum efficiency of thin film solar cells is also lower due to reduced number of collected charge carriers per incident photon.

An amorphous silicon (a-Si) solar cell is made of amorphous or microcrystalline silicon and its basic electronic structure is the p-i-n junction. A-Si is attractive as a solar cell material because it is abundant and non-toxic (unlike its CdTe counterpart) and requires a low processing temperature, enabling production of devices to occur on flexible and low-cost substrates. As the amorphous structure has a higher absorption rate of light than crystalline cells, the complete light spectrum can be absorbed with a very thin layer of photo-electrically active material. A film only 1 micron thick can absorb 90% of the usable solar energy.[64] This reduced material requirement along with current technologies being capable of large-area deposition of a-Si, the scalability of this type of cell is high. However, because it is amorphous, it has high inherent disorder and dangling bonds, making it a bad conductor for charge carriers. These dangling bonds act as recombination centers that severely reduce the carrier lifetime and pin the Fermi energy level so that doping the material to n- or p- type is not possible. Amorphous Silicon also suffers from the Staebler-Wronski effect, which results in the efficiency of devices utilizing amorphous silicon dropping as the cell is exposed to light. The production of a-Si thin film solar cells uses glass as a substrate and deposits a very thin layer of silicon by plasma-enhanced chemical vapor deposition (PECVD). A-Si manufacturers are working towards lower costs per watt and higher conversion efficiency with continuous research and development on Multijunction solar cells for solar panels. Anwell Technologies Limited recently announced its target for multi-substrate-multi-chamber PECVD, to lower the cost to US$0.5 per watt.[65]

Amorphous silicon has a higher band gap (1.7 eV) than crystalline silicon (c-Si) (1.1 eV), which means it absorbs the visible part of the solar spectrum more strongly than the infrared portion of the spectrum. As **nc-Si** has about the same band gap as c-Si, the nc-Si and a-Si can advantageously be combined in thin layers, creating a layered cell called a **tandem cell**. The top cell in a-Si absorbs the visible light and leaves the infrared part of the spectrum for the bottom cell in nc-Si.

3.5.4 Gallium arsenide multijunction:

High-efficiency multijunction cells were originally developed for special applications such as satellites and space exploration, but at present, their use in terrestrial concentrators might be the lowest cost alternative in terms of $/kWh and $/W.[40] These multijunction cells consist of multiple thin films produced using metal organic vapour phase epitaxy. A triple-junction cell, for example, may consist of the semiconductors: GaAs, Ge, and $GaInP_2$.[102] Each type of semiconductor will have a characteristic band gap energy which, loosely speaking, causes it to absorb light most efficiently at a certain color, or more precisely, to absorb electromagnetic radiation over a portion of the spectrum. The semiconductors are carefully chosen to absorb nearly all of the solar spectrum, thus generating electricity from as much of the solar energy as possible.

GaAs based multijunction devices are the most efficient solar cells to date. In April 2011, triple junction metamorphic cell reached a record high of 43.5%.[88] This technology is currently being utilized in the Mars Exploration Rover missions, which have run far past their 90 day design life.

Tandem solar cells based on monolithic, series connected, gallium indium phosphide (GaInP), gallium arsenide GaAs, and germanium Ge p-n junctions, are seeing demand rapidly rise.

3.5.5 Quantum Dot Solar Cells:

Quantum dot solar cells (QDSCs) are based on the Gratzel cell, or dye-sensitized solar cell architecture but employ low band gap semiconductor nanoparticles, also called quantum dots (such as CdS, CdSe, Sb_2S_3, PbS, etc.), instead of organic or organometallic dyes as light absorbers. Quantum dots (QDs) have attracted much interest because of their unique properties. Their size quantization allows for the band gap to be tuned by simply changing particle size. They also have high extinction coefficients, and have shown the possibility of multiple exciton generation.[84]

In a QDSC, a meso-porous layer of titanium dioxide nanoparticles forms the backbone of the cell, much like in a DSSC. This TiO_2 layer can then be made

photoactive by coating with semiconductor quantum dots using chemical bath deposition, electrophoretic deposition, or successive ionic layer adsorption and reaction. The electrical circuit is then completed through the use of a liquid or solid redox couple. During the last 3–4 years, the efficiency of QDSCs has increased rapidly [52] with efficiencies over 5% shown for both liquid-junction [83] and solid state cells.[66] In an effort to decrease production costs of these devices, the Prashant Kamat research group[87] recently demonstrated a solar paint made with TiO_2 and CdSe that can be applied using a one-step method to any conductive surface and have shown efficiencies over 1%.[34]

3.5.6 Organic/polymer solar cells:

New photovoltaic (PV) energy technologies can contribute to environmentally friendly, renewable energy production, and the reduction of the carbon dioxide emission associated with fossil fuels and biomass. One new PV technology, plastic solar cell technology, is based on conjugated polymers and molecules. Polymer solar cells have attracted considerable attention in the past few years owing to their potential of providing environmentally safe, flexible, lightweight, inexpensive, efficient solar cells. Especially, bulk-heterojunction solar cells consisting of a mixture of a conjugated donor polymer with a methanofullerene acceptor are considered as a promising approach. Here a brief introduction and overview is given of the field of polymer solar cells.

It is expected that the global energy demand will double within the next 50 years. Fossil fuels, however, are running out and are held responsible for the increased concentration of carbon dioxide in the earth's atmosphere. Hence, developing environmentally friendly, renewable energy is one of the challenges to society in the 21st century. One of the renewable energy technologies is photovoltaics (PV), the technology that directly converts daylight into electricity. PV is one of the fastest growing of all the renewable energy technologies; in fact, it is one of the fastest growing industries at present.[3] Solar cell manufacturing based on the technology of crystalline, silicon devices is growing by approximately 40% per year and this growth rate is increasing. [3] This has been realized mainly by special

market implementation programs and other government grants to encourage a substantial use of the current PV technologies based on silicon. Unfortunately, financial support by governments is under constant pressure. At present, the active materials used for the fabrication of solar cells are mainly inorganic materials, such as silicon (Si), gallium-arsenide (GaAs), cadmium-telluride (CdTe), and cadmium-indium-selenide (CIS). The power conversion efficiency for these solar cells varies from 8 to 29% (Table 3.1). With regard to the technology used, these solar cells can be divided into two classes. The crystalline solar cells or silicon solar cells are made of either (mono- or poly-) crystalline silicon or GaAs. About 85% of the PV market is shared by these crystalline solar cells. [3] Amorphous silicon, CdTe, and CIS are more recent thin-film technologies.

Table3.1: Status of the power conversion efficiencies in February 2002, as reached for inorganic solar cells and the technology used to prepare these solar cells. Source: Photovoltaic Network for the Development of a Roadmap for PV (PV-NET).

Table 3.1: shows status of the power conversion efficiencies and the technology used.

Semiconductor material	Power conversion efficiency [%]	Technology
Mono-crystalline silicon	**20-24**	**Crystalline**
Poly-crystalline silicon	**13-18**	**Thick and thin-film**
Gallium-arsenide	**20-29**	**Crystalline**
Amorphous silicon	**8-13**	**Thin-film**
Cadmium telluride	**10-17**	**Thin-film**
Cadmium indium selenide	**10-19**	**Thin-film**

The current status of PV is that it hardly contributes to the energy market, because it is far too expensive. The large production costs for the silicon solar cells are one of the major obstacles. Even when the production costs could be reduced, large-scale production of the current silicon solar cells would be limited by the scarcity of some elements required, e.g. solar-grade silicon. To ensure a sustainable technology path for PV, efforts to reduce the costs of the current silicon technology need to be balanced with measures to create and sustain variety in PV technology. It is, therefore, clear that ‘techno diversity’, implying new solar cell technologies, is

necessary. [16] In the field of inorganic thin-films, technologies based on cheaper production processes are currently under investigation.

Another approach is based on solar cells made of entirely new materials, conjugated polymers and molecules. Conjugated materials are organics consisting of alternating single and double bonds. The field of electronics based on conjugated materials started in 1977 when Heeger, MacDiarmid, and Shirakawa discovered that the conductivity of the conjugated polymer polyacetylene (PA, Figure 3.3) can be increased by seven orders of magnitude upon oxidation with iodine, [26] for which they were awarded the Nobel Prize in Chemistry in 2000.[41,42,2,6] This discovery led, subsequently, to the discovery of electroluminescence in a poly(p-phenylene vinylene) (PPV, Figure 1) by Burroughes et al. in 1990.[80,46] The first light-emitting products based on electroluminescence in conjugated polymers have already been launched at the consumer market by Philips (The Netherlands) in 2002, whereas light-emitting products based on conjugated molecules have been introduced by the joint venture of Kodak and Sanyo (Japan). Going from discovery to product within a little bit more than one decade truly holds a huge promise for the future of plastic electronics. Other emerging applications are coatings for electrostatic dissipation and electromagnetic-interference shielding.[5]

Conjugated polymers and molecules have the immense advantage of facile, chemical tailoring to alter their properties, such as the band gap. Conjugated polymers (Figure3.3) combine the electronic properties known from the traditional semiconductors and conductors with the ease of processing and mechanical flexibility of plastics. Therefore, this new class of materials has attracted considerable attention owing to its potential of providing environmentally safe, flexible, lightweight, inexpensive electronics.

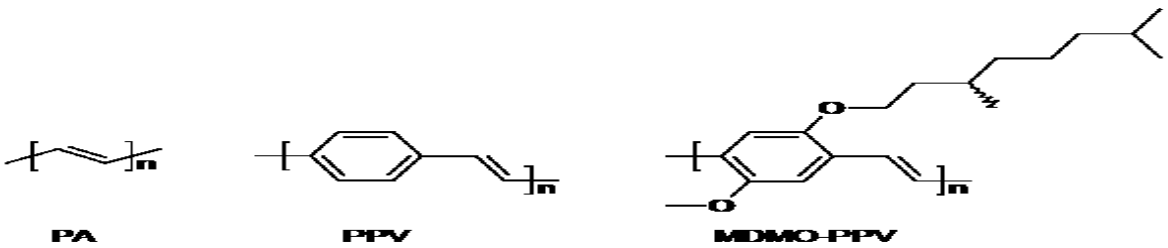

Figure 3.3: Shows the molecular structures of the conjugated polymers trans-polyacetylene (PA), poly (pphenylene vinylene) (PPV), and a substituted PPV (MDMO-PPV).

The cost reduction mainly results from the ease of processing from solution. Solution processing requires soluble polymers. Poly [p-phenylene vinylene] (PPV, Figure 1) is hardly soluble. Attachment of side-groups to the conjugated backbone, as in poly [2-methoxy-5- (3′,7′-dimethyloctyloxy)-1,4-phenylene vinylene] (MDMO-PPV, Figure(3.3), enhances the solubility of the polymer enormously. Furthermore, the nanoscale morphology, affecting the opto-electronic properties of these polymer films, can be controlled by proper choice of the position and nature of these side-groups.

Recent developments in ink-jet printing, micro-contact printing and other soft lithography techniques have further improved the potential of conjugated polymers for low-cost fabrication of large-area integrated devices on both rigid and flexible substrates. Architectures to overcome possible electronic scale-up problems related to thin film organics are being developed.[13] In contrast to conjugated polymers; conjugated molecules are mainly thermally evaporated under high vacuum. This deposition technique is much more expensive than solution processing and, therefore, less attractive.

The necessity for new PV technologies together with the opportunities in the field of plastic electronics, such as roll-to-roll production, have drawn considerable attention to plastic solar cells in the past few years. Apart from application in PV, it is expected that plastic solar cells will create a completely new market in the field of cheap electronics.

3.6 The need for two semiconductors:

Photovoltaic cell configurations based on organic materials differ from those based on inorganic semiconductors, because the physical properties of inorganic and organic semiconductors are significantly different. Inorganic semiconductors generally have a high dielectric constant and a low exciton binding energy (for GaAs the exciton binding energy is 4 meV). Hence, the thermal energy at room temperature (kT = 0.025 eV) is sufficient to dissociate the exciton created by absorption of a photon into a positive and negative charge carrier. The formed electrons and holes are easily transported as a result of the high mobility of the charge carriers and the internal field of the p-n junction. Organic materials have a

lower dielectric constant and the exciton binding energy is larger than for inorganic semiconductors, although the exact magnitude remains a matter of debate. For polydiacetylene 0.5 eV is needed to split the exciton and, hence, dissociation into free charge carriers does not occur at room temperature. To overcome this problem, organic solar cells commonly utilize two different materials that differ in electron donating and accepting properties. Charges are then created by photo induced electron transfer between the two components. This photo induced electron transfer between donor and acceptor boosts the photo generation of free charge carriers compared to the individual, pure materials, in which the formation of bound electron-hole pairs or excitons is generally favored. [78]

3.7 Basic processes in an organic solar cell:

Various architectures for organic solar cells have been investigated in recent years. In general, for a successful organic photovoltaic cell four important processes have to be optimized to obtain a high conversion efficiency of solar energy into electrical energy.

- Absorption of light.
- Charge transfer and separation of the opposite charges.
- Charge transport.
- Charge collection.

For an efficient collection of photons, the absorption spectrum of the photoactive organic layer should match the solar emission spectrum and the layer should be sufficiently thick to absorb all incidents light. A better overlap with the solar emission spectrum is obtained by lowering the band gap of the organic material, but this will ultimately have some bearing on the open-circuit voltage. Increasing the layer thickness is advantageous for light absorption, but burdens the charge transport. Creation of charges is one of the key steps in photovoltaic devices in the conversion of solar light into electrical energy. In most organic solar cells, charges are created by photo induced electron transfer. In this reaction an electron is transferred from an electron donor (D), a p-type semiconductor, to an electron acceptor (A), an n-type semiconductor, with the aid of the additional input energy of an absorbed photon (hν). In the photo induced electron transfer reaction the first

step is excition of the donor (D*) or the acceptor (A*), followed by creation of the charge-separated state consisting of the radical cation of the donor ($D^{\bullet+}$) and the radical anion of the acceptor ($A^{\bullet-}$).

$$D + A + h\nu \rightarrow D^* + A \text{ (or } D + A^*) \rightarrow D^{\bullet+} + A^{\bullet-}$$

For an efficient charge generation, it is important that the charge-separated state is the thermodynamically and kinetically most favorite pathway after photo excitation. Therefore, it is important that the energy of the absorbed photon is used for generation of the charge separated state and is not lost via competitive processes like fluorescence or non-radioactive decay. In addition, it is of importance that the charge-separated state is stabilized, so that the photo generated charges can migrate to one of the electrodes. Therefore, the back electron transfer should be slowed down as much as possible. [78]

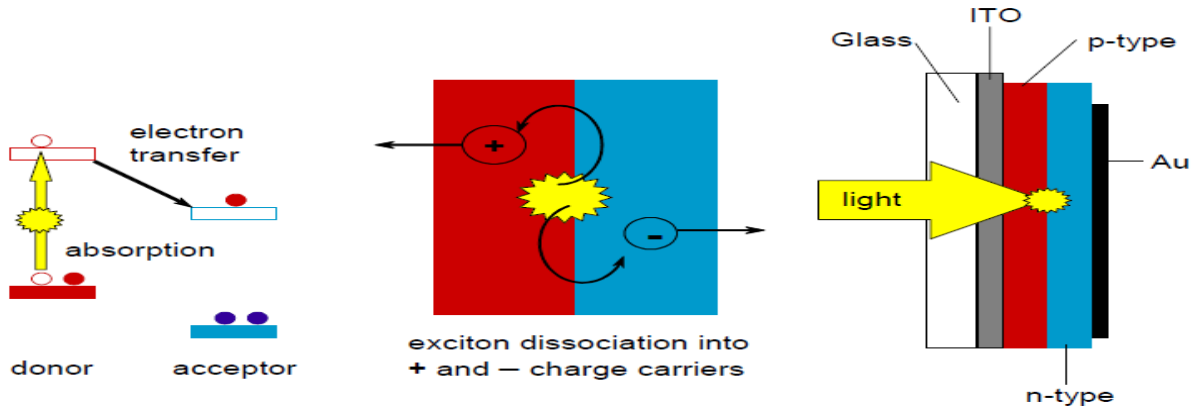

Figure 3.4: Schematic drawing of the working principle of an organic photovoltaic cell.

Illumination of donor (in red) through a transparent electrode (ITO) results in the photo excited state of the donor, in which an electron is promoted from the highest occupied molecular orbital (HOMO) to the lowest unoccupied molecular orbital (LUMO) of the donor. Subsequently, the excited electron is transferred to the LUMO of the acceptor (in blue), resulting in an extra electron on the acceptor ($A^{\bullet-}$) and leaving a hole at the donor ($D^{\bullet+}$). The photo generated charges are then transported and collected at opposite electrodes. A similar charge generation process can occur, when the acceptor is photo excited instead of the donor.

To create a working photovoltaic cell, the photoactive material (D+A) is sandwiched between two dissimilar (metallic) electrodes (of which one is transparent), to collect the photo generated charges. After the charge transfer

reaction, the photo generated charges have to migrate to these electrodes without recombination. Finally, it is important that the photo generated charges can enter the external circuit at the electrodes without interface problems. [78]

3.8 Actual organic solar cells:

In this paragraph a short overview is given of the most successful approaches towards organic solar cells to date. First, cells will be described in which organic molecules are only used for absorption light, followed by cells in which an organic or polymeric material is used for absorption of light and charge transport. [78]

3.8.1 Dye-sensitized solar cells (DSSCs):

In a dye-sensitized solar cell, an organic dye adsorbed at the surface of an inorganic wideband gap semiconductor is used for absorption of light and injection of the photo excited electron into the conduction band of the semiconductor. The research on dye sensitized solar cells gained considerable impulse, when Grätzel and co-workers greatly improved the interfacial area between the organic donor and inorganic acceptor by using nano-porous titanium dioxide (TiO_2).[19] To date, ruthenium dye-sensitized nanocrystalline TiO_2 (nc-TiO_2) solar cells reach an energy conversion efficiency of about 10% in solar light.[64] In the Grätzel cell (Figure 3), the ruthenium dye takes care of light absorption and electron injection into the TiO_2 conduction band. An I^-/I_3^- redox couple, contained in an organic solvent, is used to regenerate (i.e. reduce) the photo oxidized dye molecules. In the cells, the positive charge is transported by the liquid electrolyte to a metal electrode, where I_3^- takes up an electron from the external circuit (counter electrode), while the negative charges injected in nc-TiO_2 are collected at the fluorine doped tin oxide (SnO_2:F) electrode.

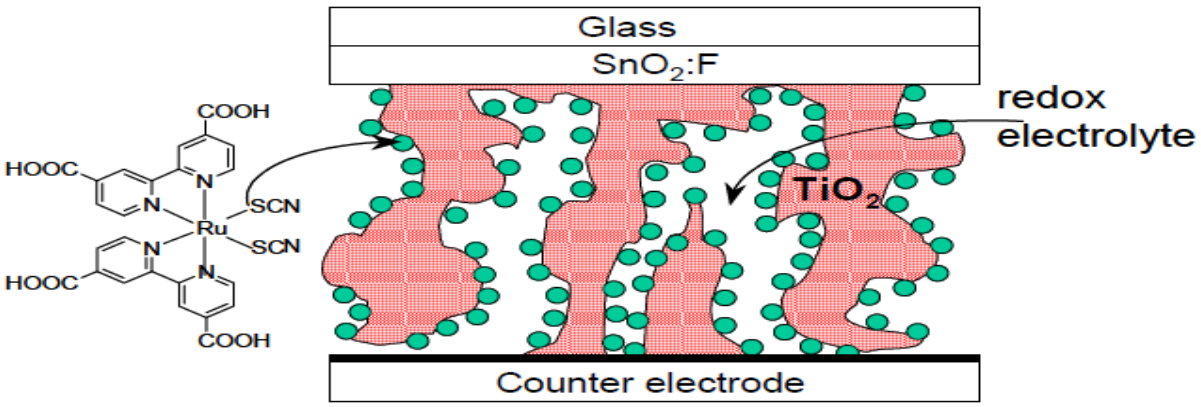

Figure3.5: The dye-sensitized solar cell. After absorption of light by the ruthenium dye, an electron is transferred to TiO_2. The dye is then reduced by a redox electrolyte, I^-/I_3^-, which in turn, is reduced at the metal counter electrode. As a result, a positive charge is transported from the dye to the metal electrode via the electrolyte. The electron in TiO_2 is transported to the SnO_2: F electrode.

The nano-porous TiO_2 ensures a dramatic enlargement of the contact area between the dye and semiconductor, compared to a flat interface. High quantum efficiencies for charge separation are achieved, because the dye molecules are directly adsorbed on the n-type semiconductor. The positive charges are transported efficiently by the liquid electrolyte and, as a consequence the thickness of the photovoltaic device can be extended to the μm range, resulting in optically dense cells. From a technology point of view, however, the liquid electrolyte represents a drawback. Hence, much research has focused on replacing the liquid electrolyte by a solid hole transporting material. The most promising replacement is a solid, wide-band gap hole transporting material resulting in power conversion efficiencies of 3%.[103]

Another new concept for a solid-state Grätzel cell consists of a polymer or organic semiconductor that combines the functions of light-absorption and charge (hole) transport in a single material and, therefore, is able to replace both the dye and hole transporting material.[71] The photo induced charge separation at the interface of an organic and inorganic semiconductor has been studied in relation to photovoltaic devices.[106] When an organic or polymeric semiconductor is excited across the optical band gap, the excitation energies and valence band offsets of this molecular semiconductor may allow electron transfer to the conduction band of an inorganic semiconductor, similar to the ruthenium dye. The dimensions of the nano-porous in TiO_2 are even more important here, because excitations are no longer created at the interface only, but throughout the whole organic material. Because essentially all excitons must be able to reach the interface with the TiO_2 for efficient charge separation and energy conversion, the distance between the site of excitation and the interface must be within the exciton diffusion length. In most organic materials, the exciton diffusion length is limited to 5-10 nm [68] by the fast intrinsic

decay processes of the photo excited molecules. Creating nano-porous TiO_2 of such dimensions, and filling it completely with an organic semiconductor, is currently one of the challenges in this area.

3.8.2 Double layer cells:

The first attempts to create all-organic solar cells were made by sandwiching a single layer of an organic material between two dissimilar electrodes.[33] In these cells, the photovoltaic properties strongly depend on the nature of the electrodes. Heavily doped conjugated materials resulted in reasonable power conversion efficiencies up to 0.3%.[33]

In 1986, a major breakthrough was realized by Tang, who introduced a double-layer structure of a p-and n-type organic semiconductor.[28] A 70 nm thick two-layer device was made using copper phthalocyanine as the electron donor, and a perylene tetra carboxylic derivative as the electron acceptor (Figure 3.6). The photoactive material was placed between two dissimilar electrodes, indium tin oxide (ITO) for collection of the positive charges and silver (Ag) to collect the negative charges. A power conversion efficiency of about 1% was achieved under simulated AM2 illumination (691 W/m^2). Important aspect in this concept is that the charge generation efficiency is relatively independent of the bias voltage.

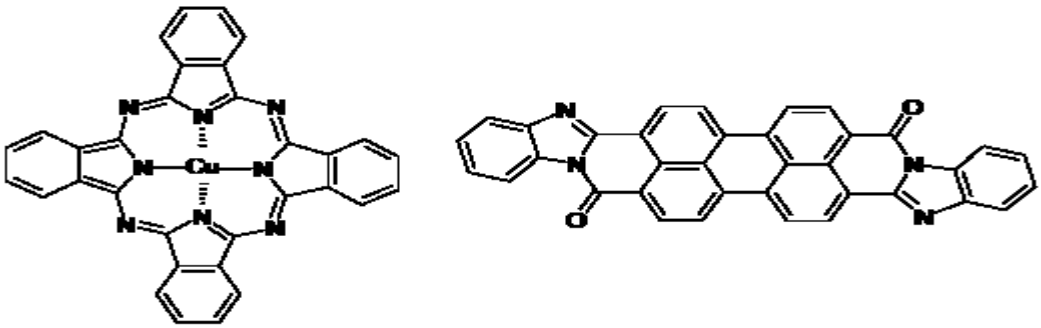

Figure 3.6: Molecular structures of copper phthalocyanine (CuPc), a perylene tetra carboxylic derivative (PTC).

In the double-layer structure the photo excitations in the photoactive material have to reach the p-n interface where charge transfer can occur, before the excitation energy of the molecule is lost via intrinsic radiative and non-radiative decay processes to the ground state. Because the exciton diffusion length of the

organic material is in general limited to 5-10nm, [68] only absorption of light within a very thin layer around the interface contributes to the photovoltaic effect. This limits the performance of double-layer devices, because such thin layer can impossibly absorb all the light. A strategy to improve the efficiency of the double-layer cell is related to structural organization of the organic material to extend the exciton diffusion length and, therefore, create a thicker photoactive interfacial area.

3.8.3 Bulk heterojunction cells:

In combining electron donating (p-type) and electron accepting (n-type) materials in the active layer of a solar cell, care must be taken that excitons created in either material can diffuse to the interface, to enable charge separation. Due to their short lifetime and low mobility, the diffusion length of excitons in organic semiconductors is limited to about ~10 nm only. This imposes an important condition to efficient charge generation. Anywhere in the active layer, the distance to the interface should be on the order of the exciton diffusion length. Despite their high absorption coefficients, exceeding 10^5 cm^{-1}, a 20 nm double layer of donor and acceptor materials would not be optical dense, allowing most photons to pass freely. The solution to this dilemma is elegantly simple.[38,47] By simple mixing the p and n-type materials and relying on the intrinsic tendency of polymer materials to phase separate on a nanometer dimension, junctions throughout the bulk of the material are created that ensure quantitative dissociation of photo generated excitons, irrespective of the thickness.

Polymer-fullerene solar cells were among the first to utilize this bulk-heterohunction principle.[38] Nevertheless, this attractive solution poses a new challenge. Photo generated charges must be able to migrate to the collecting electrodes through this intimately mixed blend. Because holes are transported by the p-type semiconductor and electrons by the n-type material, these materials should be preferably mixed into a bi-continuous, interpenetrating network in which inclusions, cul-de-sacs, or barrier layers are avoided. The close-to-ideal bulk heterojunction solar cell may look like depicted in Figure 3.7. When such a bulk-

heterojunction is deposited on an ITO substrate and capped with a metal back electrode, working photovoltaic cells is able to be obtained (Figure 3.7).

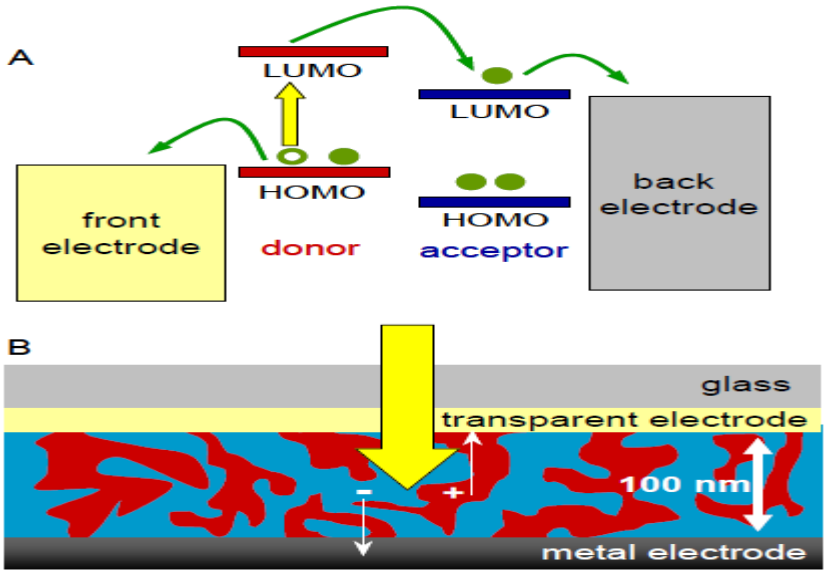

Figure 3.7: The bulk-heterojunction concept.

After absorption of light by the photoactive material, charge transfer can easily occur due to the nanoscopic mixing of the donor and acceptor (solid and dashed area). Subsequently, the photo generated charges are transported and collected at the electrodes.

The bulk heterojunction is presently the most widely used photoactive layer. The name bulk-heterojunction solar cell has been chosen, because the interface (heterojunction) between both components is all over the bulk (Figure 3.7), in contrast to the classical (bilayer-) heterojunction. As a result of the intimate mixing, the interface where charge transfer can occur has increased enormously. The exciton, created after the absorption of light, has to diffuse towards this charge-transfer interface for charge generation to occur. The diffusion length of the exciton in organic materials, however, is typically 10 nm or less. This means that for efficient charge generation after absorption of light, each exciton has to find a donor acceptor interface within a few nm, otherwise it will be lost without charge generation. An intimate bi-continuous network of donor and acceptor materials in the nanometer range should suppress exciton loss prior to charge generation. Control of morphology is not only required for a large charge-generating interface

and suppression of exciton loss, but also to ensure percolation pathways for both electron and hole transport to the collecting electrodes.

3.8.4 State-of the-arts in bulk-heterojunction solar cells:

Various combinations of donor and acceptor materials have been used to build bulk heterojunction solar cells in which the composite active layer is inserted between two electrodes. One of the most promising combinations of materials is a blend of a semiconducting polymer as a donor and a fullerene, C_{60} derivative as acceptor. It is well established that at the interface of these materials a sub-picoseconds photo induced charge transfer occurs that ensures efficient charge generation.[68,25] Surprisingly, the lifetime of the resulting charge-separated state in these blends extends into the millisecond time domain.[43,101] This longevity allows the photo generated charge carriers to diffuse away from the interface (assisted by the internal electric field in the device) to be collected in an external circuit at the electrodes.

A breakthrough to truly appealing power conversion efficiencies exceeding 2.5% under simulated AM1.5 illumination was realized for bulk-heterojunction solar cells based on MDMO-PPV as a donor and PCBM as an acceptor (names and structures of these compounds are given in Figure 3.8).[85]

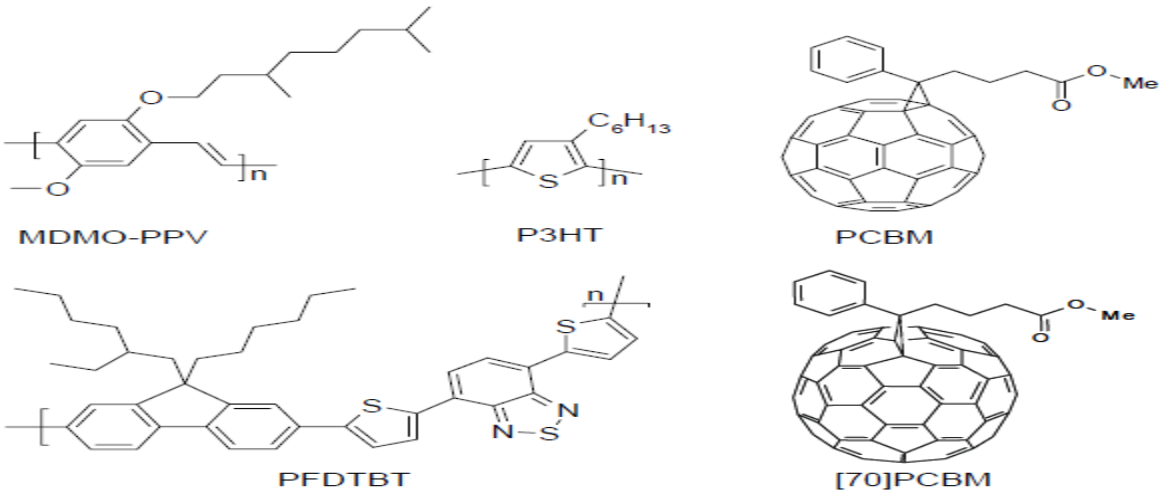

Figure3.8: Donor and acceptor materials used in polymer-fullerene bulk-heterojunction solar cells. Donors: MDMO-PPV = poly[2-methoxy-5-(3´,7´-dimethyloctyloxy)-p-phenylene vinylene]; P3HT= poly(3-hexylthiophene); PFDTBT: poly[2,7-[9-(2´-ethylhexyl)-9- hexylfluorene]-alt-5,5-(4´,7´-di-2 thienyl-2´,11´,3´-benzothiadiazole)]. Acceptors: PCBM: 3´-phenyl-3´H-

cyclopropa[1,9][5,6]fullerene C_{60}-I_h-3´-butanoic acid methyl ester; [70]PCBM: 3´-phenyl-3´H-cyclopropa[8,25][5,6]fullerene-C_{70}-D_{5h}(6)-3´-butanoic acid methyl ester.

In PCBM, the fullerene cage carries a substituent that prevents extensive crystallization upon mixing with the conjugated polymer and enhances the miscibility. In these 2.5%- efficient cells, the photoactive composite layer is sandwiched between two electrodes with different work functions: a transparent front electrode consisting of indium tin oxide covered with a conducting polymer polyethylenedioxythiophene:polystyrenesulfonate (PEDOT:PSS) for hole collection and a metal back electrode consisting of a very thin (~ 1 nm) layer of LiF covered with Al for electron collection. The layout of this device and a cross sectional transmission electron microscopy (TEM) image of an actual device slab are shown in Figure 3.9. Except for LiF, all layers are about 100 nm thick.

Although the combination MDMO-PPV and PCBM had been used several times before, the crucial step that improved the performance came from using a special solvent in the spin coating of the active layer that improves the nanoscale morphology for charge generation and transport.[85] Atomic force microscopy (AFM) and TEM studies have resolved the details of the phase separation in these blends.[48] In the best devices, which consist of a 1:4 blend (w/w) of MDMO-PPV/PCBM, nanoscale phase separation occurs in rather pure, nearly crystalline PCBM domains and an almost homogenous 1:1 mixture of MDMO-PPV and PCBM (Figure 3.9).

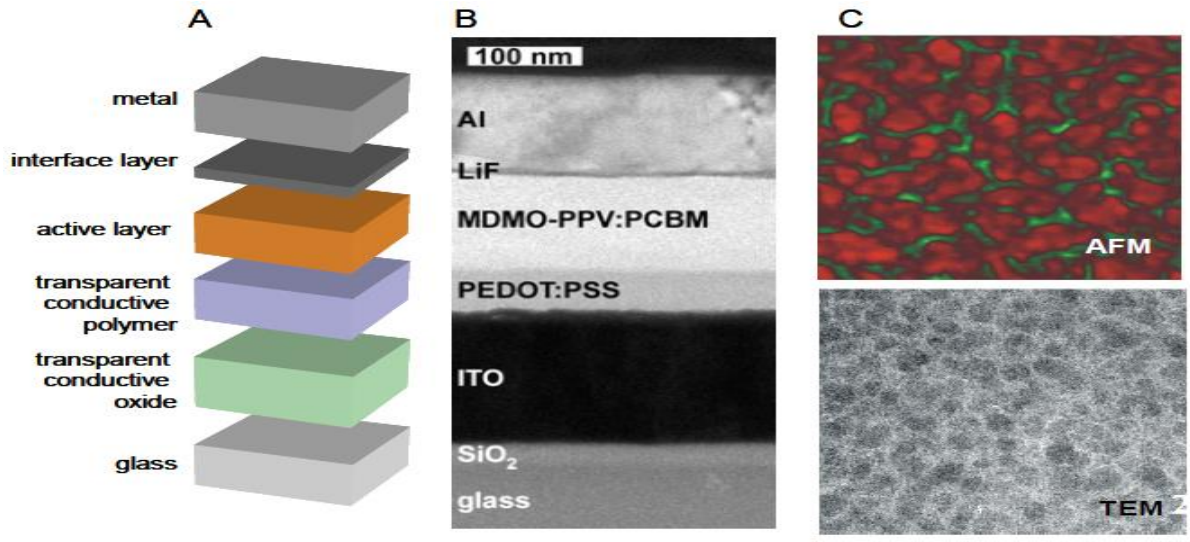

Figure 3.9: (a) Schematic layout of the device architecture of a polymer-fullerene bulk heterojunction solar cell. (b)TEM image of a thin slab of an actual device, showing the individual glass, ITO, PEDOT:PSS, MDMO-PPV/PCBM (1:4 by wt.), LiF, and Al layers. (c) AFM phase and TEM images (1 × 1 μm^2) of a MDMO-PPV/PCBM (1:4 by wt.) composite film showing phase separation into a PCBM (red in AFM, dark in TEM) and polymer-rich phase (green in AFM, light in TEM).

In recent years numerous studies have focused on a generating a deeper understanding of these MDMO-PPV/PCBM bulk heterojunctions. Investigations into the morphology, electronic structure, and charge transport have provided detailed understanding of the degree and dimensions of the phase separation in the active layer,[98] on the origin of the open-circuit voltage,[104,25] the influence of electrode materials,[104] and the magnitude of charge carrier mobilities for electrons and holes. These studies revealed that PCBM has high electron mobility compared to many other organic or polymer materials that can be deposited by spin coating. Photo physical studies have provided insights on charge generation, separation, and recombination in these layers, and more recently in working devices. These detailed insights have resulted in quantitative models describing the current voltage characteristics under illumination that serve as a guide for further development. The electrical current densities are mainly limited by incomplete utilization of the incident light due to a poor match of the absorption spectrum of the active layer with the solar emission spectrum, and low charge carrier mobilities of the organic or polymer semiconductors. In this respect, the use of P_3HT (Figure 3.8), which is known to have a high charge-carrier mobility and reduced band gap compared to MDMO-PPV, has been considered for use in solar cells in combination with PCBM. P3HT/PCBM blends indeed provide an increased performance compared to MDMO-PPV.[32,77] These higher efficiencies were obtained through the use of post-production treatment. After spin coating of the active layer and deposition of the aluminum top electrode, treating P_3HT/PCBM solar cells with a potential higher than the open circuit voltage and a temperature higher than the glass transition temperature led to an improved overall efficiency. This post-production treatment enhances the crystallinty of the P_3HT and improves the charge carrier mobility.

Photovoltaic devices of P_3HT/PCBM with external quantum efficiencies above 75% and power conversion efficiencies of up to 3.85% have been reached. Modification of the acceptor material has been considered also. In this respect it is important to note that PCBM–which may amount to as much as 75% of the weight of the photoactive layer–has a very low absorption coefficient in the visible region of the spectrum and, hence, provides a relatively small contribution to the photocurrent. The low absorption of C_{60} derivatives is due to their high degree of symmetry that makes many of the low energy transitions forbidden and hence of low intensity. When the C_{60} moiety is replaced by a less symmetrical fullerene, such as C_{70}, these transitions become allowed and a dramatic increase in light absorption can be expected. Consequently, when [70] PCBM (which is similar to PCBM but incorporates C_{70} instead of C_{60}) was used in combination with MDMO PPV instead of PCBM, the external quantum efficiency increased from ~50% to ~65% (Figure 3.10), while the current density of the solar cell increased by 50% and the power conversion efficiency to 3.0 %.[65]

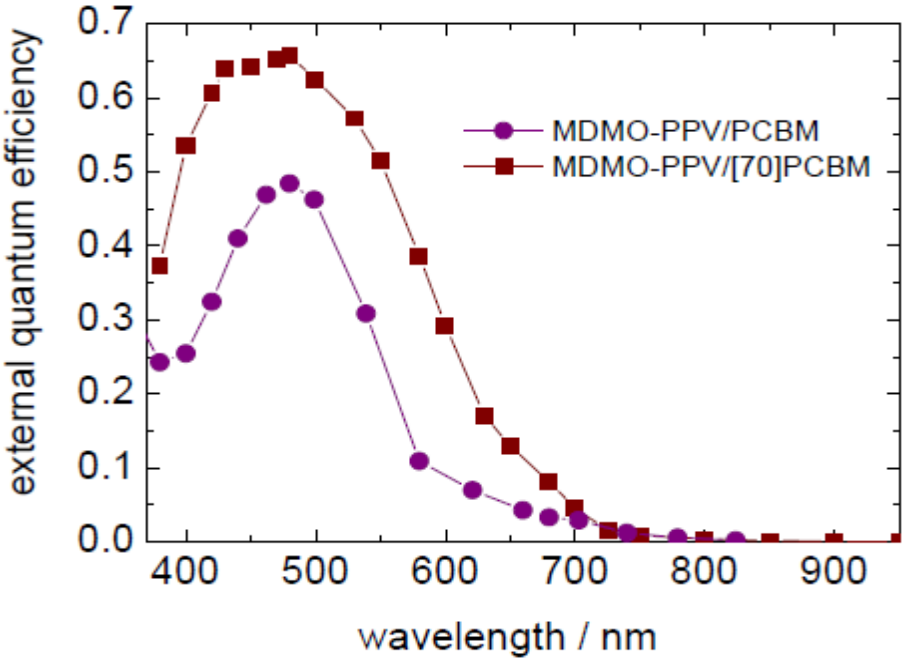

Figure 3.10: External quantum efficiency (EQE) of bulk-heterojunction solar cells with MDMOPPV/ PCBM (purple circles) and MDMO-PPV/ [70] PCBM (brown squares) active layers. The increased EQE of the layer with [70] PCBM compared to PCBM results from an increased absorption in the visible range of the spectrum.

3.9 Lifetimes of solar cells:

Of course any practical application of bulk-heterojunction polymer-fullerene solar cells requires that the cells be stable. Similar to the polymer light-emitting diodes, the present-day organic, polymer-based solar cells must be protected from ambient air to prevent degradation of the active layer and electrode materials by the effects of water and oxygen.

Even with proper protection there are several degradation processes that need to be eliminated to ensure stability. Apart from device integrity, the materials must be photo chemically stable and the nanoscale bicontinuous donor-acceptor in the active layer should preserved. A recent study revealed that MDMO-PPV/PCBM solar cells show an appreciable degradation under accelerated lifetime testing conditions (increased temperature). Interestingly, the degradation is not so much associated with the chemical stability.[93] At elevated temperatures, the PCBM molecules can diffuse through the MDMOPPV matrix and form large crystals, thereby increasing the dimension and extent of phase segregation.[107] This behavior has been observed for temperatures ~20°C below the glass transition temperature, *T*g ,of the polymer.

Fortunately, several strategies can be envisaged that may alleviate the limited thermal stability of the morphology. In general, high *T*g polymers will increase the stability of as prepared morphologies. An example has already been established for the combination of poly(3-hexylthiophene) and fullerene derivatives, where thermal annealing was used to improve the performance.

Upon cooling to operating temperatures, it may be expected that no further changes occur in the morphology. Another appealing method to preserve an as-prepared morphology in these blends is by chemical or radiation induced cross-linking, analogous to methods recently employed for polymer light-emitting diodes.[21] Finally, the use of *p-n* block copolymers seems an interesting option, because here phase separation will be dictated by the covalent bonds between the two blocks.[18] Nevertheless, creation of nanoscale bulk heterojunction morphologies that are stable in time and with temperature is one of the challenges that must be met before polymer photovoltaic's can be applied successfully.

In this respect it is important that testing of a novel semiconductor blend showed that all relevant device parameters changed less than 20% during 1000 hours of operation at 85ºC. This demonstrates that outstanding high stabilities are within reach.

3.10 Future directions for improving efficiencies:

New combinations of materials that are being developed in various laboratories focus on improving the three parameters that determine the energy conversion efficiency of a solar cell, *i.e.* the open-circuit voltage (*V*oc), the short-circuit current (*J*sc), and the fill factor that represents the curvature of the current density-voltage characteristic.

For ohmic contacts the open-circuit voltage of bulk-heterojunction polymer photovoltaic cells is governed by the energy levels of the highest occupied molecular orbital (HOMO) and the lowest unoccupied molecular orbital (LUMO) of donor and acceptor, respectively. In most polymer/fullerene solar cells, the positioning of these band levels of donor and acceptor is such that up to ~0.4–0.8 eV is lost in the electron-transfer reaction. By more careful positioning of these levels, it is possible to raise the open-circuit voltage well above 1 V. A very encouraging result in this respect is PFDTBT (Figure 2) that gives *V*oc = 1.04 V in combination with PCBM,[67] compared to 0.8–0.9 V for MDMO-PPV and 0.5–0.6 V for P_3HT.

The tradeoff of increasing the donor-HOMO to acceptor-LUMO energy is that eventually a situation will be reached in which the photo induced electron transfer is held back by a loss of energy gain.

One of the crucial parameters for increasing the photocurrent is the absorption of more photons. This may be achieved by increasing the layer thickness and by shifting the absorption spectrum of the active layer to longer wavelengths. Although the first improvement may seem trivial at first sight, an increase of the layer thickness is presently limited by the charge carrier mobility and lifetime. When the mobility is too low or the layer too thick, the transit time of photo generated charges in the device becomes longer than the lifetime, resulting in charge recombination.

The use of polymers such as P_3HT that are known to have high charge carrier mobilities allows an increase in film thickness from the usual ~100 nm to well above 500 nm, without a loss of current.

The absorption of the active layer in state-of-the-art devices currently spans the wavelength range from the UV up to about ~650 nm. In this wavelength range the monochromatic external quantum efficiency can be as high 70% under short-circuit conditions, implying that the vast majority of absorbed photons contribute to the current. The intensity of the solar spectrum, however, maximizes at ~700 nm and extends into the near infrared. Hence, a gain in efficiency can be expected when using low-band gap polymers. The preparation of low-band gap, high mobility, and process able low-band gap polymers is not trivial and requires judicious design in order to maintain the open-circuit voltage or efficiency of charge separation. Because the open-circuit voltage of bulk heterojunction solar cells is governed by the HOMO of the donor and the LUMO levels of the acceptor, the most promising strategy seems to lower the band gap by adjusting the other two levels, *i.e.* decrease the LUMO of the donor, or increase the HOMO of the acceptor, or both. Several groups are actively pursuing low-band gap polymers and the first, promising results are emerging.

A high fill factor (strongly curved *J-V* characteristic) is advantageous and indicates that fairly strong photocurrents can be extracted close to the open-circuit voltage. In this range, the internal field in the device that assists in charge separation and transport is fairly small. Consequently a high fill factor can be obtained when the charge mobility of both charges is high. Presently the fill factor is limited to about 60% in the best devices, but values up to 70% have been achieved recently.[7]

Apart from developing improved materials, a further gain in device performance can be expected from the combined optimization of the optical field distribution present in the device. Optical effects, such as interference of light in multilayer cavities, have received only limited attention so far but will likely contribute to a better light-management in these devices.

CHAPTER FOUR

LITERATURE REVIEWS

PREVIOUS STUDIES IN POLYMER CELLS AND THE MECHANSIM OF POLYMER CELLS

4.1 Introduction:

The chapter is divided into two sections. One presents the previous studies in polymer solar cells and second one presenting the mechanism of polymer cells and the way of comparing them.

4.2 Previous Studies in Polymer Solar Cells

Studies and researches in the field of polymer solar cells competed in order to access lower-cost production and to obtain the highest efficiency solar cell. Some of these studies used different dyes beside polymer.

In this section we will address some of these studies and compare the results that have been reached with the results that we have acquired in this search.

4.2.1 Charge transport in TiO_2/MEH-PPV polymer photovoltaics

A. J. Breeze, Z. Schlesinger, and S. A. Carter*
Physics Department, University of California, Santa Cruz, California 95064
P. J. Brock
IBM Almaden Research Center, San Jose, California
~Received 5 June 2000; revised manuscript received 28 November 2000; published 10 September 2001!

We study the effect of polymer thickness, hole mobility, and morphology on the device properties of polymer-based photovoltaics consisting of MEH-PPV as the optically active layer, TiO_2 as the exciton dissociation surface, and ITO and Au electrodes. We demonstrate that the conversion efficiency in these polymerbased photovoltaics is primarily limited by the short exciton diffusion length combined

with low carrier mobility. For MEH-PPV devices with optimal device geometry, we achieve quantum efficiencies of 6% at the maximum absorption of the polymer, open circuit voltages of 1.1 V, current densities of 0.4 mA/cm^2 and rectification ratios greater than 105 under 100 mW/cm^2 white light illumination. In addition, we achieve fill factors up to 42% at high light intensities and as high as 69% at low light intensities. We conclude by presenting a model that describes charge transport in solid-state polymer/TiO_2-based photovoltaics and suggest methods for improving energy conversion efficiencies in polymer-based photovoltaics.

4. 2.2 Conjugated Polymer Photovoltaic Cells

Kevin M. Coakley and Michael D. McGehee*
Department of Materials Science and Engineering, Stanford University, 476 Lomita Mall,
Stanford, California 94305-4045
Received March 2, 2004. Revised Manuscript Received June 29, 2004

Conjugated polymers are attractive semiconductors for photovoltaic cells because they are strong absorbers and can be deposited on flexible substrates at low cost. Cells made with a single polymer and two electrodes tend to be inefficient because the photogenerated excitons are usually not split by the built-in electric field, which arises from differences in the electrode work functions. The efficiency can be increased by splitting the excitons at an interface between two semiconductors with offset energy levels. Power conversion efficiencies of almost 4% have been achieved by blending polymers with electron-accepting materials such as C_{60} derivatives, cadmium selenide, and titanium dioxide. We predict that efficiencies higher than 10% can be achieved by optimizing the cell's architecture to promote efficient exciton splitting and charge transport and by reducing the band gap of the polymer so that a larger fraction of the solar spectrum can be absorbed.

4.2.3 Efficient polymer-based interpenetrated network photovoltaic cells

Salima Alem, Remi de Bettignies, and Jean-Michel Nunzia)
Equipe de Recherche Technologique Cellules Solaires Photovoltaı¨ques Plastiques and Proprie´te´s Optiques
des Mate´riaux et Applications, Laboratoire Associe´ au Centre National de la Recherche Scientifique 6136, Universite´ d'Angers, 49045 Angers, France
Michel Cariou
Equipe de Recherche Technologique Cellules Solaires Photovoltaı¨ques Plastiques and Inge´nierie Mole´culaire et Mate´riaux Organiques, Laboratoire Associe´ au Centre National de la Recherche Scientifique 6501 , Universite´ d'Angers, 49045 Angers, France
~Received 5 September 2003; accepted 15 January 2004!

Organic solar cells based on an interpenetrated network of conjugated polymer as donor and fullerene derivative as acceptor materials have a great potential for improving efficiency. We fabricated a device based on a composite of poly(2-methoxy-5-(28-ethylhexyloxy)-1, 4-phenylenevinylene and [6,6]-phenyl C_{60} butyric acid methyl ester. Surface treatment, insertion of interfacial layers, and improvement of the morphology of the active layer significantly increase the photovoltaic performances of the structure. We obtain an open circuit voltage of 0.87 V and short circuit current density of 8.4 mA/cm^2 under 100 mW/cm^2 air-mass 1.5 solar simulator illumination, yielding a 2.9% power conversion efficiency.

4.2.4 Lead Sulphide Nanocrystal: Conducting Polymer Solar Cells

Andrew A. R. Watt*, David Blake, Jamie H. Warner, Elizabeth A. Thomsen, Eric L. Tavenner, Halina Rubinsztein-Dunlop & Paul Meredith.
Soft Condensed Matter Physics Group and Centre for Biophotonics and Laser Science, School of Physical Sciences, University of Queensland, Brisbane, QLD 4072 Australia [2005]

In this paper we report photovoltaic devices fabricated from PbS nanocrystals and the conducting polymer poly (2-methoxy-5-(2'-ethyl-hexyloxy)-p-phenylene vinylene (MEH-PPV). This composite material was produced via a new single-pot synthesis which solves many of the issues associated with existing methods. Our devices have white light power conversion efficiencies under AM1.5 illumination of 0.7% and single wavelength conversion efficiencies of 1.1%. Additionally, they exhibit remarkably good ideality factors (n=1.15). Our measurements show that these composites have significant potential as soft optoelectronic materials.

4.2.5 Improved morphology of polymer-fullerene photovoltaic devices with thermally induced concentration gradients

M. Dreesa!
Department of Physics, Virginia Tech, Blacksburg, Virginia 24061
R. M. Davis
Department of Chemical Engineering, Virginia Tech, Blacksburg, Virginia 24061
J. R. Heflinb!
Department of Physics, Virginia Tech, Blacksburg, Virginia 24061
Received 22 July 2004; accepted 9 November 2004; published online 11 January 2005

Gradient concentration profiles for efficient charge transfer and transport can be created in polymer-fullerene organic photovoltaics by thermally induced inter

diffusion of an initial bilayer. Prior demonstrations with poly [2 methoxy-5-(2-ethylhexyloxy)-1,4-phenylenevinylene] [MEH-PPV] and C_{60} have been limited by the low miscibility of the two component materials. The morphology of the inter diffused films and resultant photovoltaic efficiency are improved by the use of the more miscible electron donor/electron acceptor pair of poly (3-octylthiophene) and C_{60}. The resultant concentration gradient profile is demonstrated by Auger spectroscopy and ion-beam milling. Increases in the short-circuit currents and fill factors relative to inter diffused MEH -PPV/C_{60} devices lead to monochromatic power conversion efficiencies of 1.5% at 470 nm.

4.2.6 Single-molecule imaging and spectroscopy of the π-conjugated polymer MEH-PPV

Oleg Mirzov
Licentiate thesis, Lund University [2006]

This licentiate thesis is intended to give a short introduction into the field of single molecule spectroscopy of π-conjugated polymers (Chapter 1) and to present a part of the work done by the author (in collaboration with other researchers) in this area. In this work single-molecule imaging and spectroscopy techniques, whose experimental implementation is described in (Chapter 2), were used to study the π-conjugated polymer MEH-PPV. The spectroscopy technique was used to establish a "bridge" between single-molecule and "bulk" spectroscopy by investigating a range of samples with different concentrations of MEH-PPV: from films to single chains (Chapter 3). Single-molecule imaging was employed to study fluorescence intensity distributions of single MEH-PPV chains, thereby addressing the problem of a single-molecule quantum yield (Article I).

4.2. 7 Polymer solar cells

Jacob Lund Rasmus Røge Ren´e Petersen Tom Larsen
1st June 2006

As mentioned in Section 6.2 only five functional polymer solar cells were produced. When comparing solar cell A with solar cell B and C (Figure 6.4 and Figure 6.5) it can be seen that V_{OC} is highest for solar cell B and C. V_{OC} for A, B, and C is 0.47, 0.87, and 1.05 V respectively. The increased voltages are probably caused by the introduction of the PEDOT: PSS layer, due to the difference in work function between ITO and PEDOT: PSS. The observed value of I_{SC} for the three

solar cells was 2.61, 6.41, and 7.44 μA/cm2 for A, B, and C. As it can be seen the current is more than doubled for solar cell B and C compared to A. This increase is probably a consequence of a better junction at the high work function electrode caused by the PEDOT: PSS layer and the increased open circuit voltages. When comparing the IV-curves from solar cell B and C, present in Figure 6.4 and Figure 6.5, there is a similar behavior between them. This similar behavior was expected since the two solar cells have been made using the same procedure. The active layer in solar cell D and E have been made from a solution where MEH-PPV and PCBM was dissolved in toluene and that might have had an impact on the active layer. When comparing D and E with A is it clear that ISC was increased significantly. I_{SC} was increased from 2.61 74 7.3. CALCULATIONS μA/cm2 for solar cell A to 8.23 and 28.7 μA/cm2 for solar cell D and E. This increase may indicate that MEH-PPV and PCBM are dissolved more homogeneously in toluene than in THF. The concentration difference in the two solutions used in solar cell D and E is probably the reason why I_{SC} is highest in solar cell E. Since the high concentration of MEH-PPV: PCBM will give a better absorbing layer and thereby increasing the amount of produced charges. Both layers were spin coated at 750 rpm. V_{OC} is almost the same for solar cell A and D, 0.47 and 0.415 V, as expected since no improvements have been made at any of the electrodes. V_{OC} of solar cell E is the highest measured for all the polymer solar cells, 1.1 V. This high V_{OC} is unexpected since no improvements have been made in order to increase the built-in potential difference. The origin for this high V_{OC} could be an exceptional high work function of the ITO layer. The dark IV-curves from the polymer solar cells are presented in Figure 6.6 and Figure 6.7. As it can be seen the dark IV-curve for solar cell D differs from the rest. The reason for this can be that the dark IV-curves were not measured in absolute darkness and that might have affected the measurement. The rest of the dark IV-curves show low values of voltages and currents as expected.

4 .2. 8 A strong regioregularity effect in self-organizing conjugated polymer films and high-efficiency polythiophene:fullerene solar cells

YOUNGKYOO KIM[1]*, STEFFAN COOK[2], SACHETAN M. TULADHAR[1], STELIOS A. CHOULIS[1], JENNY NELSON[1]*, JAMES R. DURRANT[2], DONAL D. C. BRADLEY[1]*, MARK GILES[3], IAIN MCCULLOCH[3],

CHANG-SIK HA[4] AND MOONHOR REE[5]
[1]Department of Physics, Blackett Laboratory, Imperial College London, London SW7 2BW, UK
[2]Department of Chemistry, Imperial College London, London SW7 2AZ, UK
[3]Merck Chemicals, Chilworth Science Park, Southampton SO16 7QD, UK
[4]Department of Polymer Science and Engineering, Pusan National University, Pusan 609-735, South Korea
[5]Department of Chemistry & Pohang Accelerator Laboratory, Pohang University of Science and Technology, Pohang 790-784, South Korea
*e-mail: y.kim@ic.ac.uk; jenny.nelson@imperial.ac.uk; d.bradley@imperial.ac.uk Published online: 5 February 2006

The devices with P3HT: PCBM (1:1) blend films (approximately 200 nm thick): symbol and line colours are as in Fig. 2. Solar-cell characteristics are summarized as follows: for not-annealed device with 95.2% RR P3HT, J_{SC} =7.26 mA cm^{-2}, open circuit voltage V_{OC} =0.56 V, fill factor FF=43.9%, PCE=2.1%; for annealed device with 95.2% RR, J_{SC} =7.28 mA cm^{-2}, V_{OC} =0.57V , FF=49.7%, PCE=2.4%; for not-annealed device with 93% RR, J_{SC} =5.1 mA cm^{-2}, V_{OC} =0.57 V, FF=37.8%, PCE=1.3%; for annealed device with 93% RR, J_{SC} =6.28 mA cm^{-2}, V_{OC} =0.6 V, FF=39.4%, PCE=1.8%; for not-annealed device with 90.7% RR, J_{SC} =3.27 mA cm^{-2}, V_{OC} =0.62 V, FF=37.0%, PCE=0.9%; for annealed device with 90.7% RR, J_{SC} =3.07 mA cm^{-2}, V_{OC} =0.61 V, FF=32.1%, PCE=0.7%. **c**,**d**, Dark *J*–*V* characteristics of not-annealed devices with pristine P3HT films (**c**) and P3HT:PCBM (1:1) blend films (**d**). **e**,**f**, Hole (**e**) and electron (**f**) mobilities (TOF) of P3HT:PCBM (1.2:1) blend films (approximately 1–2 μm thick) as a function of the square-rooted electric field (*E*1/2): black squares, red circles and blue triangles, which were excited at 355 nm, denote the blend films prepared with 95.2%, 93% and 90.7% RR P3HT. **g**,**h**, Normalized _OD transients (**g**, line colours as in Fig. 2) of not-annealed (NAN) and annealed (AN) blend films (approximately 200 nm thick), and resulting slope (α) changes with respect to RR (**h**, hatched bar for not-annealed; grey bar for annealed blend films).

4.2.9 Efficiency enhancement in low-bandgap polymer solar cells by processing with alkane dithiols

J. PEET, J. Y. KIM, N. E. COATES, W. L. MA, D. MOSES, A. J. HEEGER* AND G. C. BAZAN*
Center for Polymers and Organic Solids, University of California at Santa Barbara, Santa Barbara, California 93106, USA
*e-mail: ajhe@physics.ucsb.edu; Bazan@chem.ucsb.edu
Published online: 27 May 2007; doi:10.1038/nmat1928

Device optimization involved over 1,000 devices made from over 250 independently prepared PCPDTBT:C_{71}-PCBM films; optimum photovoltaic efficiencies of between 5.2% and 5.8% were obtained. The most efficient devices comprised a polymer/fullerene ratio of between 1:2 and 1:3, a spin speed of

between 1,200 and 1,600 r.p.m., a polymer concentration of between 0.8 and 1% by weight and a 1,8-octanedithiol concentration of between 17.5 and 25 mg ml−1. The most repeatable series of high-efficiency devices had an average power-conversion efficiency of 5.5% under 100mWcm−2, with short-circuit current I_{sc} = 16.2mAcm−2, FF = 0.55 and open circuit voltage V_{oc} = 0.62 V. More than 40 devices gave efficiencies of over 5.2%. Nevertheless, as implied by the measured FF=0.55, there are significant improvements to be made that could lead to more efficient solar-energy conversion.

4.2.10 Efficient Conjugated-Polymer Optoelectronic Devices Fabricated by Thin-Film Transfer-Printing Technique

By Keng-Hoong Yim, Zijian Zheng, Ziqi Liang, Richard H. Friend, Wilhelm T. S. Huck,* and Ji-Seon Kim*

As the P3HT thickness was gradually increased to 40 nm and 70 nm, the short-circuit photocurrent spectrum approached the absorption spectrum of P3HT, and the maximum EQE increased to 32% and 45%, respectively. Under AM 1.5 illumination, the short-circuit current of these devices also increased from 3.1mAcm^{-2} to 3.8mAcm^{-2} then 7.6mAcm^{-2} with increasing P3HT film thickness (Fig. 3c), as expected from the EQE spectra. The maximum power-conversion efficiency of 1.7% with a fill factor of 40% was achieved for the 70 nm/70 nm bilayer device. When the thickness of P3HT layer was kept constant at 70 nm, the EQE gradually dropped to 32% and 23% with decreasing PCBM film thickness. The photocurrent-action spectra show only slight blue shifts with respect to the absorption band of P3HT, indicating that the main contribution to photocurrent comes from the P3HT layer, rather than the PCBM layer that is directly next to the metal electrode. Considering that the light intensity is virtually zero near the aluminum electrode, we attribute the decrease of EQE to reduced photogeneration of charge carriers, as the distance between the polymer-polymer heterojunction (charge dissociation zone) and electrode decreases with decreasing PCBM thickness. Under AM 1.5 illumination (Fig. 3c), the short-circuit current rapidly dropped to 2.7mAcm^{-2} and 2.4mAcm^{-2} when the PCBM thickness was reduced to 50 nm and 20 nm, respectively. We consider the imbalance of charge-carrier

mobilities in the P3HT and PCBM layers important for such a rapid decrease in the short-circuit current under high-intensity illumination (100 mW cm^{-2}).

4.2. 11 Polymer–Fullerene Composite Solar Cells

Barry C. Thompson and Jean M. J.Fr_chet*

Fossil fuel alternatives, such as solar energy, are moving to the forefront in a variety of research fields. Polymer-based organic photovoltaic systems hold the promise for a cost-effective, lightweight solar energy conversion platform, which could benefit from simple solution processing of the active layer. The function of such excitonic solar cells is based on photoinduced electron transfer from a donor to an acceptor. Fullerenes have become the ubiquitous acceptors because of their high electron affinity and ability to transport charge effectively. The most effective solar cells have been made from bicontinuous polymer–fullerene composites, or so-called bulk heterojunctions. The best solar cells currently achieve an efficiency of about 5%, thus significant advances in the fundamental understanding of the complex interplay between the active layer morphology and electronic properties are required if this technology is to find viable application.

4.2.12 Polymer solar cell by blade coating

Yu-Han Chang a, Shin-Rong Tseng a, Chun-Yu Chen a, Hsin-Fei Meng a,*, En-Chen Chen b,
Sheng-Fu Horng b, Chian-Shu Hsu c
Institute of Physics, National Chiao Tung University, Hsinchu 300, Taiwan, Republic of China
Department of Electrical Engineering, National Tsing Hua University, Hsinchu 300, Taiwan, Republic of China
Department of Applied Chemistry, National Chiao Tung University, Hsinchu 300, Taiwan, Republic of China [2009]

The result of the device with the bladed PEDOT: PSS and blade and spin coated P3HT: PCBM layer is also shown in Fig. 3a. The efficiency of device G is 2.5% with J_{sc} of 8.35 mA/cm^2, V_{oc} of 0.59 V, and fill factor of 52%. The relative low performance of device G results from the thick PEDOT: PSS film (120 nm), which causes high series resistance. Two devices are made by conventional high boiling points solvents chlorobenzene (device E) and dichlorobenzene (device F). Fig. 3b shows the results of the devices by the fast-drying blade and spin process with different solvents. There is no slow solvent evaporation in the fabrication process. The power conversion efficiencies are 2.5% in the device from chlorobenzene solution (device E) and 3.5% in that from dichlorobenzene solution (device F). The Jsc are both about 8.8 mA/cm^2, which is significantly smaller than

Jsc of 11.4 mA/cm^2 in device D from toluene. Interestingly high boiling point solvents give higher J_{sc} for spin coating but smaller J_{sc} for blade coating. There are probably more P3HT/PCBM interfaces in toluene solution than those in chlorobenzene and dichlorobenzene solutions, resulting in more efficient exciton dissociation.

4.2. 13 Dye-Sensitized Solar Cells with Nanotechnologies

Liyuan Han
Advanced Photovoltaics Center（NIMS) [2009]

The I-V curve of the DSC was independently measured by the public test center (AIST JAPAN) and the result of the device are J_{sc} : 18.9 mA/cm^2 J_{sc} : 20.9 mA/cm^2 V_{oc} : 0.693 V, V_{oc} : 0.73 V, FF : 0.686, F.F. : 0.72 and the efficiency of DSC > 11% in small cell.

4.2. 14 Highly Efficient Tandem Polymer Photovoltaic Cells

By Srinivas Sista, Mi-Hyae Park, Ziruo Hong,* Yue Wu, Jianhui Hou, Wei Lek Kwan, Gang Li, and Yang Yang*

Dr. Z. Hong, Prof. Y. Yang, S. Sista, M.-H. Park, Dr. Y. Wu, Dr. J. Hou, W. L. Kwan
Department of Materials Science and Engineering
University of California Los Angeles
Los Angeles, CA 90095 (USA)
E-mail: zrhong@ucla.edu; yangy@ucla.edu
Dr. Y. Wu, Dr. J. Hou, Dr. G. Li
Solarmer Energy, Inc.
El Monte, CA 91731 (USA) [2010]

The current density versus voltage (J–V) characteristics of the tandem and reference single cells were taken under AM1.5G 100mW cm^{-2} illumination as shown in Figure 2a and photovoltaic parameters are listed in Table 1. The tandem cell yields a PCE of 5.84% with a V_{oc} of 1.25 V. From P3HT: PC70BM BHJs with a thickness of 150nm PCE of 3.77% is obtained with a J_{sc} of 9.27mA cm^{-2}. The low-bandgap PSBTBT: PC70BM BHJ with a thickness of 100nm exhibits a Jsc of 10.71mA cm^{-2} and a PCE of 3.94%. In this case, the rear subcell becomes the photocurrent-limiting cell, giving a low FF of 55% for tandem cells.[23] After scratching, the front cell limits the overall photocurrent, resulting in a FF higher than 60%. According to our observation, extra care over efficiency estimation has to be taken when using highly conductive materials in the interlayer. In summary, we demonstrate an efficient photovoltaic cell with a tandem structure. Mechanism studies indicate that a metal. Semiconductor contact between the conductive

polymer and the semiconducting metal oxide, which connects individual subcells in a series, works effectively as an interlayer. It is worth emphasizing that the front cell with a larger bandgap should offer higher V_{oc} to explore the full potential of the tandem cells.[24] In this sense, P3HT is used mainly to demonstrate the concept, rather than efficiency improvement, because large bandgap of P3HToffers a mediocre V_{oc} of 0.6 V. With a suitable combination of donor–acceptor systems, which are able to deliver higher V_{oc} from the front cell[25] and all other parameters remaining the same as for P3HT, the PCE of tandem cells can be significantly improved.

4.2. 15 Increasing Polymer Solar Cell Efficiency with Triangular Silver Gratings

Aimi Abass, Honghui Shen, Peter Bienstman, Bjorn Maes
Photonics Research Group, Ghent University – imec, Department of Information Technology, St.-Pietersnieuwstraat 41, 9000 Ghent, Belgium
aimi.abass@ugent.be [2010]

Figure 1(b) shows an example of enhancement in the absorption spectrum that can be achieved by the introduction of a triangular grating (grating periodicity 400nm, fill factor 0.5 and triangle height 120nm). The peak at 640nm (for TM) is due to excitation of a plasmonic mode. The plot of the field profile at this wavelength is shown in figure 1(c). The field is distributed mostly in the polymer, leading to a huge enhancement at this wavelength. The integrated absorption efficiency for a planar unpatterned structure is 48% while for a patterned structure it is 63.6% for TM polarization and 56% for the TE Polarization. The absorption enhancement for the TE polarization is due to scattering by the grating profile. The geometric parameters of the grating were optimized to obtain a large integrated absorption efficiency, but also to have a significant enhancement at the **a1005_1.pdf** OSA / PV 2010 **PWA5.pdf** absorption edge of the active layer. Therefore we aimed for resonances in the wavelength range of 600 to 650nm. A recent publication indicated that the internal quantum efficiency of P3HT: PCBM is still around 70% in this range [4].

4.2. 16 Mobility and photovoltaic performance studies on polymer blends: effects of side chains volume fraction

Getachew Adam,[ab] Almantas Pivrikas,[a] Alberto M. Ramil,[a] Sisay Tadesse,[ab] Teketel Yohannes,[b] Niyazi S. Sariciftci[a] and Daniel A. M. Egbe*[a]
Received 13th August 2010, Accepted 4th November 2010

The current–voltage (I–V) characteristics of the solar cells are given in Fig. 3. Statistical studies were also made in order to ensure the reproducibility of results and the characteristic average values of these solar cells made are shown in Table 1.The IV characteristics of the solar cells in Fig. 3 reveal a dark rectification ratio of approximately 103 at 2 V. The solar cells made from D2: PCBM (1 : 3) showed an average open circuit voltage (V_{OC}) value of 735 mV and that of D1 : PCBM (1 : 3) showed 842 mV. The average V_{OC} of the ternary blend of 860 mV in contrast is higher than that of the respective binary systems. It is reported that V_{OC} is a function of the HOMO of the polymer and that of the LUMO of the acceptor,1b,9 so this result shows that by mixing two polymers of the same backbone but with different side chain volume fraction, the open circuit voltage can be improved.38 When we compare the solar cells made from the individual polymers with PCBM, D2 : PCBM showed an average short circuit current density (JSC) of 4.9 mA cm^{-2} which is higher than that of D1 : PCBM which showed an average 4.5 mA cm^{-2}. This trend is consistent with the photoluminescence (PL) spectra of the blends where D2 : PCBM showed the strongest PL quenching due to more efficient photo-induced electron transfer to the acceptor PCBM as compared to D1 : PCBM. The highest average JSC of 5.7 mA cm^{-2} obtained for the ternary blend is due to its better active layer nanomorphology than the binary blends. The fill factor FF values observed for the ternary blend (40%) are very close to the highest average value of 41% obtained for D1 : PCBM binary system.

4.2. 17 π-Conjugated Polymers for Organic Electronics and Photovoltaic Cell Applications

Antonio Facchetti*
Polyera Corporation, 8045 Lamon Avenue, Skokie, Illinois 60077, United States, and Department of Chemistry and the Materials Research Center, Northwestern University, 2145 Sheridan Road, Evanston, Illinois 60208-3113, United States
Received August 23, 2010. Revised Manuscript Received November 21, 2010

OPV cell model consisting of P66 PC61BM cell (Figure 30) was fabricated with and without an organic interlayer. Marks et al. found that aTPDSi2TFB cross linked electron-blocking layer (EBL) chemisorbed between the active layer and the anode produces a record V_{oc} = 1.08 V for a materials system having a theoretical maximum V_{oc} ~ 1.2 V (Figure 30).[52,53] This interfacial layer substantially increases

PCE and thermal stability.107 In a different approach, the same group used NiO as an inorganic interlayer to fabricate P3HT-based cells. NiO is a transparent conducting p-type oxide, and considering the relevant energy levels for P3HT PC61BM cells indicates that a thin layer of NiO on the ITO anode could enhance hole extraction while blocking electron leakage to the anode. Both NiO and ITO are wide-band gap transparent conducting oxides to the P3HT-PCBM materials. The highest PCE reported at the time for optimized P3HT-PC61BM cells, using standard fabrication procedures, were ~4.0% efficiency.108 Using the same fabrication procedure, NU used a thin (5 -70 nm) NiO films grown on ITO anodes by PLD (pulsed laser deposition) and P3HT PC61BM cells fabricated on top of this anode. For optimum NiO thicknesses of 5-10 nm, the NU team achieved record cell power efficiencies of 5.2% (NREL measured 5.6%)109 Importantly, control experiments with n-type TCOs both at NU and elsewhere do not show this effect which is attributable, among other factors, to the good hole transport characteristics of NiO. Note that the greatest effect of the NiO layer was to increase the fill factor and V_{oc}.

4.2. 18 Development and Characterization of New Donor-Acceptor Conjugated Polymers and Fullerene Nanoparticles for High Performance Bulk Heterojunction Solar Cells

Kung-Hwa Wei
Institution: National Chiao Tung University, Department of Materials Science & Eng.;
University of Washington. Jan. [2011]

We have prepared a bithiophene/thieno[3,4-*c*]pyrrole-4,6-dione (TPD)–based donor acceptor polymer, **PBTTPD**, that exhibits high crystallinity and a low-lying highest occupied molecular orbital. An optimal device incorporating a **PBTTPD**/[6,6]-phenyl C_{61}-butyric acid methyl ester blend (1:1.5, w/w) displayed an open circuit voltage of 0.95 V and a power conversion efficiency of 4.7%. A novel molecular design concept was introduced to develop a series of new conjugated polymers with donor-π-bridge-acceptor side chains for high efficiency polymer solar cells. Different from the commonly used linear D-A conjugated polymers, the acceptor of the polymers are located at the end of the side chains and connected with the electron-rich unit on the main chain through a π-bridge. This

method provides a facile way to tune the bandgaps and energy levels of the polymers by simply varying the acceptors on the side chains. A systematic study was performed in this project to elucidate the relationship among molecular structure-morphology-device properties to explore the full potential of applying these new materials for OPV applications.

4.2. 19 Charge Carrier Mobility, Photovoltaic, and Electroluminescent Properties of Anthracene-Based Conjugated Polymers Bearing Randomly Distributed Side Chains

Ozlem Usluer,[1,2] Christian K€astner,[3] Mamatimin Abbas,[1,4] Christoph Ulbricht,[1] Vera Cimrova,[5] Andreas Wild,[6] Eckhard Birckner,[7] Nalan Tekin,[8] Niyazi Serdar Sariciftci,[1] Harald Hoppe,[3] Silke Rathgeber,[9] Daniel A. M. Egbe[1]

To investigate the photovoltaic performance of the polymers, solar cell devices were fabricated and tested. Figure 11 shows the I–V curves of the fabricated solar cells. In general, for the investigated AnE-PV: PCBM blends, high open-circuit voltages are expected. The highest V_{OC} (872 mV) has been achieved with AnE-PVstat4. As expected from the optical and AFM data, AnE-PVstat shows the best performance because of efficient charge generation and percolation. Its I–V curve exhibits the highest FF and current density. Only the open-circuit voltage is a little bit lower than the one of AnE-PVstat4. It is also obvious that the side-chain ratio has no distinct influence on the open-circuit voltage in case of linear and branched side chains. AnE PVstat, stat1, and stat2 exhibit very similar open-circuit voltage because of similar side-chain volume of linear and branched substitution. The altered side-chain distribution of AnE-PVstat1 and stat2 dramatically decreases the short-circuit current, FF, and efficiency compared to AnE-PVstat. The observed open circuit voltages for AnE-PVstat3, stat4, and stat5 are in accord with former results. The side-chain volume and the position of the side chains are reasonable for the value of the open-circuit voltage. Table 4 shows the complete set of photovoltaic parameters under AM1.5 illumination for the best solar cell device of each polymer: PCBM blend.

TABLE 4 Photovoltaic Parameters of the Solar Cells Build From Polymer:PCBM Blends (1:2 Weight Ratio)

AnE-PV	I_{sc} (mA cm^{-2})	V_{oc} (mV)	FF (%)	PCE (%)	R_s (Ω)	R_p (Ω)
-stat	6.27	828	58.42	3.03	14.6	1,929
-stat1	2.52	844	34.03	0.72	75.7	1,295
-stat2	2.93	844	35.67	0.88	89	1,120
-stat3	2.733	613	31	0.52	8.3	690
-stat4	4.628	872	40.89	1.65	15.3	1,091
-stat5	3.211	779	34.66	0.87	49.9	837

4.2. 20 Hybrid Silicon Nanocone−Polymer Solar Cells

Sangmoo Jeong,† Erik C. Garnett,‡ Shuang Wang,† Zongfu Yu,† Shanhui Fan,† Mark L. Brongersma,‡ Michael D. McGehee,*,‡ and Yi Cui*,‡,§
†Department of Electrical Engineering and ‡Department of Materials Science and Engineering, Stanford University, Stanford, California 94305, United States
§Stanford Institute for Materials and Energy Sciences, SLAC National Accelerator Laboratory, 2575 Sand Hill Road, Menlo Park, California 94025, United States [2012]

Recently, hybrid Si/organic solar cells have been studied for low-cost Si photovoltaic devices because the Schottky junction between the Si and organic material can be formed by solution processes at a low temperature. In this study, we demonstrate a hybrid solar cell composed of Si nanocones and conductive polymer. The optimal nanocone structure with an aspect ratio (height/diameter of a nanocone) less than two allowed for conformal polymer surface coverage via spin-coating while also providing both excellent antireflection and light trapping properties. The uniform heterojunction over the nanocones with enhanced light absorption resulted in a power conversion efficiency above 11%. Based on our simulation study, the optimal nanocone structures for a 10 μm thick Si solar cell can achieve a short-circuit current density, up to 39.1 mA/cm2, which is very close to the theoretical limit. With very thin material and inexpensive processing, hybrid Si nanocone/polymer solar cells are promising as an economically viable alternative energy solution.

4.3 The Mechanism of organic solar cells

In this section we will deal with the mechanism of organic solar cells and address some of the important factor to compare between solar cells.

4.3.1 Energy levels in organic semiconductors

The semiconducting properties of organic materials primarily originate from the delocalization of electrons in molecules with double bonds. In covalently bonded atoms, the shape of the electron orbitals around the atoms will be dependent on the atom and the number and type of bonds made with surrounding atoms. A

conjugated system is formed where carbon atoms covalently bond with alternating single and double bonds; in other words these are chemical reactions of hydrocarbons. These hydrocarbons' electrons pz orbitals delocalize and form a delocalized bonding π orbital with a π* antibonding orbital. The delocalized π orbital is the highest occupied molecular orbital (HOMO), and the π* orbital is the lowest unoccupied molecular orbital (LUMO). The voltage separation between HOMO and LUMO is considered the band gap of organic electronic materials. The band gap is typically in the range of 1–4 eV.[2]

The disorder of organic semiconductors significantly complicates the theoretical understanding of what is happening at a molecular level. Orientation of the molecules affects how the orbitals overlap. Geometry relaxations in different excited states change molecular shape and energy levels. Energy levels shift as more molecules are packed together. These, and many other considerations, all ultimately affect the charge transport properties in organic semiconductors and are not easily understood when dealing with systems involving billions of molecules. While advances continue to be made in understanding organic semiconductor processes at the molecular level, primarily considering the HOMO and LUMO levels gives a simplified framework that has worked well for visualizing a very complex system. However, considerations at the molecular level need to be considered more and more to keep advancing organic electronics.

4.3.2 Photocurrent generation

The absorption of a photon in an inorganic solar cell can promote an electron from the valence band into the conduction band and lead to a free electron-hole pair because the binding energy between the electron and hole is small and easily overcome by the thermal energy (kT) at room temperature. The low binding energy is largely the result of the high dielectric constant of the materials and the periodicity and rigidity that create in the band structure. However, geometry relaxation effects, lower dielectric constant and electron correlation, and stronger Coulomb attraction in organic materials lead to a bound electron-hole pair, called an exciton, when light (photon) is absorbed in an organic semiconductor an excited state is created and confined to a molecule or a region of a polymer chain. The

excited state can be regarded as an electron-hole pair bound together by electrostatic interactions, i.e. excitons. In photovoltaic cells, excitons are broken up into free electron-hole pairs by effective fields. The effective fields are set up by creating a heterojunction between two dissimilar materials. Effective fields break up excitons by causing the electron to fall from the conduction band of the absorber to the conduction band of the acceptor molecule. It is necessary that the acceptor material has a conduction band edge that is lower than that of the absorber material [5]

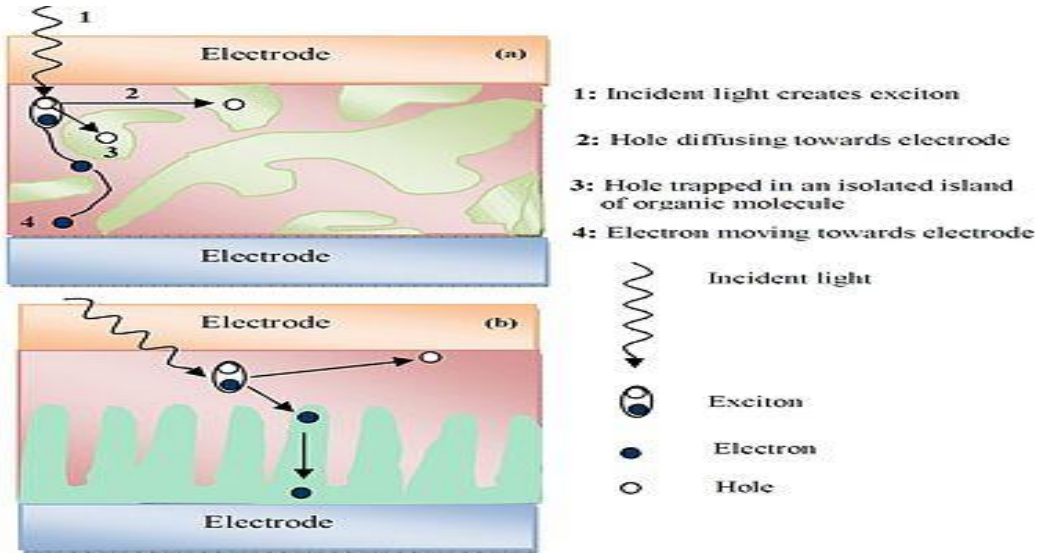

Figure 4.1. Show the creation of excitons in organic solar cell.

The excitons in organics, which typically have large binding energies on the order of 500 meV [106], must be dissociated into separate charges before they can contribute to photocurrent in an organic cell. This dissociation can be accomplished at the interface between an appropriately chosen electron donating material (donor) and an electron accepting material (acceptor) where it is energetically favorable for the exciton to dissociate with the electron in the acceptor and the hole in the donor. Figure 4.2(a) shows a simple energy-level diagram of this situation.

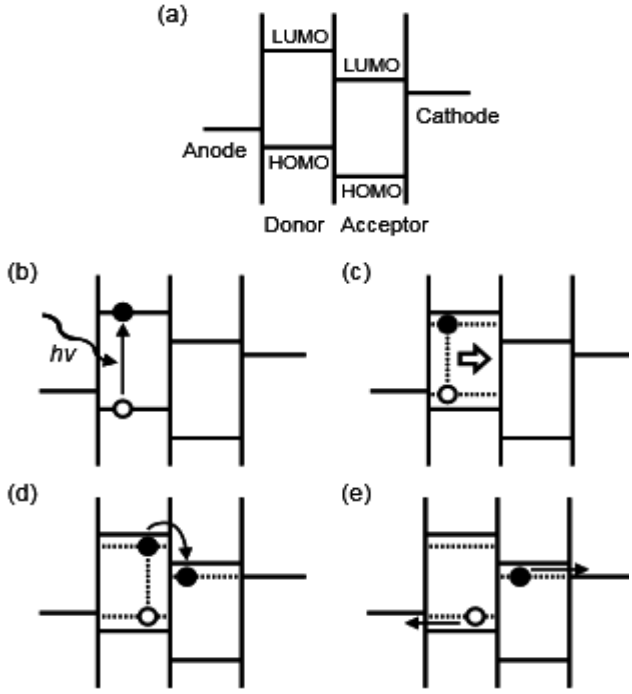

Figure 4.2. (a) Basic energy-level diagram for an organic solar cell. Based on the energy- level diagram, overview of the photocurrent generation process: (b) light absorption to create an exciton; (c) exciton diffusion to donor / acceptor interface; (d) exciton dissociation and charge separation; and (e) charge transport and collection at the electrodes.

Photocurrent generation in an organic solar cell generally occurs in four main steps (Figure 4.2). First, the absorption of a photon excites an electron from the HOMO of the organic material to create an exciton (Figure 4.2b). Next, the exciton must diffuse to the donor / acceptor interface to dissociate into charge carriers (Figure 4.2c). Because excitons have no net charge, their diffusion is generally treated as a random process based on concentration gradients without influence from electric fields [106]. However, excitons can recombine during the diffusion process before reaching the donor / acceptor interface, leading to absorbed photons that do not contribute to the current. The characteristic length an exciton travels before recombining is described by the exciton diffusion length. Exciton diffusion length affects device design because of the trade-off between light absorption and recombination as layer thickness is changed. Excitons that do reach the donor / acceptor interface can then dissociate into electrons and holes (Figure 4.2d). However, there is still no clear understanding of exactly how exciton dissociation occurs on a molecular level [106]. Generally, the process is described as the changing of the exciton state at the interface into a charge transfer state between an adjacent

donor and acceptor followed by either recombination or dissociation into a charge-separated state. While this is the most repeated description, the entire picture is most likely more complicated, involving processes such as the interaction of additional states, the possibility of energy transfer, and the formation of different types of excitons, with the ultimate outcome determined by the relative rates of all the interactions [106]. While the full story is still the subject of much research, it appears that the energy change in going from a bound electron-hole pair to a hole in the donor (with an energy roughly estimated by the ionization potential) and an electron in the acceptor (roughly estimated by the electron affinity) is what ultimately leads to free charges.

Finally, the charges are transported through the semiconductors and collected by their respective electrodes (Figure 4.2e). Unlike inorganic semiconductors, the charges in organic materials are generally more localized and travel through hopping processes. The different transport mechanisms lead to mobility values typically below 1 $cm^2V^{-1}s^{-1}$ that can have different dependences on temperature and electric field compared to in inorganic materials. Also, choice of electrode materials and modification of the contact between the electrodes and organic is another area undergoing active research that can significantly affect the ability to extract the generated charges.

4.3.2.1 Operation mode in dye sensitized polymer solar cells

In this project the cell consists of two metallic plates (ITO, Solder Sn/Pb). Above the lower plate a polymer layer is located, then a dye sensitized layer is formed, beside the ITO layer just below the upper plate. When the sun light is incident on the cell it well penetrated the upper transparent layer plate ITO. The incident photon on dye atoms gives electrons enough energy to be free while that incident on the polymer produces excitons in the form of electron-hole pairs. The exciton is formed since the energy of the photon is not sufficient to remove the electron from valence to conduction band (Eg > hf). The hole is located in the valence band whereas the electron is located on one of the levels (donor or acceptor) that exists in the forbidden band. The free electrons in the dye are highly

concentrated, thus electrons flow by diffusion to ITO layer then to the upper plate at which electrons are accumulated to form a negative electrode. On the other hand the excitons which are highly concentrated at the polymer moves by diffusion towards the dye positive ions layer. The dye ions have small energy band gap (Eg (dye) < E (excitons)). Thus it can attract easily the electrons from the excitons and leaving the holes at polymer layer. Thus charge separation takes place at the interface between dye and polymer layer. The holes have high concentration compared to that of the lower plate. The holes thus moves towards the lower plate to pick free electrons from it. As a result the lower plate (Sn/Pb) act as a positive electrode due to the accumulation of large amount of positive ions.

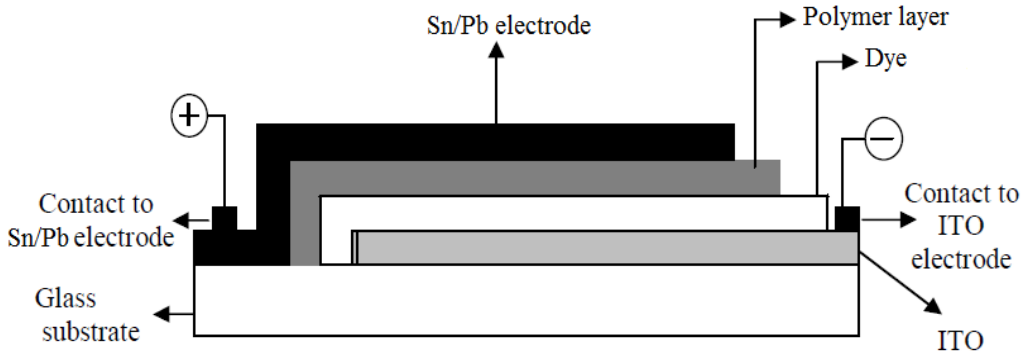

Figure 4.3. Show a designed cell used in this project.

4.3.3 Comparisons

In order to compare various solar cells it is necessary to measure the characteristic values: V_{oc}, I_{sc}, the fill factor and the efficiency η. All these factors can be determined from the IV characteristic of a solar cell.

4.3.3.1 IV curve:

The IV curve of a solar cell is the superposition of the IV curve of the solar cell diode in the dark with the light-generated current.[1] The light has the effect of shifting the IV curve down into the fourth quadrant where power can be extracted from the diode. Illuminating a cell adds to the normal "dark" currents in the diode. The equation for the IV curve in the first quadrant is:

$$I = I_L - I_0\left[\exp\left(\frac{qV}{nkT}\right) - 1\right] \qquad (4\text{-}1)$$

Where I_L = light generated current.

The -1 term in the above equation can usually be neglected. The exponential term is usually >> 1 except for voltages below 100 mV. Further, at low voltages the light generated current I_L dominates the I_0 (...) term so the -1 term is not needed under illumination.

$$I = I_L - I_0\left[\exp\left(\frac{qV}{nkT}\right)\right] \quad (4\text{-}2)$$

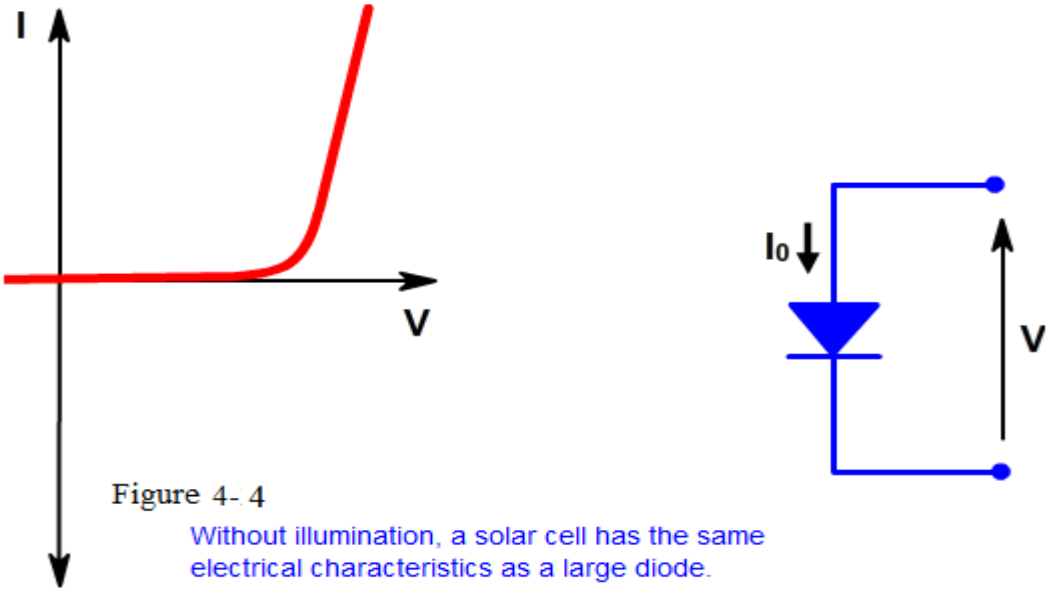

Figure 4- 4

Without illumination, a solar cell has the same electrical characteristics as a large diode.

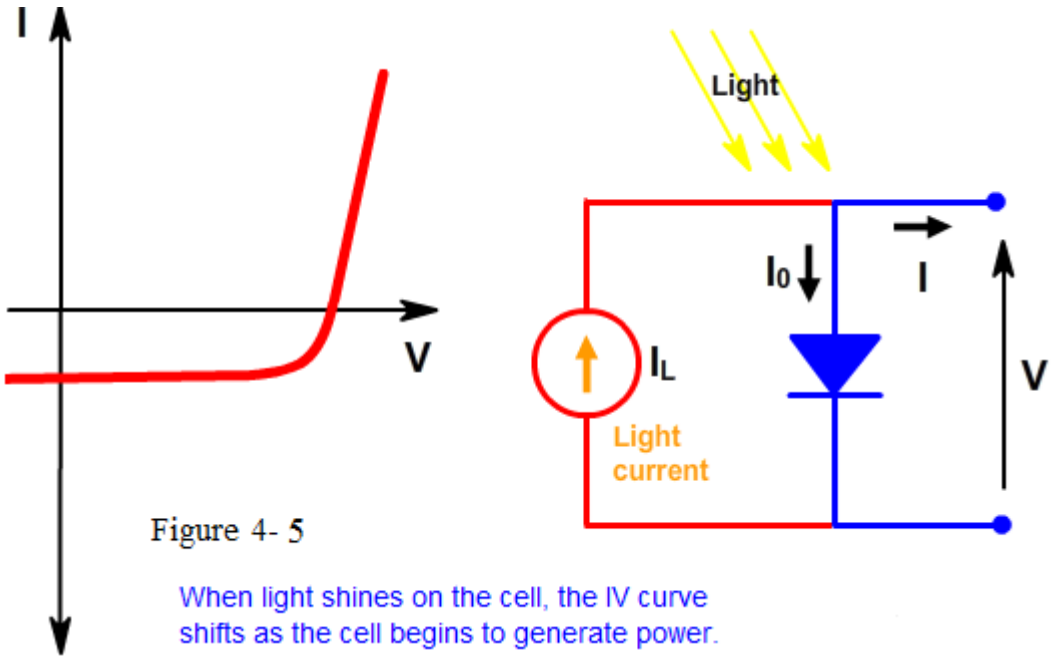

Figure 4- 5

When light shines on the cell, the IV curve shifts as the cell begins to generate power.

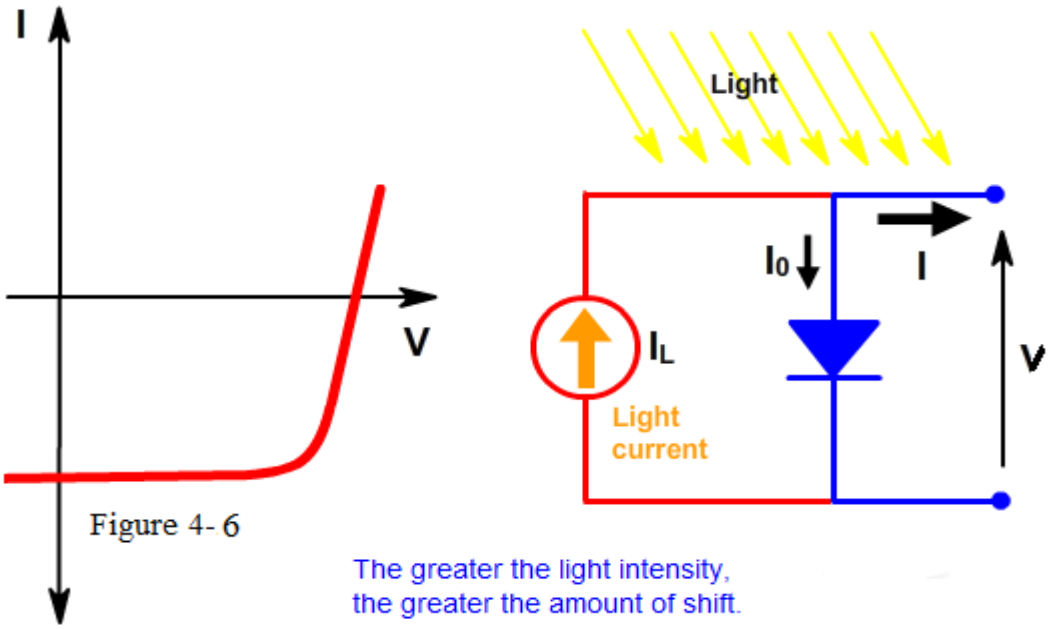

Figure 4- 6

The greater the light intensity, the greater the amount of shift.

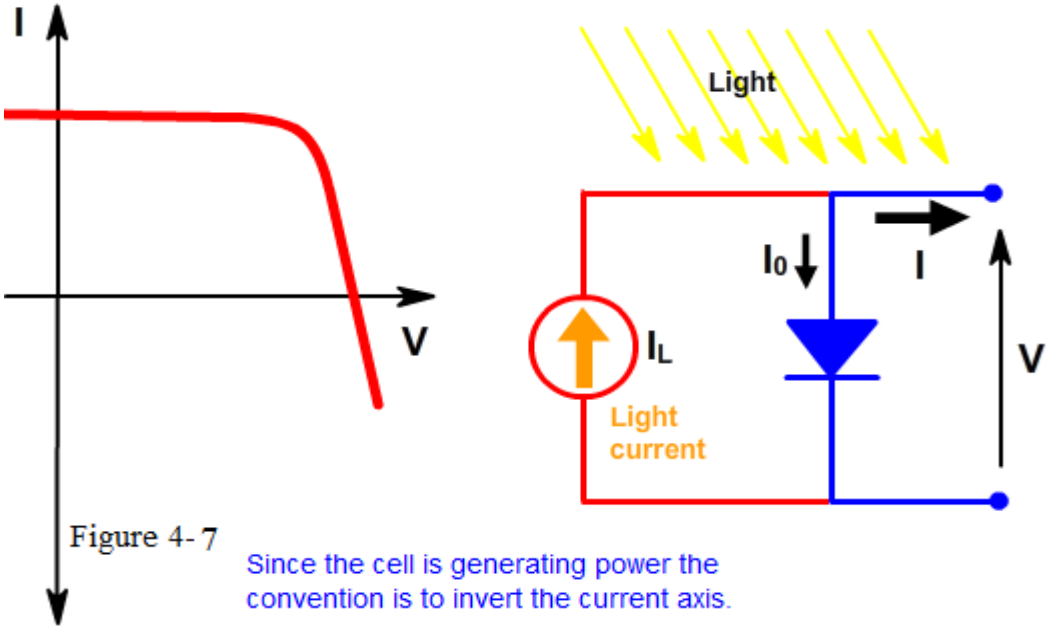

Figure 4- 7

Since the cell is generating power the convention is to invert the current axis.

Several important parameters which are used to characterize solar cells are discussed in the following pages. The short-circuit current (I_{SC}), the open-circuit voltage (V_{OC}), the fill factor (FF) and the efficiency are all parameters determined from the IV curve.

4.3.3.2 Short-circuit current:

The short-circuit current is the current through the solar cell when the voltage across the solar cell is zero (i.e., when the solar cell is short circuited). Usually written as I_{SC}, the short-circuit current is shown on the IV curve below.

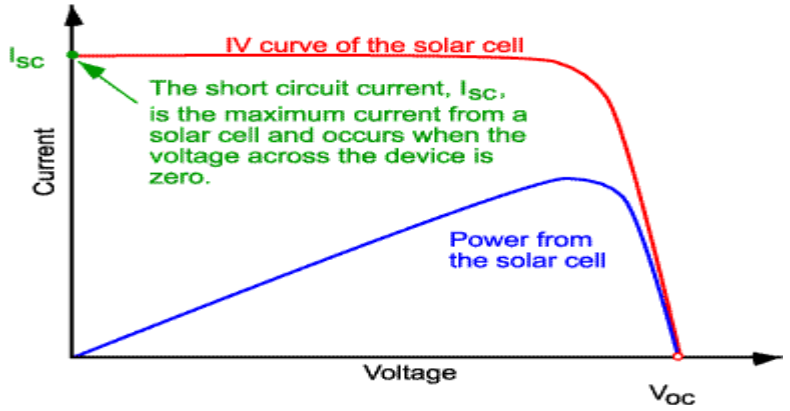

Figure 4-8: IV curve of a solar cell showing the short-circuit current.

The short-circuit current is due to the generation and collection of light-generated carriers. For an ideal solar cell at most moderate resistive loss mechanisms, the short-circuit current and the light-generated current are identical. Therefore, the short-circuit current is the largest current which may be drawn from the solar cell.

The short-circuit current depends on a number of factors which are described below:

1-The area of the solar cell: To remove the dependence of the solar cell area, it is more common to list the short-circuit current **density** (J_{sc} in mA/cm^2) rather than the short-circuit current.

2-The number of photons: (i.e., the power of the incident light source). I_{sc} from a solar cell is directly dependent on the light intensity.

3-The spectrum of the incident light: For most solar cell measurement, the spectrum is standardized to the AM1.5 spectrum.

4-The optical properties (absorption and reflection) of the solar cell

5-The collection probability: The collection probability of the solar cell, which depends chiefly on the surface passivation and the minority carrier lifetime in the base.

When comparing solar cells of the same material type, the most critical material parameter is the diffusion length and surface passivation. In a cell with perfectly passivated surface and uniform generation, the equation for the short-circuit current can be approximated as:

$$J_{SC} = qG\left(L_n + L_p\right) \qquad (4\text{-}3)$$

Where G is the generation rate, and L_n and L_p are the electron and hole diffusion lengths respectively. Although this equation makes several assumptions which are not true for the conditions encountered in most solar cells, the above equation nevertheless indicates that the short-circuit current depends strongly on the generation rate and the diffusion length.

Silicon solar cells under an AM1.5 spectrum have a maximum possible current of 46 mA/cm^2. Laboratory devices have measured short-circuit currents of over 42 mA/cm^2, and commercial solar cell have short-circuit currents between about 28 mA/cm^2 and 35 mA/cm^2.

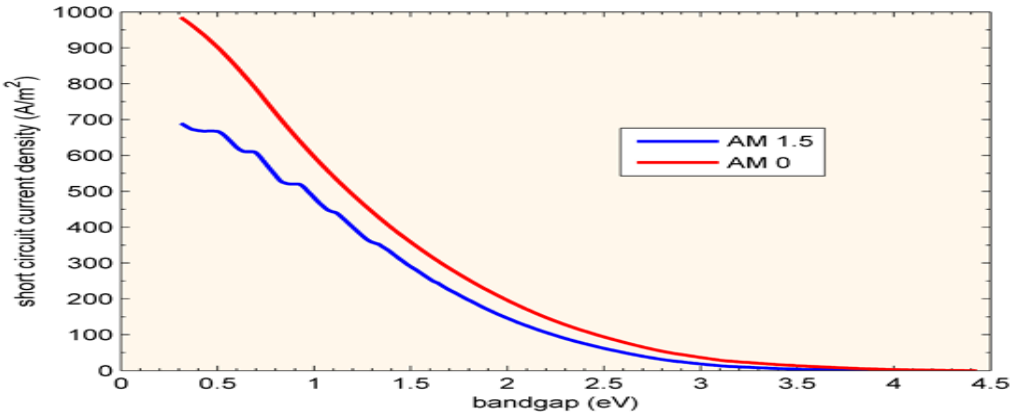

Figure 4- 9: In an ideal device every photon above the bandgap gives one charge carrier in the external circuit so the the highest current is for the lowest bandgap.

4 .3.3.3 Illuminated Current and Short Circuit Current (I_L and I_{sc}):

I_L is the light generated current inside the solar cell and is the correct term to use in the solar cell equation. At short circuit conditions the externally measured current is $I_{sc.}$ Since I_{sc} is usually equal to I_L, the two are used interchangeably and for simplicity and the solar cell equation is written with I_{sc} in place of I_L. In the case of very high series resistance (> 10 Ωcm^2) I_{sc} is less than I_L and writing the solar cell equation with I_{sc} is incorrect.

Another assumption is that the illumination current I_L is solely dependent on the incoming light and is independent of voltage across the cell. However, I_L varies with voltage in the case of drift-field solar cells and where carrier lifetime is a function of injection level such as defected multicrystalline materials.

4 .3.3.4 Open-circuit voltage:

The open-circuit voltage, V_{OC}, is the maximum voltage available from a solar cell, and this occurs at zero current. The open-circuit voltage corresponds to the amount of forward bias on the solar cell due to the bias of the solar cell junction with the light-generated current. The open-circuit voltage is shown on the IV curve below.

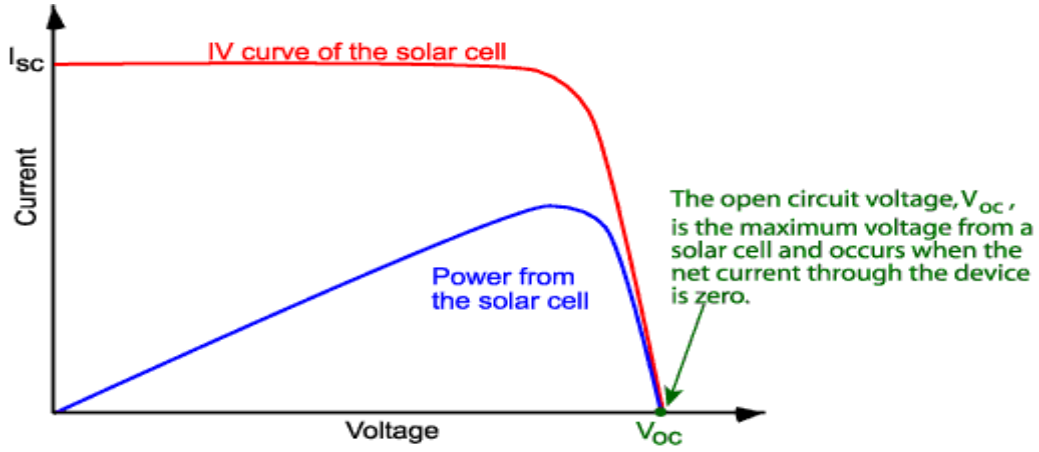

Figure 4-10: IV curve of a solar cell showing the open-circuit voltage.

An equation for V_{oc} is found by setting the net current equal to zero in the solar cell equation to give:

$$V_{OC} = \frac{nkT}{q} \ln\left(\frac{I_L}{I_0} + 1\right) \qquad (4-4)$$

The above equation shows that V_{oc} depends on the saturation current of the solar cell and the light-generated current. While I_{sc} typically has a small variation, the key effect is the saturation current, since this may vary by orders of magnitude. The saturation current, I_0 depends on recombination in the solar cell. Open-circuit voltage is then a measure of the amount of recombination in the device. Silicon solar cells on high quality single crystalline material have open-circuit voltages of

up to 730 mV under one sun and AM1.5 conditions, while commercial devices on multicrystalline silicon typically have open-circuit voltages around 600 mV.

The V_{OC} can also be determined from the carrier concentration:

$$V_{OC} = \frac{kT}{q} \ln\left(\frac{(N_A + \Delta n)\Delta n}{n_i^2}\right) \qquad (4-5)$$

Where kT/q is the thermal voltage, N_A is the doping concentration, Δn is the excess carrier concentration and n_i is the intrinsic carrier concentration. The determination of V_{OC} from the carrier concentration is also termed Implied V_{OC}.

4.3.3.5 Fill Factor:

The short-circuit current and the open-circuit voltage are the maximum current and voltage respectively from a solar cell. However, at both of these operating points, the power from the solar cell is zero. The "fill factor", more commonly known by its abbreviation "FF", is a parameter which, in conjunction with V_{oc} and I_{sc}, determines the maximum power from a solar cell. The FF is defined as the ratio of the maximum power from the solar cell to the product of V_{oc} and I_{sc}. Graphically, the FF is a measure of the "squareness" of the solar cell and is also the area of the largest rectangle which will fit in the IV curve. The FF is illustrated below.

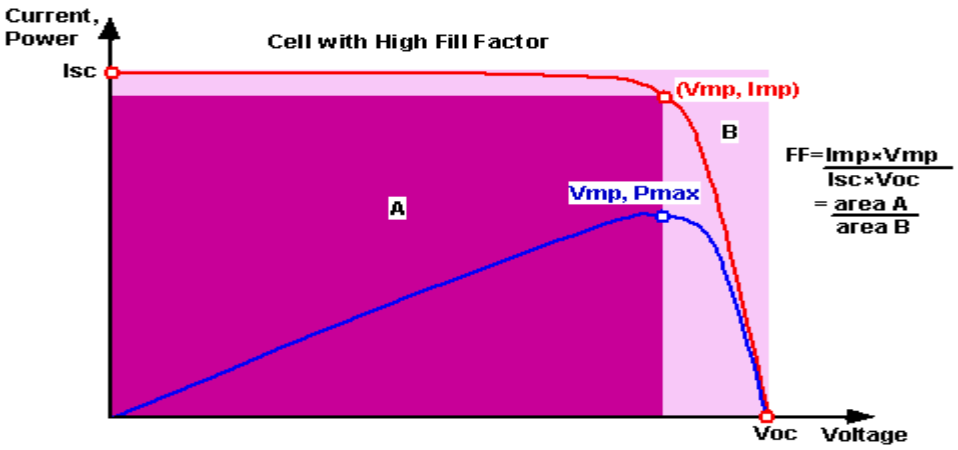

Figure 4- 11: Graph of cell output current (red line) and power (blue line) as function of voltage. Also shown are the cell short-circuit current (I_{sc}) and open circuit voltage (V_{oc}) points, as well as the maximum power point (V_{mp},I_{mp}).

As FF is a measure of the "squareness" of the IV curve, a solar cell with a higher voltage has a larger possible FF since the "rounded" portion of the IV curve takes

up less area. The maximum theoretical FF from a solar cell can be determined by differentiating the power from a solar cell with respect to voltage and finding where this is equal to zero. Hence:

$$\frac{d(IV)}{dV} = 0 \qquad (4-6)$$

Giving:

$$V_{MP} = V_{OC} - \frac{nkT}{q} \ln\left(\frac{V_{mp}}{nkT/q} + 1\right) \qquad (4-7)$$

However, the above technique does not yield a simple or closed form equation. The equation above only relates V_{oc} to V_{mp}, and extra equations are needed to find I_{mp} and FF. A more commonly used expression for the FF can be determined empirically as: [1]

$$FF = \frac{V_{OC} - \ln(V_{OC} + 0.72)}{V_{OC} + 1} \qquad (4-8)$$

Where v_{oc} is defined as a "normalized V_{oc}":

$$V_{OC} = \frac{q}{nkT} V_{OC} \qquad (4-9)$$

The above equations show that a higher voltage will have a higher possible FF. However, large variations in open-circuit voltage within a given material system are relatively uncommon. For example, at one sun, the difference between the maximum open-circuit voltage measured for a silicon laboratory device and a typical commercial solar cell is about 120 mV, giving maximum FF's respectively of 0.85 and 0.83. However, the variation in maximum FF can be significant for solar cells made from different materials. For example, a GaAs solar cell may have a FF approaching 0.89.

The above equation also demonstrates the importance of the ideality factor, also known as the "n-factor" of a solar cell. The ideality factor is a measure of the junction quality and the type of recombination in a solar cell. For the simple recombination mechanisms discussed in Types of Recombination, the n-factor has a value of 1. However, some recombination mechanisms, particularly if they are

large, may introduce recombination mechanisms of 2. A high n-value not only degrades the FF, but since it will also usually signal high recombination, it gives low open-circuit voltages.

A key limitation in the equations described above is that they represent a maximum possible FF, although in practice the FF will be lower due to the presence of parasitic resistive losses, which are discussed in Effects of Parasitic Resistances. Therefore, the FF is most commonly determined from measurement of the IV curve and is defined as the maximum power divided by the product of I_{sc}*V_{oc}, i.e.:

$$FF = \frac{V_{MP} I_{MP}}{V_{OC} I_{SC}} \qquad (4-10)$$

4.3.3.6 The Efficiency:

The efficiency is the most commonly used parameter to compare the performance of one solar cell to another. Efficiency is defined as the ratio of energy output from the solar cell to input energy from the sun. In addition to reflecting the performance of the solar cell itself, the efficiency depends on the spectrum and intensity of the incident sunlight and the temperature of the solar cell. Therefore, conditions under which efficiency is measured must be carefully controlled in order to compare the performance of one device to another. Terrestrial solar cells are measured under AM1.5 conditions and at a temperature of 25°C. Solar cells intended for space use are measured under AM0 conditions. Recent top efficiency solar cell results are given in the page Solar Cell Efficiency Results.

The efficiency of a solar cell is determined as the fraction of incident power which is converted to electricity and is defined as:

$$P_{\max} = V_{OC} I_{SC} FF \qquad (4-11)$$

$$\eta = \frac{V_{OC} I_{SC} FF}{P_{in}} \qquad (4-12)$$

Where V_{oc} is the open-circuit voltage; I_{sc} is the short-circuit current; FF is the fill factor and η is the efficiency.[58]

CHAPTER FIVE

MATERIALS AND METHODS

5.1 Introduction:

This chapter includes a description of the major experimental methods and setups used in this research. To make a solar cell, different materials are needed, and the materials have to be processed by different methods. In this section, the processing of making solar cell will be specified.

5.2 Materials:

The materials we were used in this work are listed as follows:

1. Indium Tin Oxide (ITO).
2. Poly [2-methoxy-5-(2-ethylhexyloxy)-1,4-phenylenevinylene] (MEH-PPV).
3. Different types of dyes (Rhodamine 6G ; Coumarin 500 and Dibenzocyanin 45 (DDTTCI).
4. Solder (Sn/Pb).

5.2.1 ITO

ITO (Indium Tin Oxide) is a transparent conductive material. It is a mixture of indium oxide (In_2O_3) and tin oxide (SnO_2). ITO is used as one of the electrodes in the solar cell.[45]

5.2.2 MEH-PPV

Poly[2-methoxy-5-(2-ethyl-hexyloxy)-1,4-phenylenevinylene] (MEH-PPV) seen in Figure 5.1 is the active material of the solar cell. It is a modification of PPV, modified by the MEH-group, which makes it more soluble in some liquids. It is appearance in dark brown or red granules.[45]

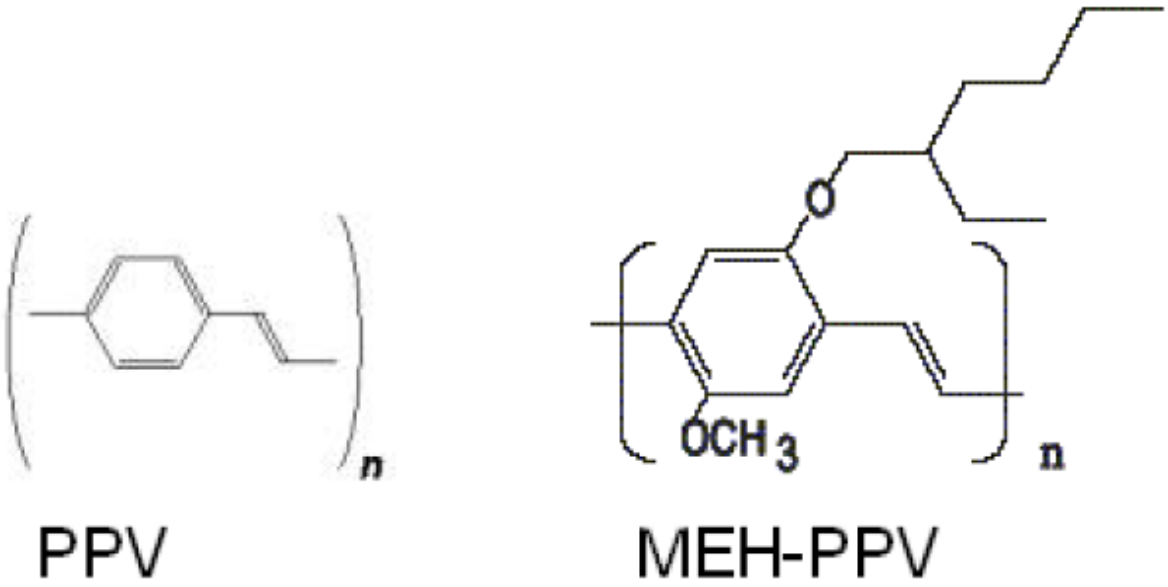

Figure 5.1: The two figures in the monomer of MEH-PPV(right) and the monomer of PPV(left).

5.2.3 Rhodamine 6G

Benzoic Acid, 2-[6-(ethylamino)-3-(ethylimino)-2,7-dimethyl-3H-xanthen-9-yl]- ethyl ester, monohydrochloride ($C_{28}H_{31}N_2O_3Cl$). It is appearance in red crystalline solid.[104]

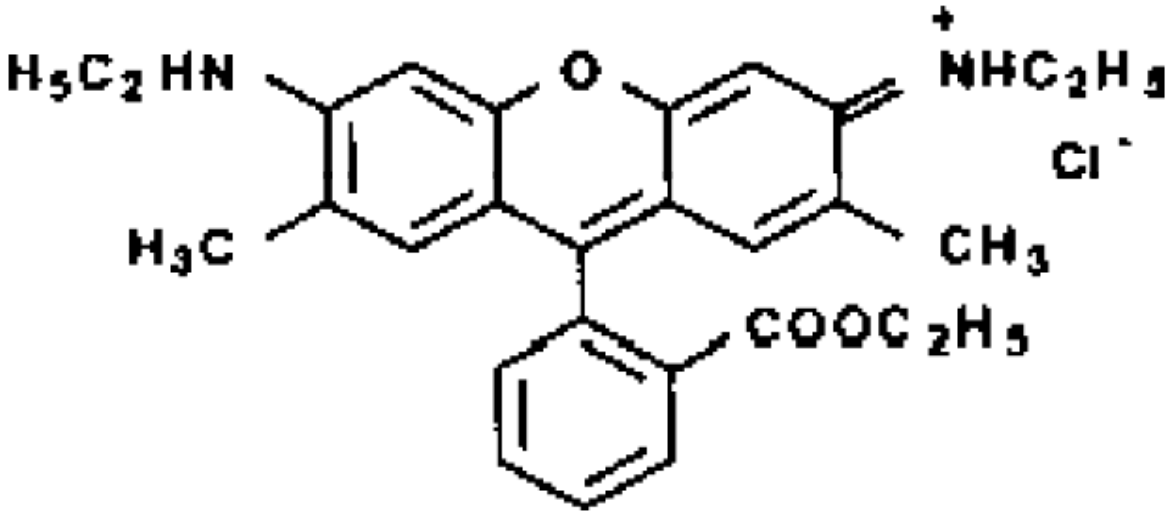

Figure 5.2: The figure shows the structure of Rhodamine 6G.

5.2.4 Coumarin 500

7-Ethylamino-4-trifluormethylcoumarin ($C_{12}H_{10}NO_2F_3$).It is appearance in yellow crystalline solid. [104]

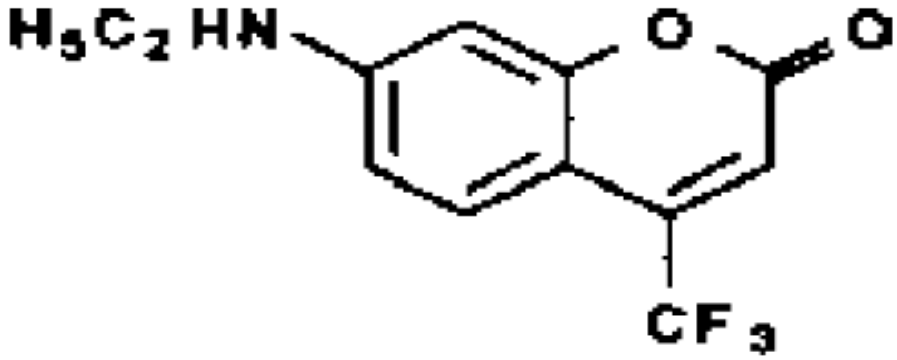

Figure 5.3: The figure shows the structure of Coumarin 500.

5.2.5 Dibenzocyanin 45 (DDTTCI)

3,3'-Diethyl-4,4',5,5'-dibenzothiatricarbocyanine Iodide Hexadibenzocyaini 45 ($C_{33}H_{29}N_2S_2I$). It is appearance in bronze crystalline solid.[104]

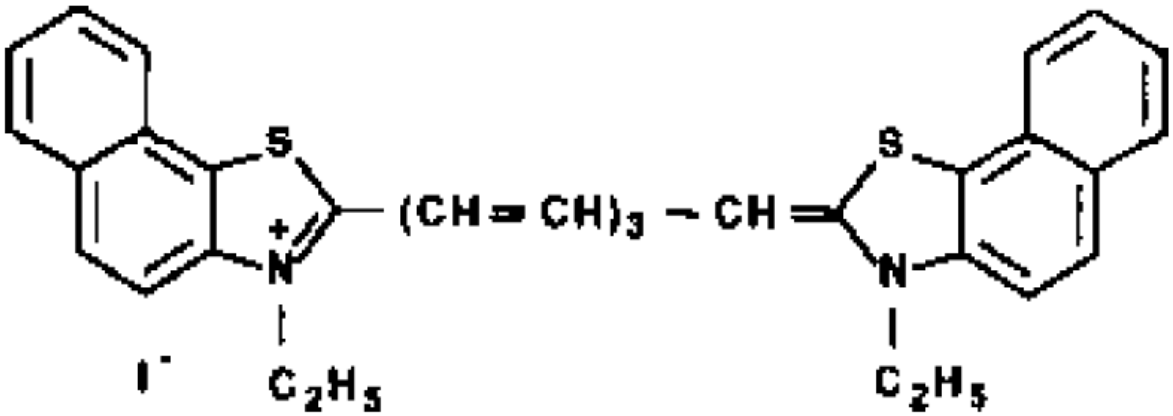

Figure 5.4: The figure shows the structure of DDTTCI.

5.2.6 Solder (Sn/Pb)

Tin/lead solders, also called soft solders, are commercially available with tin concentrations between 5% and 70% by weight. The greater the tin concentration, the greater the solder's tensile and shear strengths. Alloys commonly used for electrical soldering are 60/40 Tin/lead (Sn/Pb) which melts at 370 °F or 188 °C and 63/37 Sn/Pb used principally in electrical/electronic work.

5.3 METHODS

5.3.1 Making the Solar Cell

First of all, a clean glass plate with a thin layer of ITO (Indium Tin Oxide) is needed. These plates are getting from Alneelain University- Department of Physics – laser laboratory. The ITO acts as the first part of the solar cell, the first electrode. When a solar cell is made, it is important that the materials are clean. To clean the

plate, it is first washed with soap; then water and finally washed with ethanol and dried for 1 minute.

5.3.1.1 Solutions

Two solutions have been made, MEH-PPV solution, and dyes solution. The MEH-PPV solution has been treated carefully, the chemical MEH-PPV (PolyPhenylene Venylene) is very light sensitive so it has to be wrapped in silver paper to keep the MEH-PPV from reacting with sunlight. The dyes solutions are added in order to make the dissociation of excitons more efficient. The concentrations of the different chemicals solutions are described in table 5.1

Table 5.1: The concentrations of different chemicals solutions for the solar cells

Material	Solvent	Concentration
MEH-PPV	Ethanol	0.1 mg/ml
Rhodamine 6G	Ethanol	0.5 mg/ml
Coumarin 500	Ethanol	0.5 mg/ml
Dibenzocyanin 45 (DDTTCI)	Ethanol	1 mg/ml

5.3.1.2 Spin Coating

To deposit the polymer layers, a standard spin-coating technique was employed. Spin-coating implies either putting a droplet of a solution onto the center of a rotating substrate, or first putting the solution onto the substrate and then spinning it up (Figure 5.5). In this work the first approach was used.

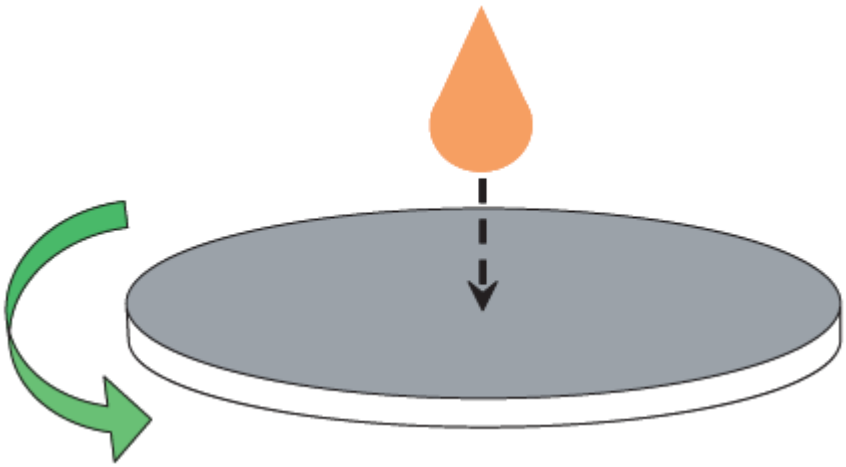

Figure5.5: An illustration of the spin-coating technique. [68]

Figure 5.6: Actual spin coating machine used in this work

Two solutions have been spun over the plate. The first layer is the dye and the second layer is MEH-PPV which functions as the active layer in the solar cell. Then the plates were heated in oven at 80 ^{0}C for 30 minute in order to evaporate the water from the solution. Both layers MEH-PPV and the dye were spun for 1 minute. Table 5.2 shows the parameters of spin coating machine for MEH-PPV and dyes.

Table 5.2: The Parameters of spin coating machine for MEH-PPV and Dyes for the samples.

Samples	Dyes	Parameters of spin coating machine for dyes	Parameters of spin coating machine for MEH-PPV	Groups
A3	Rhodamine 6G	V = 0.7 v , I = 500 mA	V = 0.9 v , I = 500 mA	A
A6	Rhodamine 6G			
A9	Coumarin 500			
A12	Dibenzocyanin-45			
A15	Dibenzocyanin-45			
B2	Rhodamine 6G		V = 1.1 v , I = 500 mA	B
B5	Rhodamine 6G			
B8	Coumarin 500			
B11	Dibenzocyanin-45			
B14	Dibenzocyanin-45			
C1	Rhodamine 6G		V = 1.3 v , I = 500 mA	C
C4	Rhodamine 6G			
C7	Coumarin 500			
C10	Dibenzocyanin-45			
C13	Dibenzocyanin-45			

The last layer is Solder Sn/Pb we spun it for 25 seconds as a second electrode. According to the parameters of spin coating machine in table 5.2 the

thickness of samples will increase from Group C to Group A that means samples in Group A thicker than the others.

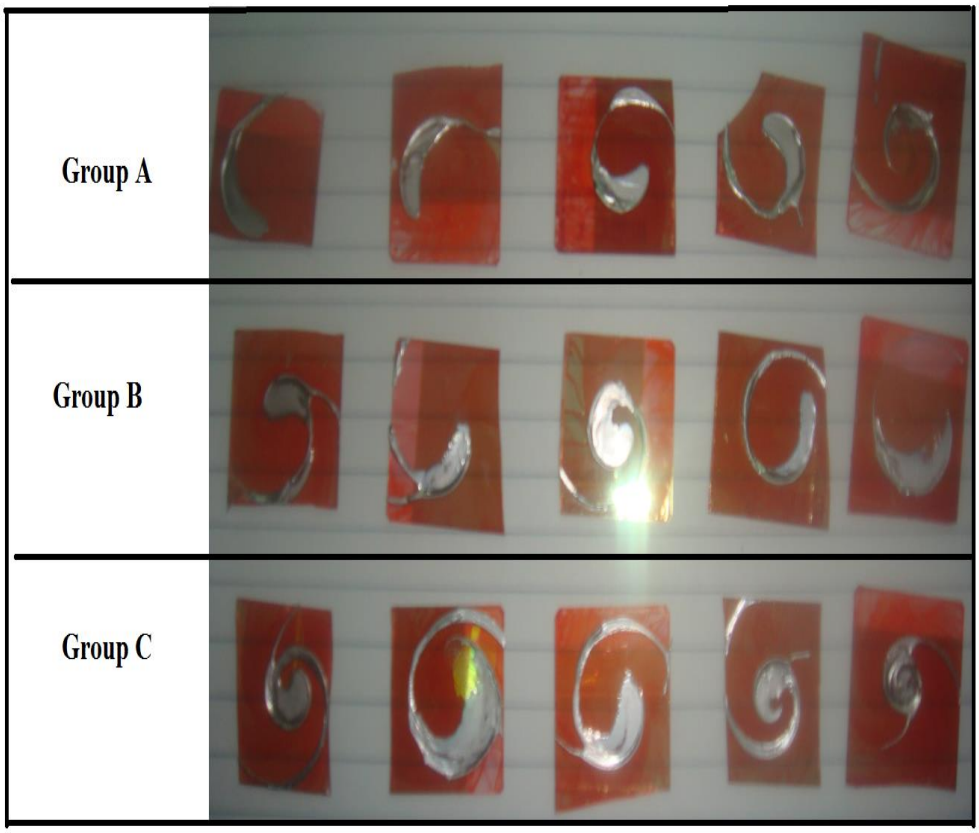

Figure 5.7: Actual conjugate polymers solar cells have been fabricated in this work

5.3.2 The measurement of ultra violet spectra

Optical absorption spectra were recorded with a UV-VIS spectrophotometer (model: UV mini-1240) within the wavelength range of 200–800 nm, at room temperature.

Absorption spectra are usually registered by instruments known as spectrophotometers. Figure 5.8 shows a schematic diagram with the main elements of the simplest spectrophotometer. Basically, it consists of the following components: (i) a light source (usually a deuterium lamp for the UV spectral range and a tungsten lamp for the VIS and IR spectral ranges) that is focused on the entrance to (ii) a monochromator, which is used to select a single wavelength (frequency) from all of those provided by the lamp source and to scan over a desired frequency range. (iii) a sample holder, followed by (iv) a light detector, to measure the intensity of each monochromatic beam after traversing the sample and

finally (v) a computer, to display and record the absorption spectrum. (Sole, etal., 2005).

The UV-VIS spectrophotometer (model: UV mini-1240) used in this work. A glass slide that had been treated the same way as the slides with films but with no film on it was used as the reference slide. The wavelength was varied in units of 10 from 200 nm to 800 nm and the corresponding absorbance reading recorded.[68]

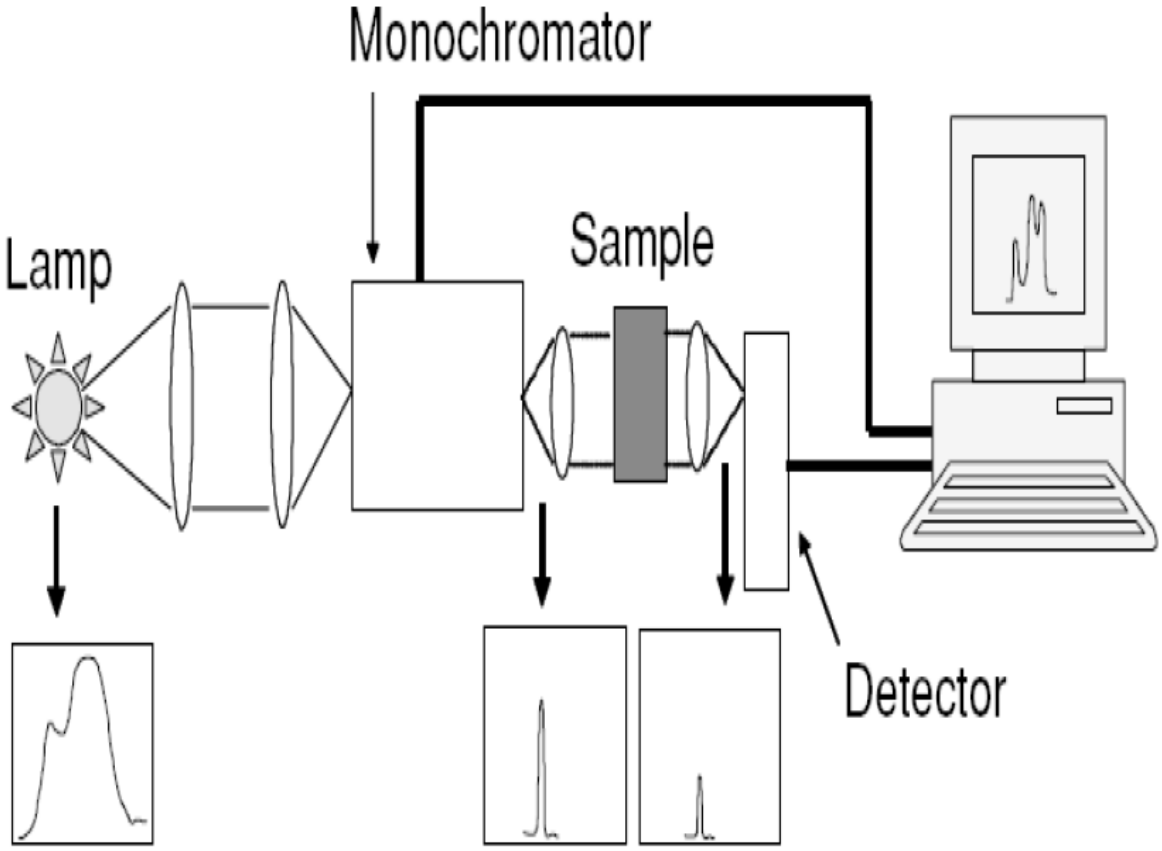

Figure 5.8: Schematic diagram of a single-beam spectrophotometer.

5.3.3 Measuring the IV Characteristic

In order to compare various solar cells it is necessary to measure the characteristic values: Voc, Isc, the fill factor and the efficiency, ɳ. All these factors can be determined from the IV characteristic of a solar cell and the power output from the lamp. Therefore an IV characteristic was performed under illumination for each solar cell in this project.

The IV characteristic is a measurement of the current as a function of the applied voltage. There are various ways to achieve this. In This work we used a simple circuit consist of electrical source, Rheostat, Ammeter, Voltmeter, solar cell

and light source of output power 100 w. The setups were done in room temperature as displayed in figure 5.9.

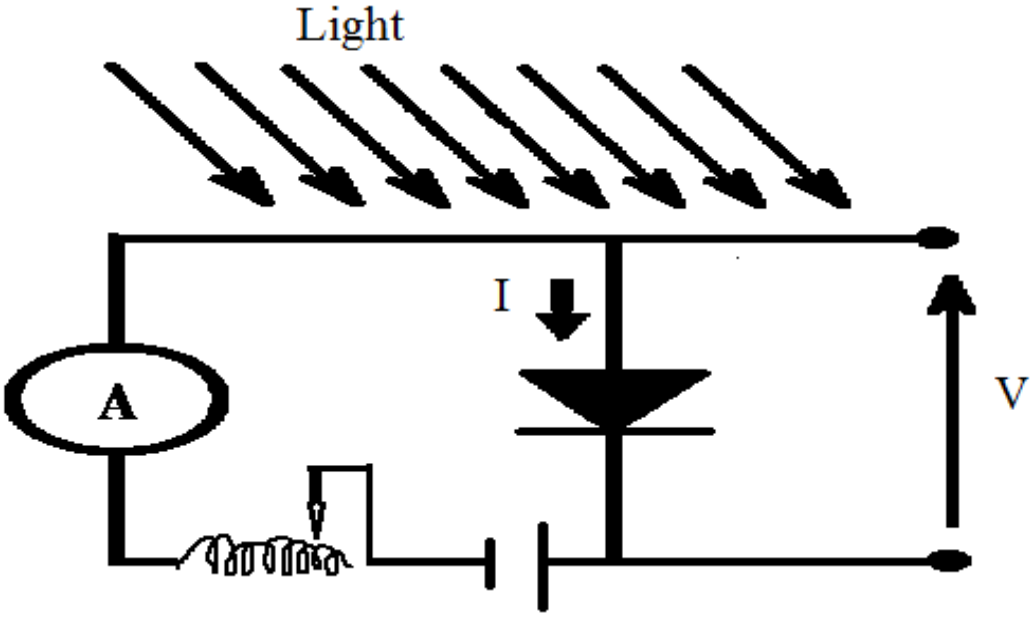

Figure 5.9: The setup for measuring the IV characteristics of solar cells.

CHAPTER SIX

RESULTS AND DISCUSSION

6.1 Results:

This chapter presents the results obtained from the experiments, which have been carried out in the laboratory during this project. In this work we fabricated 15 samples of solar cells and we distributing it in three groups A, B and C according to the spin coating machine parameters for (MEH-PPV) as shown in table 5.2 (chapter five).

6.1.1 Absorbance

The absorbance of the separate parts of the conjugate polymer solar cells has been measured, and their schemes are shown by groups in Figures (6.1 - 6.15).

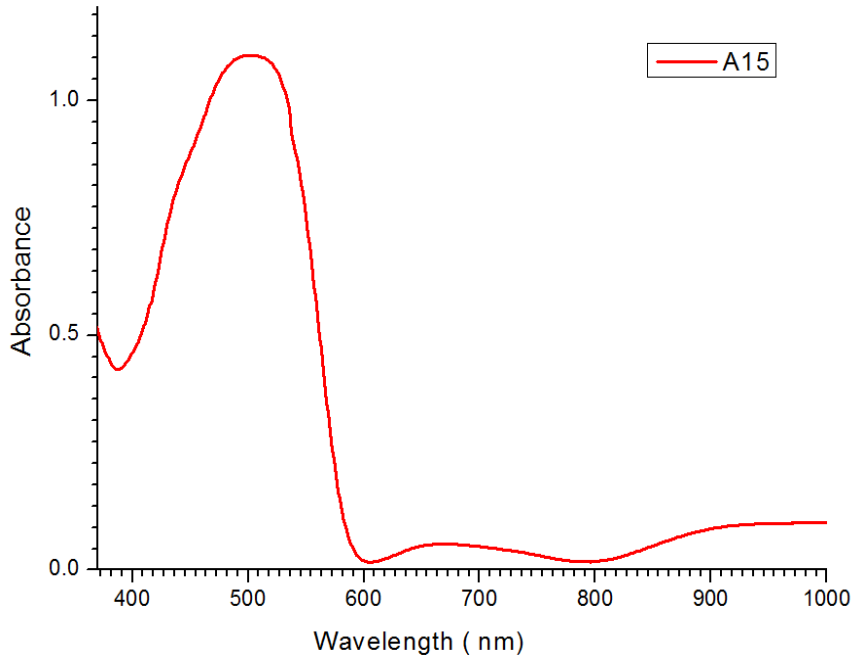

Figure 6.1: UV spectrum of sample A15 (the highest absorbance).

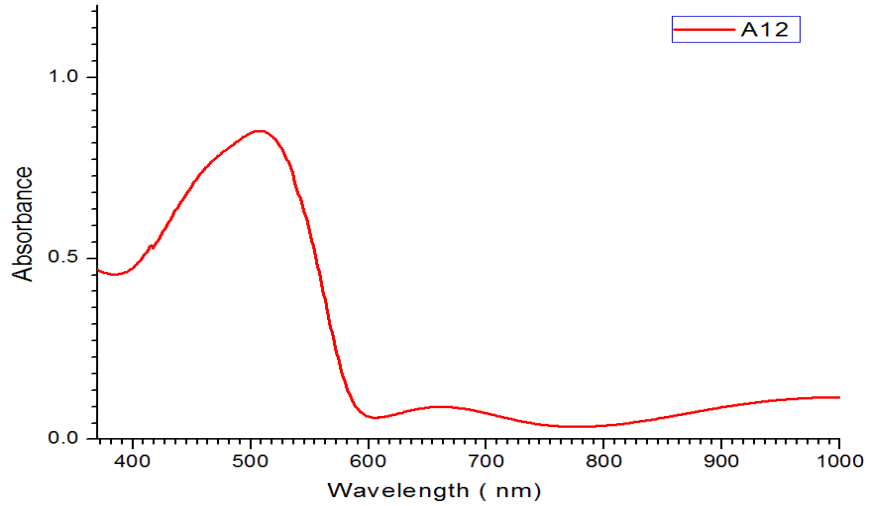

Figure 6.2: UV spectrum of sample A12.

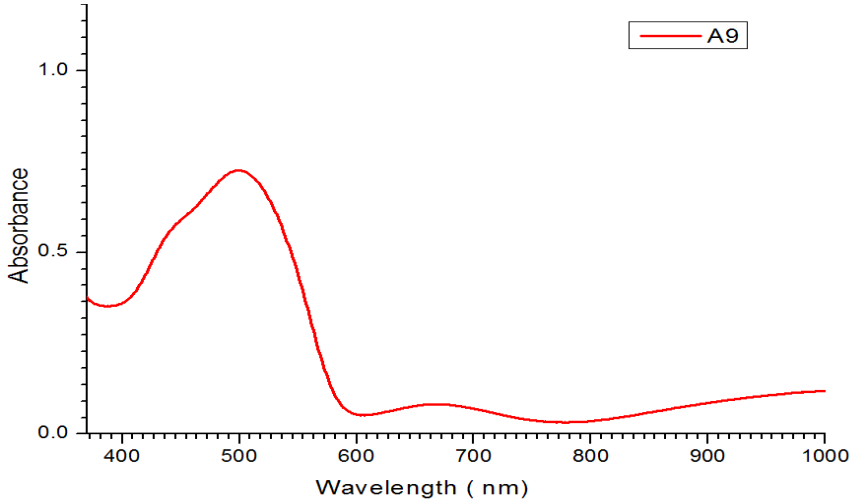

Figure 6.3: UV spectrum of sample A9.

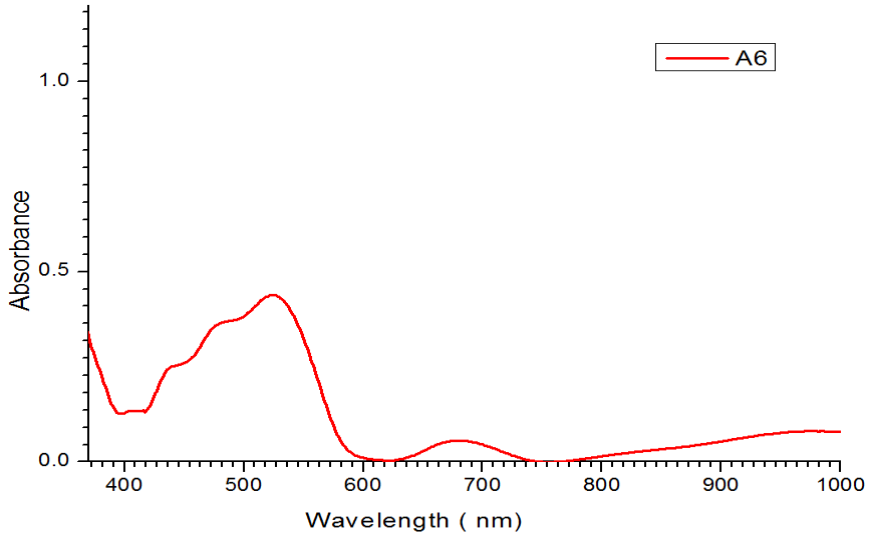

Figure 6.4: UV spectrum of sample A6.

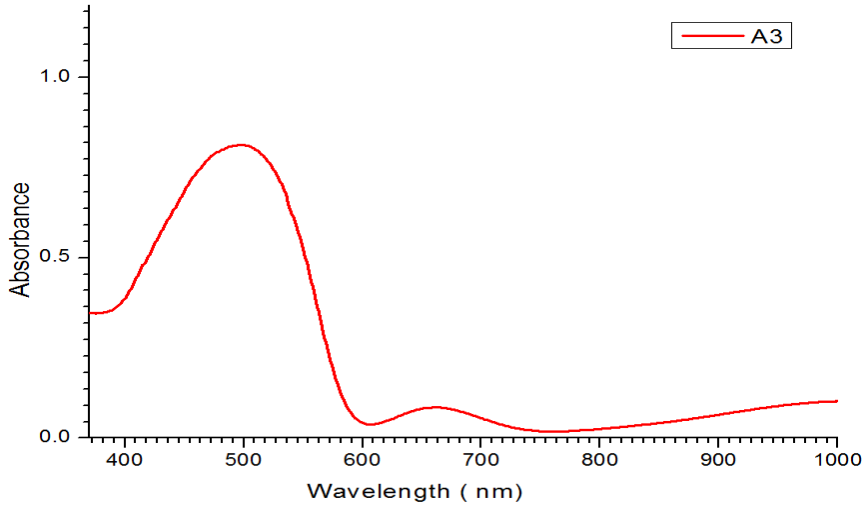

Figure 6.5: UV spectrum of sample A3.

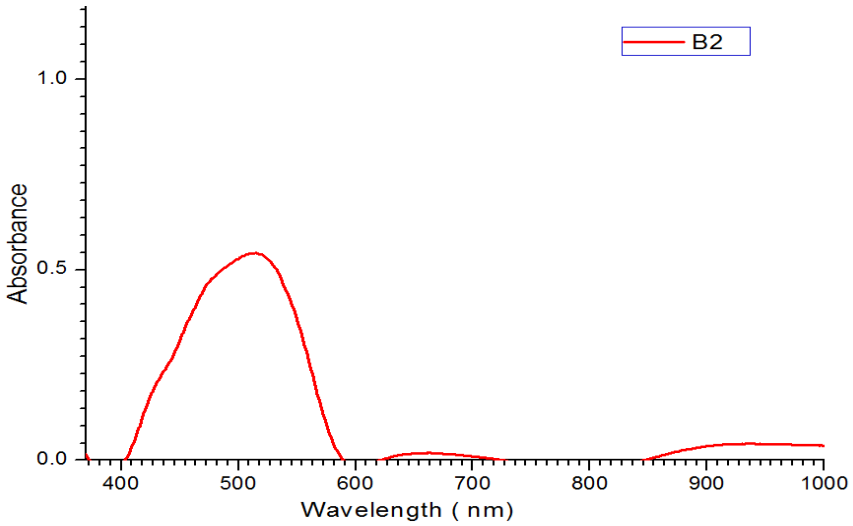

Figure 6.6: UV spectrum of sample B2.

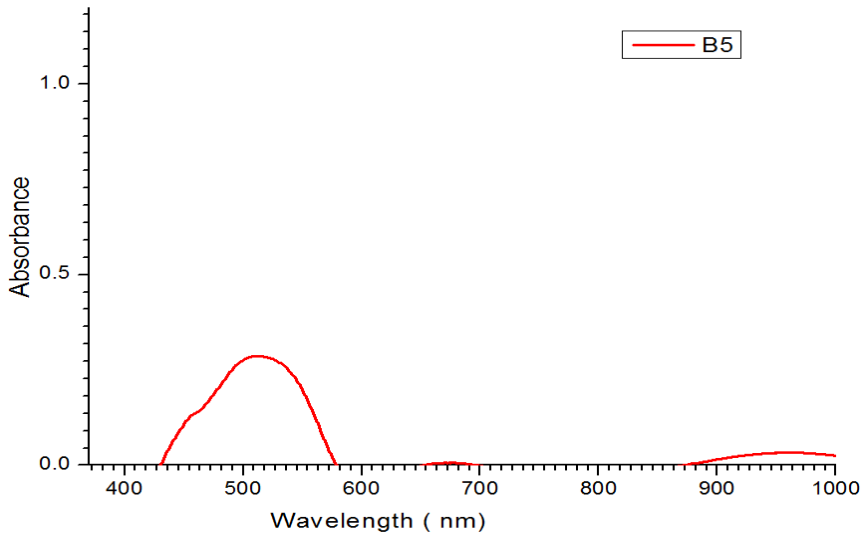

Figure 6.7: UV spectrum of sample B5.

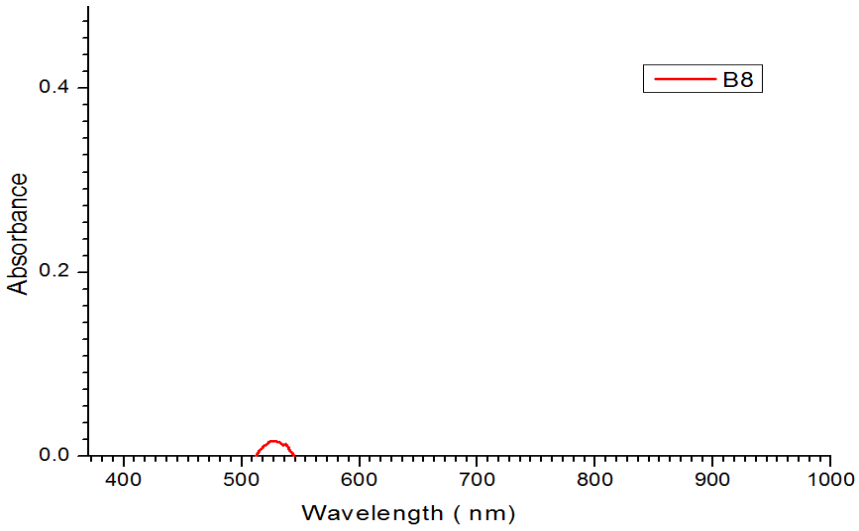

Figure 6.8: UV spectrum of sample B8 (the lowest absorbance).

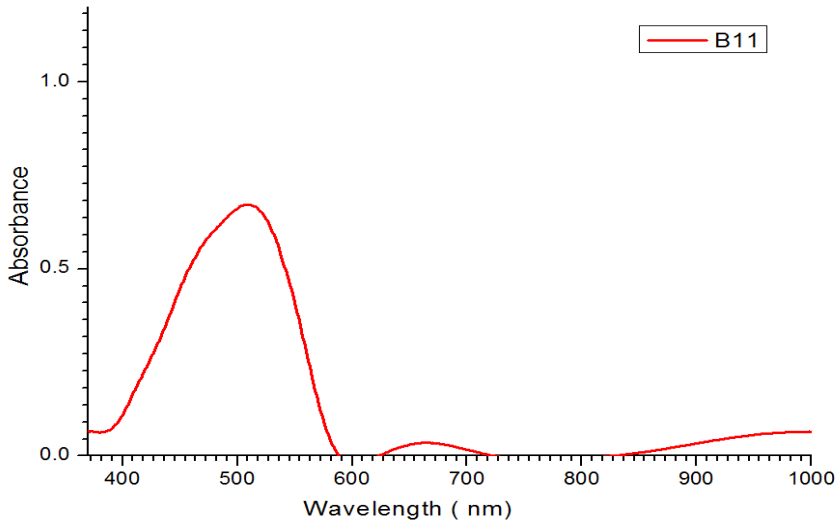

Figure 6.9: UV spectrum of sample B11.

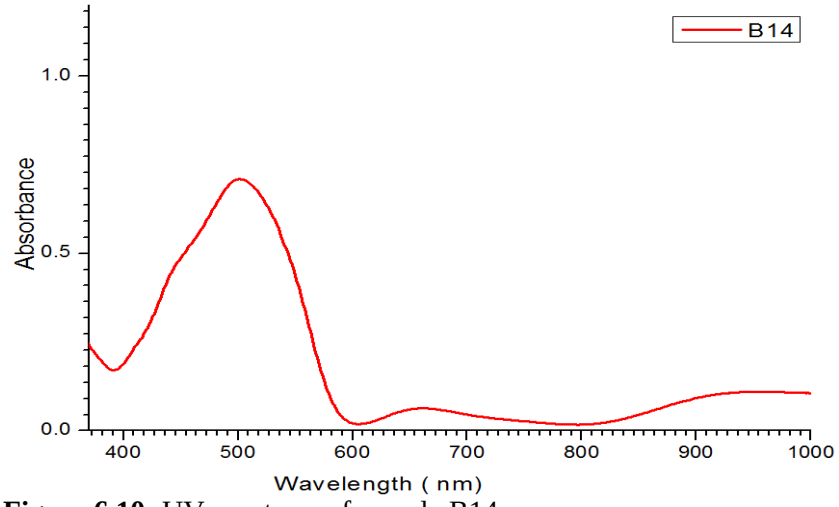

Figure 6.10: UV spectrum of sample B14.

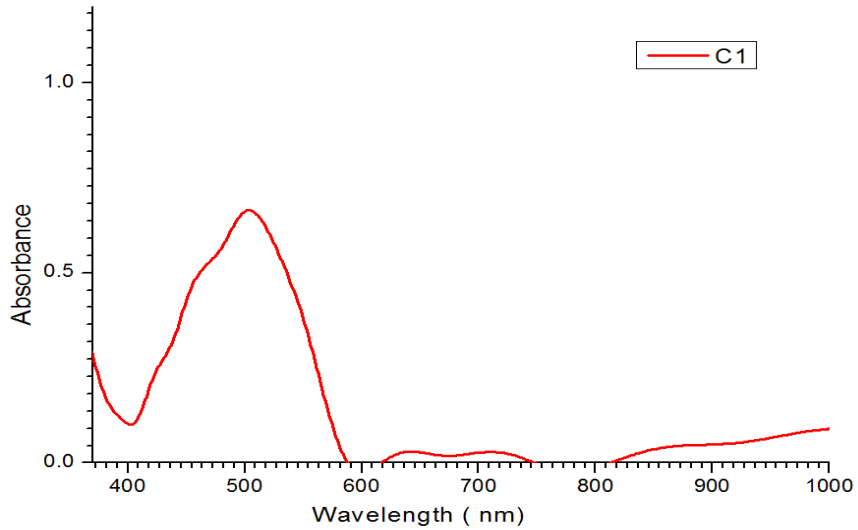

Figure 6.11: UV spectrum of sample C1.

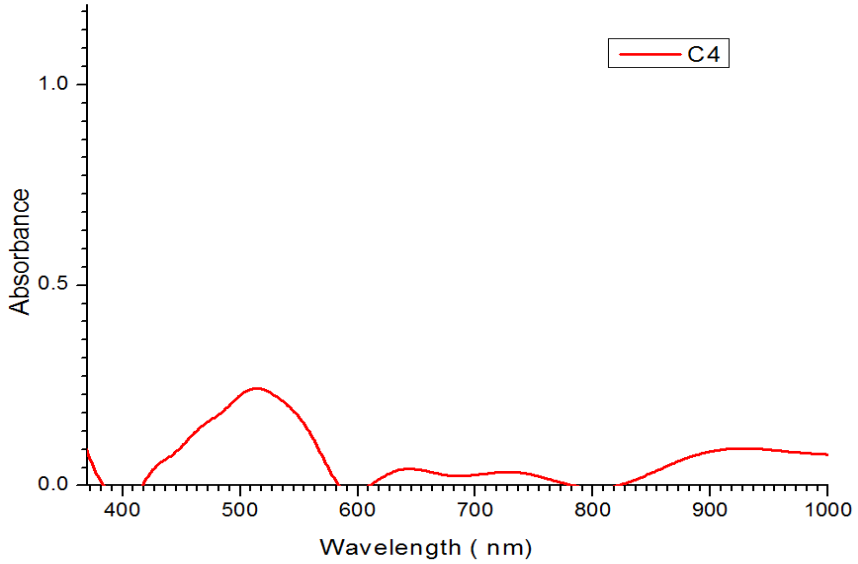

Figure 6.12: UV spectrum of sample C4.

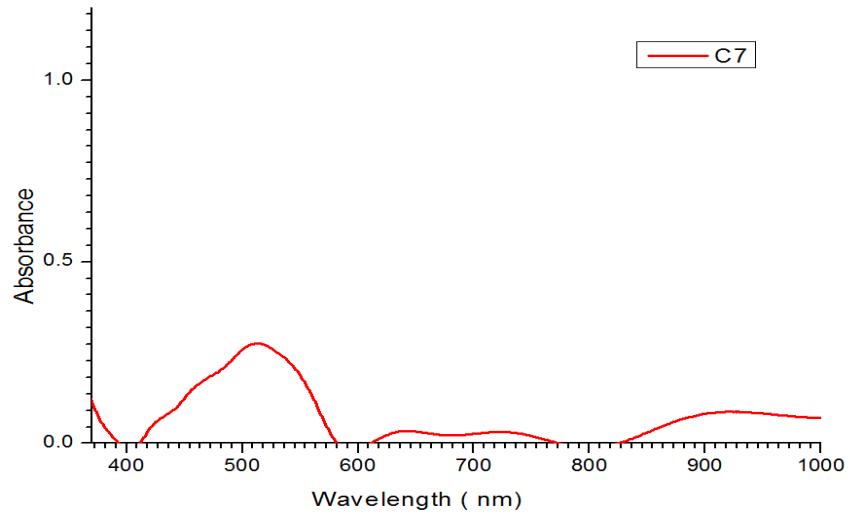

Figure 6.13: UV spectrum of sample C7.

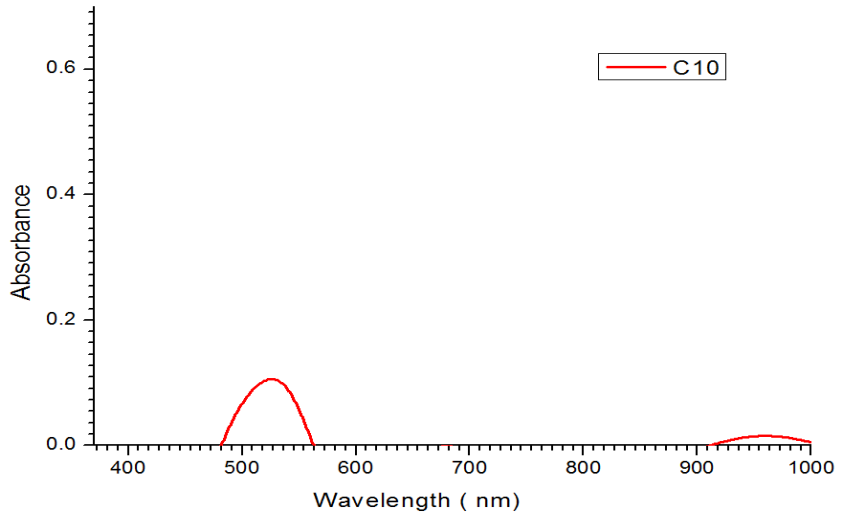

Figure 6.14: UV spectrum of sample C10.

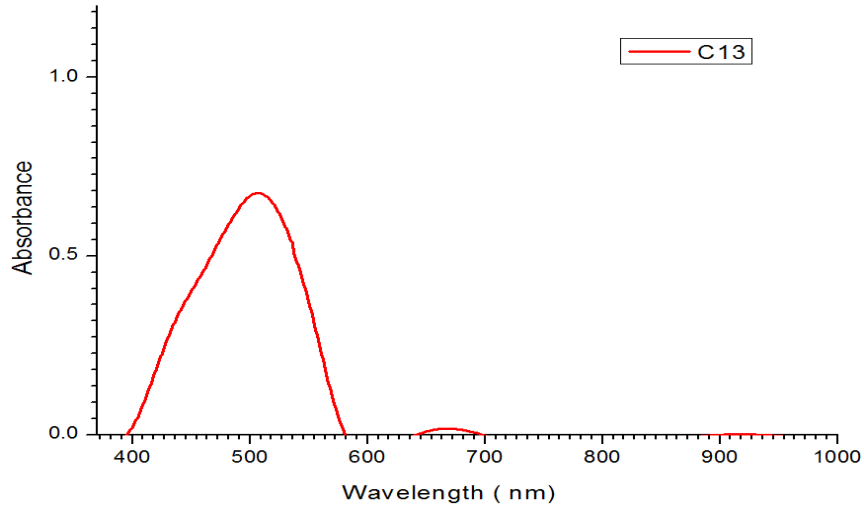

Figure 6.15: UV spectrum of sample C13.

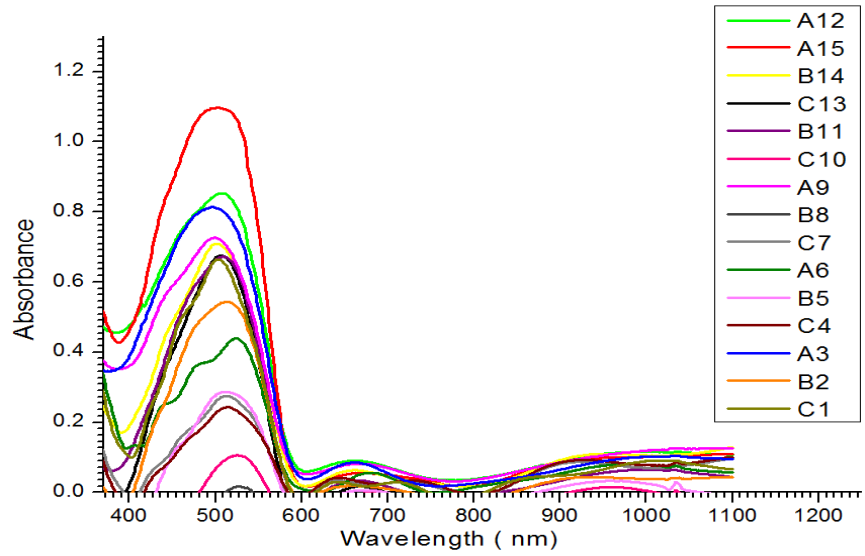

Figure 6.16: UV spectra for all samples.

6.1.2 IV characterization

The IV-curve from the solar cells has been analyzed in the laboratory. Figure 6.17 shows an IV-curve obtained from an ordinary conjugate polymer solar cell under illumination. I_{SC}, I_{mp}, V_{mp}, and V_{OC} are marked on the curve.

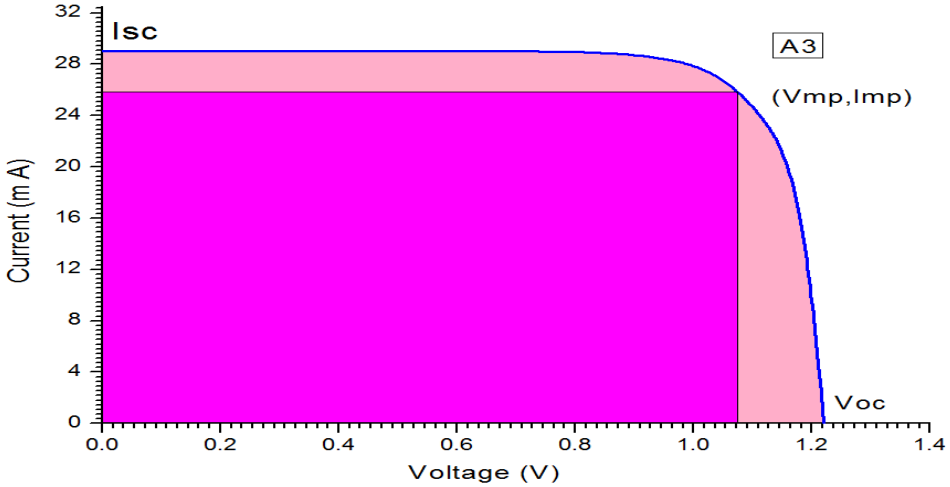

Figure 6.17: The IV curve for sample A3.

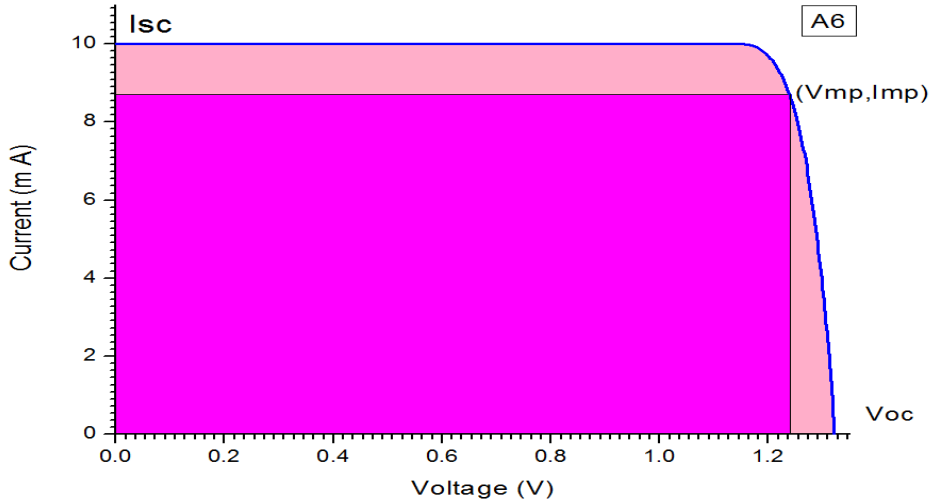

Figure 6.18: The IV curve for sample A6.

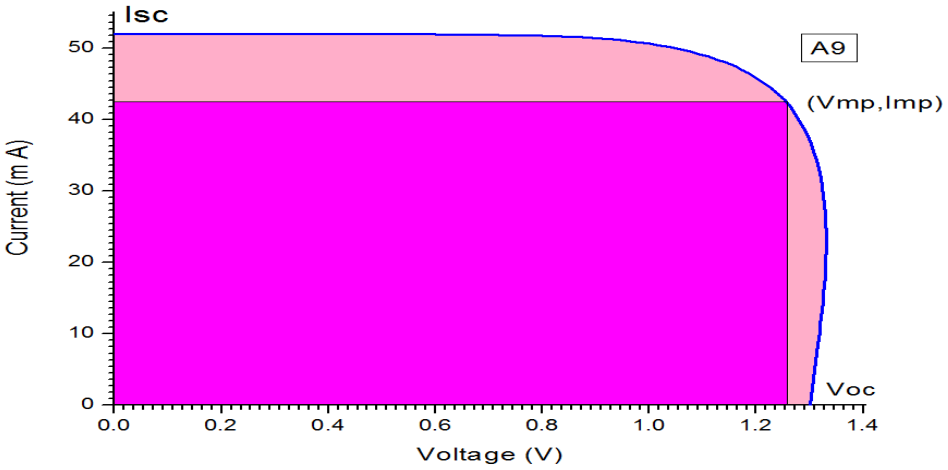

Figure 6.19: The IV curve for sample A9.

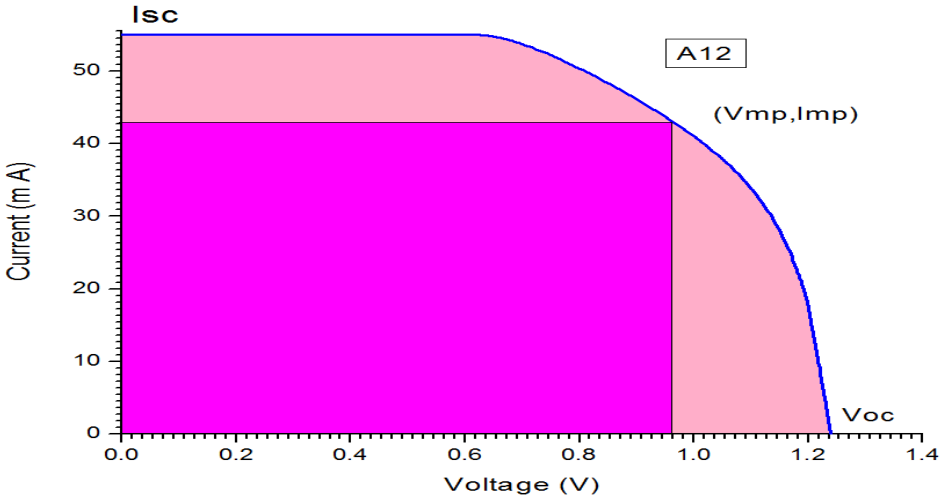

Figure 6.20: The IV curve for sample A12.

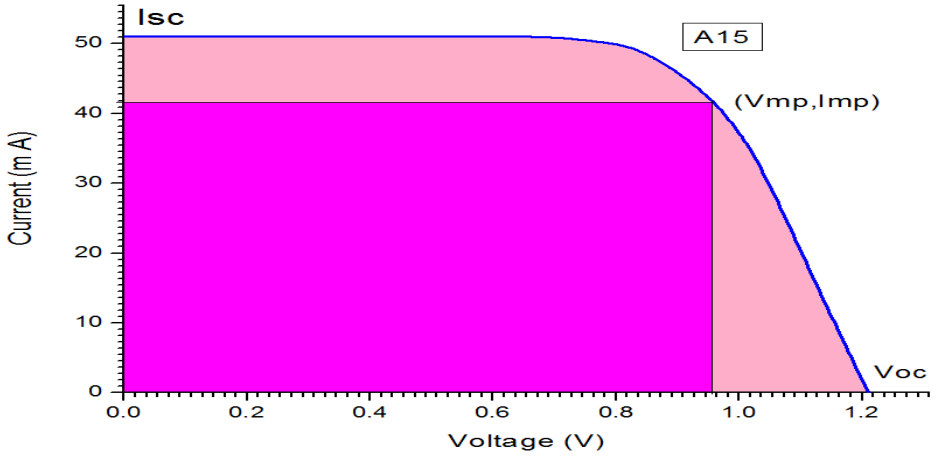

Figure 6.21: The IV curve for sample A15.

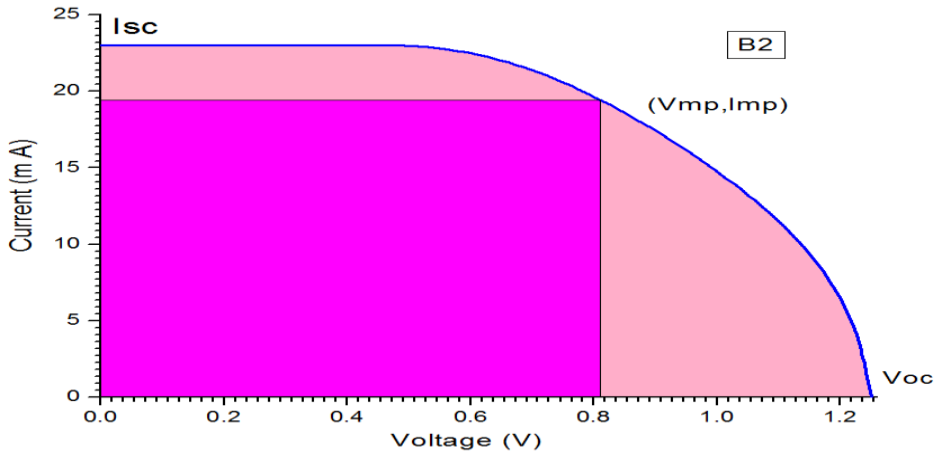

Figure 6.22: The IV curve for sample B2.

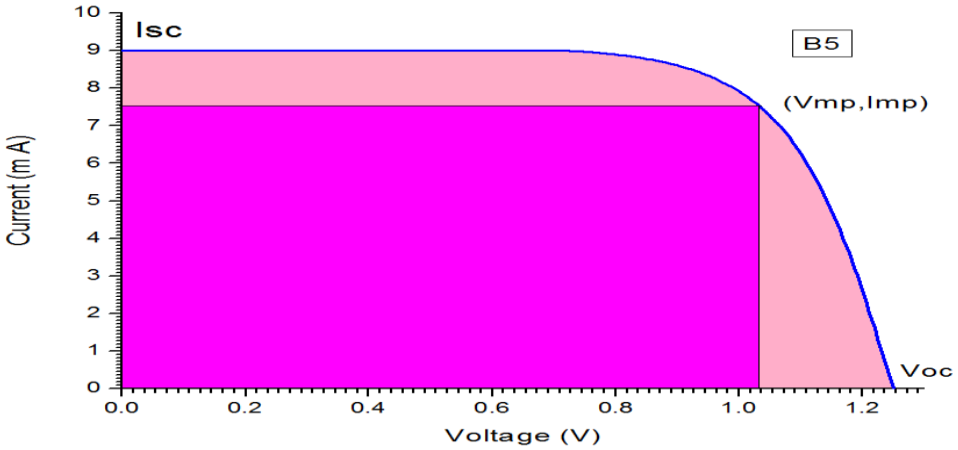

Figure 6.23: The IV curve for sample B5.

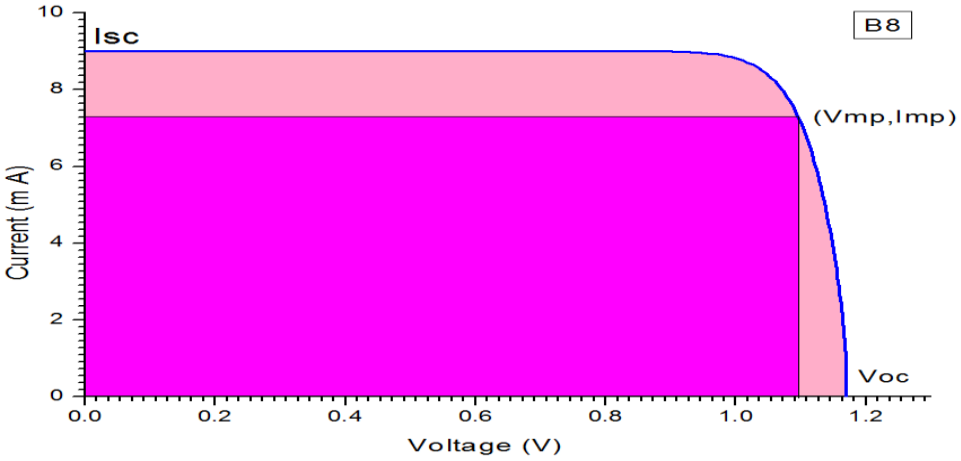

Figure 6.24: The IV curve for sample B8.

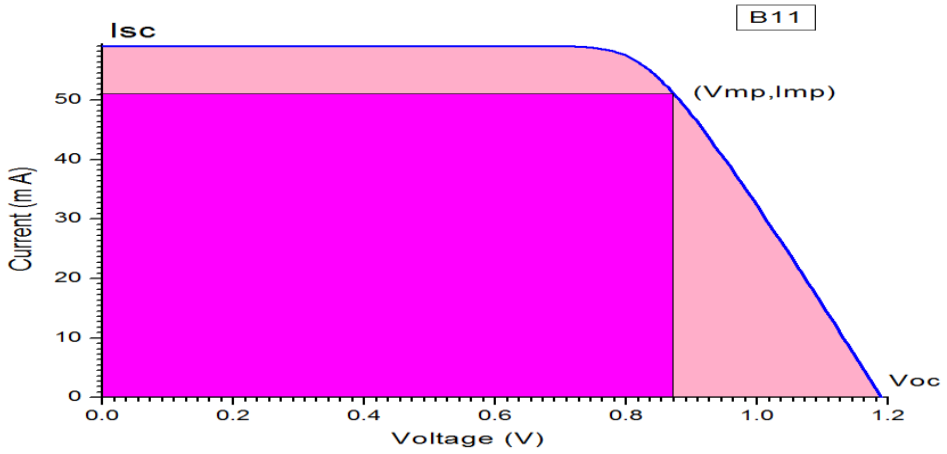

Figure 6.25: The IV curve for sample B11.

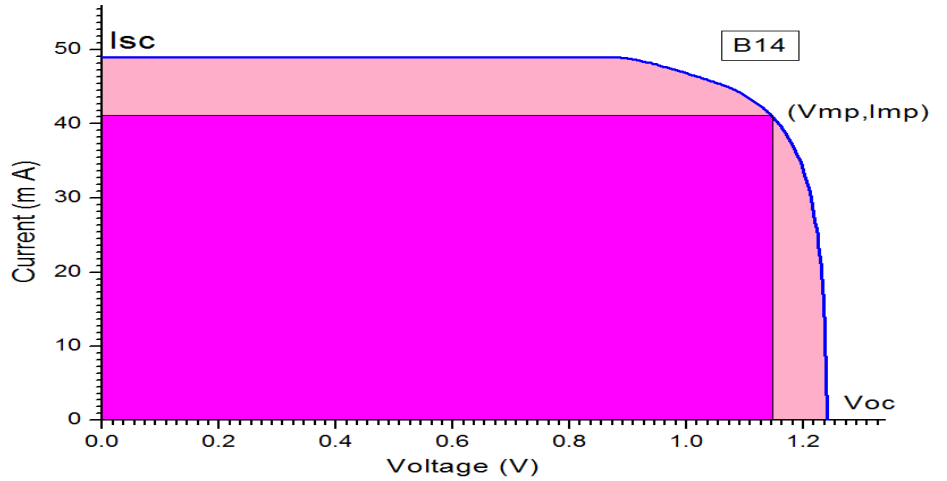

Figure 6.26: The IV curve for sample B14.

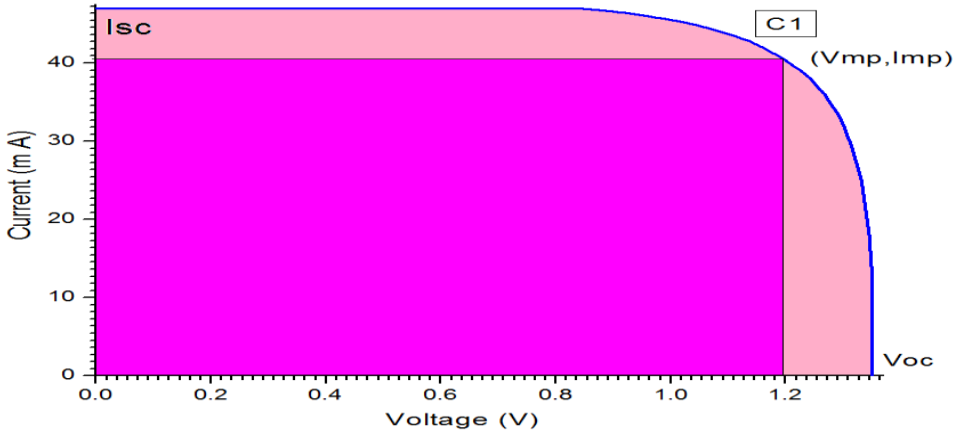

Figure 6.27: The IV curve for sample C1.

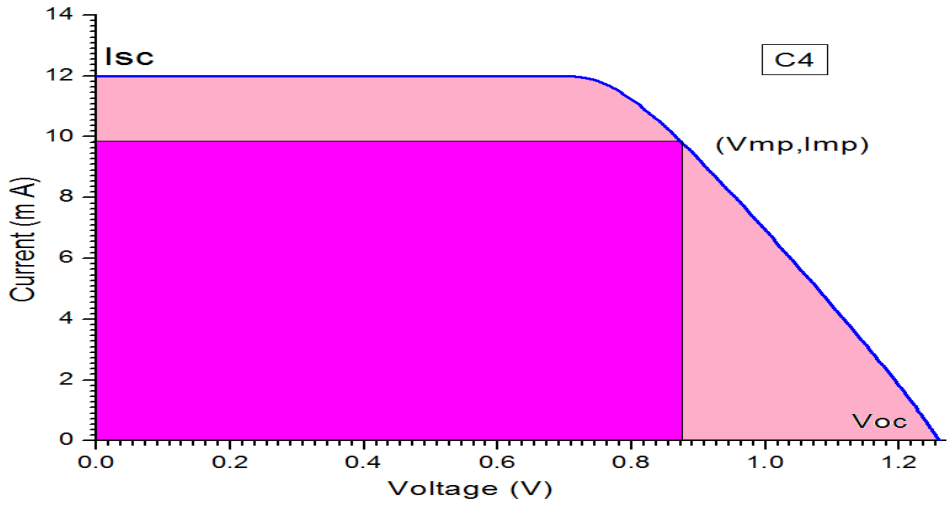

Figure 6.28: The IV curve for sample C4.

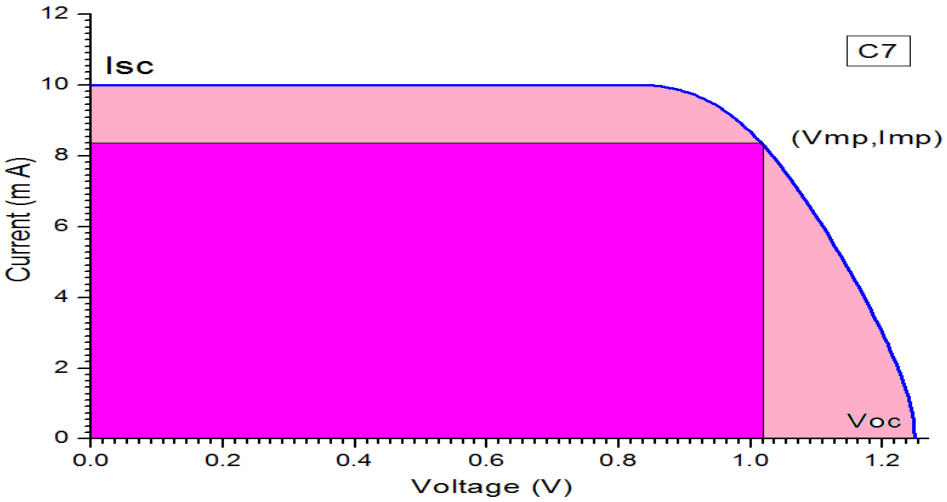

Figure 6.29: The IV curve for sample C7.

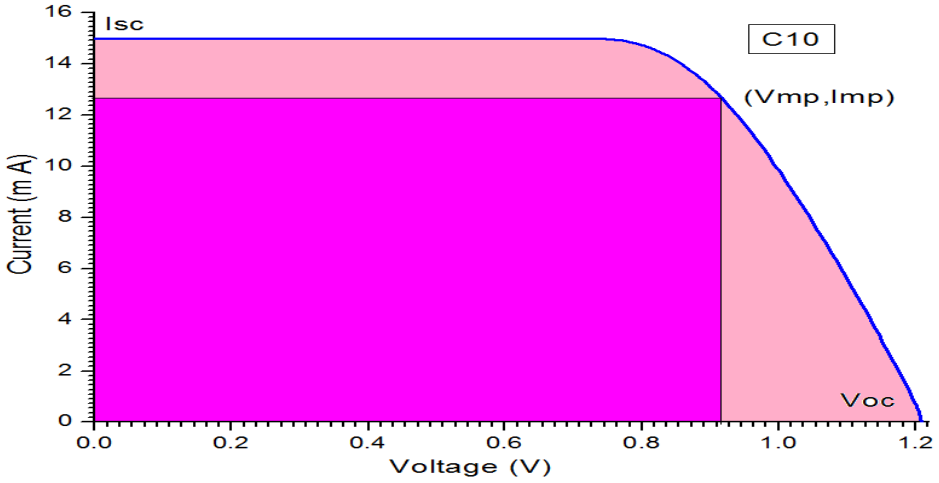

Figure 6.30: The IV curve for sample C10.

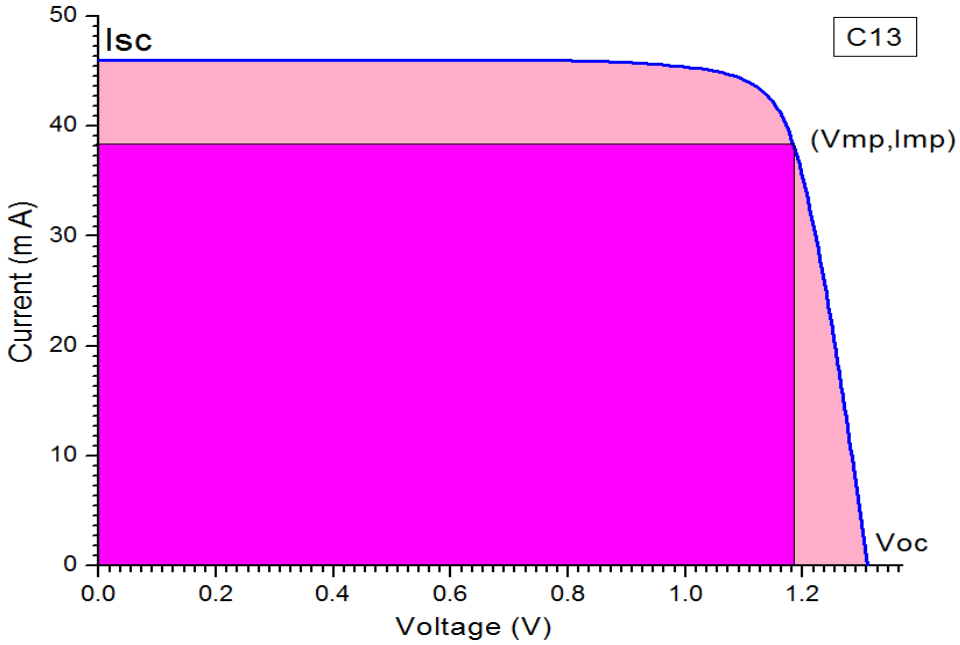

Figure 6.31: The IV curve for sample C13.

6.2 Discussions:

This part of the discussion will deal with the performance of the analyzed solar cells. As mentioned in Section 6.1 there was 15 functional polymer solar cells were produced.

6.2.1 Absorption

The majority of the samples showed a similar absorption of spectra. For all samples the absorption peak shifts towards its maximum at a wavelength range 505-528 nm with decreasing of the thickness of the thin films as shows in figure 6.16. The highest absorbance recorded of the samples is sample A15 it absorbs at most visible wavelengths with a maximum absorption at cyan wavelengths of the solar spectrum as shown in figure 6.1. The lowest absorbance recorded of the samples is sample B8 it absorbs at green wavelengths as shows in figure 6.8 and this may be attributed to the thickness of the two layers of MEH-PPV. Also organic dye is not thick enough and the sample surface is not perfectly homogeneous.

Table 6.1 shows colors region of the solar spectrum.

Table 6.1: Colors regions of the solar spectrum.[31]

color region	wavelength (nm)
violet	380 – 435
blue	435 – 500
cyan	500 – 520
green	520 – 565
yellow	565 – 590
orange	590 – 625
red	625 – 740

6.2.2 IV Characterization

The obtained IV-curves for conjugate polymer solar cells are similar to that of the optimal model, described in chapter 4 Section 4.3.3. Sample A12 recorded the highest value of the short-circuit current as recorded samples C1 and A6 gave the highest values for each of the open circuit voltage and fill factor, respectively, as shown in figures 6.20 ,6.27 ,6.18 , respectively. All samples showed a variation in terms of efficiency which was obtained in range 10.28 % - 1.744 %.

The highest efficiency of the solar cell has been obtained from the sample A15. The lowest efficiency was obtained from the sample B8 this could be due to weak absorption coefficient of light exhibited by the sample, which was already discussed in the previous section.

The samples which we produced have shown good results in the efficiency compared to the results obtained in the previous studies in chapter 4 sections 4.2. Table 6.2 shows the short-circuit current, open circuit voltage, the fill factor, the current density and the efficiency obtained from all samples. The results of efficiency obtained from the samples are summarized in the histogram in Figure 6.32.

The calculations were made for each of the fill factor; the current density and the efficiency for all samples were attached on Appendix page.

Table 6.2: Isc, Voc, Jsc, FF and the conversion efficiency for all samples.

Samples	Isc (mA)	Voc (V)	Area (cm^2)	Jsc (mA/cm^2)	FF (%)	Efficiency (ɳ) (%)
A15	51	1.21	4	12.75	0.66699	10.28
A9	52	1.3	6.25	8.32	0.8014	8.66
A12	55	1.24	5.25	10.47619	0.60527	7.862
C1	47	1.35	6.25	7.52	0.7509	7.62
B14	49	1.24	6.25	7.84	0.7827	7.609
A3	29	1.22	3.75	7.733	0.793668	7.487
C13	46	1.31	6	7.66	0.7441	7.466
B11	59	1.19	6.25	9.44	0.639	7.178
B2	23	1.25	3.75	6.133	0.5561	4.263
A6	10	1.32	3.5	2.857	0.8266	3.117
C10	15	1.21	5.25	2.857	0.6629	2.291
C4	12	1.26	4	3	0.5703	2.155
C7	10	1.25	4.24	2.352	0.68544	2.015
B5	9	1.25	4	2.25	0.7118	2.0019
B8	9	1.17	4.75	1.894	0.787	1.744

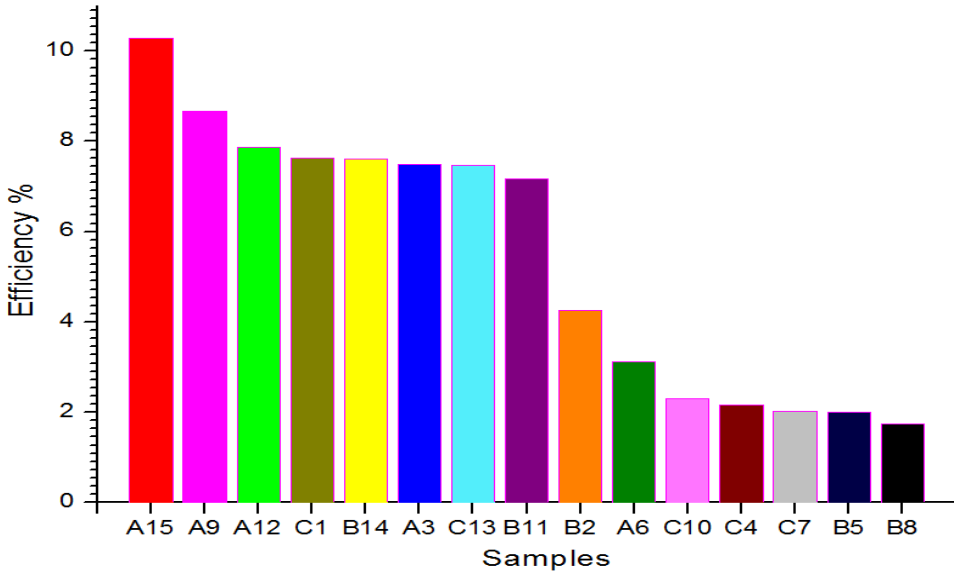

Figure 6.32: The conversion efficiency for all samples.

6.2.3 Low-Cost

In order to reduce the cost of manufacturing solar cells we used conjugate polymer as the main materials in this work because its improve lowest cost according to many studies in this field as reported in references [21] and [22].

Polymer solar cells (PSC) are one of the possible replacements. These solar cells add some very interesting properties to the solar cell as well as reducing the price considerably. Krebs[55]have demonstrated that the production of large area

PSC ($1m^2$) can be done at a cost 100 times lower than that of monocrystalline silicon solar cells in terms of material cost.

Recent developments in ink-jet printing, micro-contact printing, and other soft lithography techniques have further improved the potential of conjugated polymers for low-cost fabrication of large-area integrated devices on both rigid and flexible substrates.

6.3 Conclusion

In this project calculations of IV Characterization and absorbance spectra of conjugated polymers have been made and different types of polymer solar cells have been produced. As mentioned above we fabricated 15 samples of solar cells and we distributing it in three groups A, B and C according to the spin coating machine parameters for (MEH-PPV) as show in table 5.2 in chapter five.

The optical absorbance of these films was measured by UV-VIS spectrophotometer (model: UV mini-1240) within wavelength range of 200-800 nm. The samples show a wide range of absorption of the solar spectrum. Sample A15 and sample B8 was recorded the highest absorbance and the lowest absorbance, respectively.

For the IV-curve we obtained from the conjugate polymer solar cells a curve similar to the curve from the optimal model, described in chapter 4 Section 4.3.3. The samples which we produced have shown good results in the efficiency compared to the results obtained in the previous studies in chapter 4 sections 4.2.

6.4 Recommendations

Further research work is required to optimize blend composition, processing conditions and device structure to achieve more improved photovoltaic properties.

In order to get better photovoltaic properties many properties like band gap, molecular energy level, mobility, solubility, etc., should be considered, and how to balance these parameters is the most important part to molecular design.

References

[1] A. De Vos, "Detailed balance limit of the efficiency of tandem solar cells", Journal of Physics D: Applied Physics Volume **13**, Issue 5 (14 May 1980), page 839-846 doi:10.1088/0022-3727/13/5/018.

[2] A. G. MacDiarmid, Angew. Chem. Int. Ed. 2001, **40**, 2581.

[3] A. Jäger-Waldau, PV Status Report 2003 2003, European Commission, EUR 20850 EN.

[4] A. J. Breeze, Z. Schlesinger, and S. A. Carter "Charge transport in TiO_2/MEH-PPV polymer photovoltaics" Physics Department, University of California, Santa Cruz, California **95**,64 IBM Alma den Research Center, San Jose, California -Received 5 June 2000; revised manuscript received 28 November 2000; published 10 September 2001.

[5] A. J. Epstein, Y. Yang (Eds.), Polymeric and Organic Electronic Materials: from Scientific Curiosity to Applications, MRS Bull. 1997, **22**, 13.

[6] A. J. Heeger, Angew. Chem. Int. Ed. 2001, **40**, 2591.

[7] A. J. Mozer, P. Denk, M. C. Scharber, H. Neugebauer, N. S. Sariciftci, P. Wagner, L. Lutsen, D. Vanderzande, J. Phys. Chem. B 2004, **108**, 5235.

[8] Aimi Abass, Honghui Shen, Peter Bienstman, Bjorn Maes "Increasing Polymer Solar Cell Efficiency with Triangular Silver Gratings" Photonics Research Group, Ghent University – imec, Department of Information Technology, St.-Pietersnieuwstraat **41**, 900 Ghent, Belgium aimi.abass@ugent.be [2010].

[9] Alfred Smee (1849). Elements of electro-biology,: or the voltaic mechanism of man; of electro-pathology, especially of the nervous system; and of electro-therapeutics. London: Longman, Brown, Green, and Longmans.**15** p. 15. *http://books.google.com/?id=CU0EAAAAQAAJ&pg=PA15.*

[10] Andrew A. R. Watt*, David Blake, Jamie H. Warner, Elizabeth A. Thomsen, Eric L. Tavenner, Halina Rubinsztein-Dunlop & Paul Meredith "Lead Sulphide Nanocrystal: Conducting Polymer Solar Cells". Soft Condensed Matter Physics Group and Centre for Biophotonics and Laser Science, School of Physical Sciences, University of Queensland, Brisbane, **40**, 72 Australia [2005].

[11] Antonio Facchetti. (2010). *π-Conjugated Polymers for Organic Electronics and Photovoltaic Cell Applications*. Journal of Chemistry and the Materials Research Center United States, Northwestern University **214**: 202-211.

[12] Anwell "produces its first solar panel". NextInsight. 2009-09-01. *http://nextinsight.com.sg/index.php/story-archive-mainmenu-60/36-2009* , **14** 80. anwell-produces-its-first-solar-panel.

[13] A. R. Duggal, D. F. Foust, W. F. Nealon, C. M. Heller, Appl. Phys. Lett. 2003, 82, 2580.

[14] Barry C. Thompson and Jean M. J.Fr_chet*"Polymer–Fullerene Composite Solar Cells" 2008 Wiley-VCH Verlag GmbH & Co. KGaA, Weinheim Angew. Chem. Int. Ed. 2008.

[15] Baruch P, De Vos A, Landsberg PT, Parrott JE. On some thermodynamic aspects of photovoltaic solar energy conversion. Solar Energy Materials and Solar Cells. 1995;36:201-222.

[16] B. A. Sandén, Materials Availability for Thin-Film PV and the Need for 'Technodiversity', at the EUROPV 2003 Conference 2003, Bologna (Spain).

[17] Bassam Z. Shakhashiri A Handbook for Teachers of Chemistry 'Polymers' Journal Chemical of the week, Volume 1 (1983), page 241.

[18] B. de Boer, U. Stalmach, P. F. van Hutten, C. Melzer, V. V. Krasnikov, G. Hadziioannou, Polymer 2001, 42, 9097.

[19] B. O'Regan, M. Grätzel, Nature 1991, 335, 737.

[20] Br´edas, J. L.; Cornil, J.; Beljonne, D.; dos Santos, D.; Shuai, Z. G. Accounts Chem. Res. 1999, 32(3), 267–276.

[21] C. D. Müller, A. Falcou, N. Reckefuss, M. Rojahn, V. Wiederhirn, P. Rudati, H. Frohne, O. Nuyken. (2003). *Organic–Metallic Hybrid Polymers: Fundamentals and Device Applications Nature*. Polymer Journal **41**: 511–520.

[22] Chang, R.; Hsu, J. H.; Fann, W. S.; Liang, K. K.; Chiang, C. H.; Hayashi, M.; Yu, J.; Lin, S. H.; Chang, E. C.; Chuang,(2000). *Investigations of Ultrafast Dynamics in Light-emitting Polymers*. Journal of Chinese Chemical Society (**1-2**): 142–152.

[23] Charting a Path to Low-Cost Solar. Greentech Media (2008-07-16). Retrieved on 2011 01-19.

[24] Chiang, C. K.; Fincher, C. R.; Park, Y. W.; Heeger, A. J.; Shirakawa, H.; Louis, E. J.; Gau, S. C.; MacDiarmid, A. G. Phys.Rev.Lett. 1977, 39(17), 1098–1101.

[25] C. J. Brabec, G. Zerza, G. Cerullo, S. De Silvestri, S. Luzzati, J. C. Hummelen. (2001). *Tracing photoinduced electron transfer process in conjugated polymer/fullerence bulk heterojunctions in real time*. Journal of Chemical Physics Letters **340**: 232-236.

[26] C. K. Chiang, C. R. Fincher, Y.W. Park, A. J. Heeger, H. Shirakawa, E. J. Louis, S. C. Gau, A. G. MacDiarmid, Phys. Rev. Lett. 1977, 39, 1098.

[27] Collins, R; Ferlauto, A.S.; Ferreira, G.M.; Chen, Chi; Koh, Joohyun; Koval, R.J.; Lee, Yeeheng; Pearce, J.M. et al. (2003). "Evolution of microstructure and phase in amorphous, protocrystalline, and microcrystalline silicon studied by real time spectroscopic ellipsometry". Solar Energy Materials and Solar Cells 78 (1–4): 143. doi:10.1016/S0927-0248(02)00436-1.

[28] C. W. Tang, Appl. Phys. Lett. 1986, 48, 183.

[29] D. Choudhury, A. Thompson, A. Thompson, V. Stojanoff, S. Langerman, J. Pinkner, S. J. Hultgren, S. Knight "Introduction to Materials Science", Chapter 15, Polymer Structures University Tennessee, Dept. of Materials Science and Engineering

[30] D.S. Kim, A.M. Gabor, V. Yelundur, A.D. Upadhyaya, V. Meemongkolkiat, A. Rohatgi (18 May 2003). "String ribbon silicon solar cells with 17.8% efficiency". Proceedings of 3rd World Conference on Photovoltaic Energy Conversion, 2003

[31] Energy Information Administration. (2006*). International Energy Outlook*. report # DOE/EIA-0484. www.eia.doe.gov/oiaf/ieo/index.html.

[32] F. Padinger, R. S. Rittberger, N. S. Sariciftci, (2003). *Effects of Postproduction Treatment on Plastic Solar Cells*, Journal of Advanced Functional Materials **13**: 85–88.

[33] G. A. Chamberlain, Solar Cells 1983, 8, 47.

[34] Genovese, Matthew P.; Lightcap, Ian V.; Kamat, Prashant V. (2012). "Sun-BelievableSolar Paint. A Transformative One-Step Approach for Designing Nanocrystalline Solar Cells". ACS Nano 6 (1): 865–72. doi:10.1021/nn204381g. PMID 22147684.

[35] Getachew Adam,ab Almantas Pivrikas,a Alberto M. Ramil,a Sisay Tadesse,ab Teketel Yohannes,b
Niyazi S. Sariciftcia and Daniel A. M. Egbe* "Mobility and photovoltaic performance studies on polymer blends: effects of side chains volume fraction" Received 13th August 2010, Accepted 4th November 2010.

[36] Graham, S. C.; Bradley, D. D. C.; Friend, R. H.; Spangler, (1991). *Raman and photoluminescence spectra of PPV oligomers*. Journal article in the OhioLINK Electronic **41**: 1277-1280.

[37] Green MA. Solar cell fill factors: General graph and empirical expressions. Solid-State Electronics. 1981;24:788 - 789.

[38] G. Yu, Y. Gao, J. C. Hummelen, F. Wudl, A. J. Heeger, Science 1995, 270, 1789.

[39] Heeger, A. J. Angew. Chem. Int. Edit. 2001, 40(14), 2591–2611.

[40] Hermann, W. & Simon, A. J. 2007. Global Climate and Energy Project. [online]. [Accessed 9th of June 2009]. Available form World Wide Web: http://gcep.stanford.edu/pdfs/GCEP_Exergy_Poster_web.pdf

[41] H. Shirakawa, A. G. MacDiarmid, A. J. Heeger, Chem. Commun. 2003, 1.

[42] H. Shirakawa, Angew. Chem. Int. Ed. 2001, 40, 2574.

[43] I. Montanari, A. F. Nogueira, J. Nelson, J. R. Durrant, C. Winder, M. A. Loi, N. S. Sariciftci. (2002). *Experimental determination of the rate law for charge carrier decay in a polythiophene: Fullerene solar cell*. Journal of Applied Physics Letters **92**: 9- 81.

[44] International Energy Agency. (2007). *Renewables in Global Energy Supply* - An IEA Fact Sheet. IEA Publications. Paris. France.

[45] Jacob Lund, Rasmus Røge ,Ren´e Petersen ,Tom Larsen. (2006). *Polymer solar cells*., Aalborg University. Journal of Nanoscience and Nanotechnology. **156**: 4-75

[46] J. H. Burroughes, D. D. C. Bradley, A. R. Brown, R. N. Marks, K. Mackay, R. H. Friend, P. L. Burns, A. B. Holmes, Nature 1990, 347, 539.

[47] J. J. M. Halls, C. A. Walsh, N. C. Greenham, E. A. Marseglia, R. H. Friend, S. C. Maratti, A. B. Holmes, Nature 1995, 376, 498.

[48] J. K. J. van Duren, X. N. Yang, J. Loos, C. W. T. Bulle-Lieuwma, A. B. Sieval, J. C. Hummelen and R. A. J. Janssen, Adv. Funct. Mater. 2004, 14, 425.

[49] J. M. Pearce, N. Podraza, R. W. Collins, M.M. Al-Jassim, K.M. Jones, J. Deng, and C. R. Wronski (2007). "Optimization of Open-Circuit Voltage in Amorphous Silicon Solar Cells with Mixed Phase (Amorphous + Nanocrystalline) p-Type Contacts of Low Nanocrystalline Content". Journal of Applied Physics 101 (11): 114301. doi:10.1063/1.2714507.
http://me.queensu.ca/people/pearce/publications/documents/t14.pdf.

[50] J. PEET, J. Y. KIM, N. E. COATES, W. L. MA, D. MOSES, A. J. HEEGER* AND G. C. BAZAN*"Efficiency enhancement in low-bandgap polymer solar cells by processing with alkane dithiols" Center for Polymers and Organic Solids, University of California at Santa Barbara, Santa Barbara, California 93106, USA *e-mail: ajhe@physics.ucsb.edu; Bazan@chem.ucsb.edu Published online: 27 May 2007; doi:10.1038/nmat1928

[51] K. A. Tsokos, "Physics for the IB Diploma", Fifth edition, Cambridge University Press, Cambridge, 2008, ISBN 0-521-70820-6

[52] Kamat, Prashant V. (2012). "Boosting the Efficiency of Quantum Dot Sensitized Solar Cells through Modulation of Interfacial Charge Transfer". Accounts of Chemical Research: 120411095315008. doi:10.1021/ar200315d.

[53] Keng-Hoong Yim, Zijian Zheng, Ziqi Liang, Richard H. Friend, Wilhelm T. S. Huck,* and Ji-Seon Kim*"Efficient Conjugated-Polymer Optoelectronic Devices Fabricated by Thin-Film Transfer-Printing Technique" -2008 Wiley-VCH Verlag GmbH & Co. KGaA, Weinheim Adv. Funct. Mater. 2008.

[54] Kevin M. Coakley and Michael D. McGehee "Conjugated Polymer Photovoltaic Cells" Department of Materials Science and Engineering, Stanford University, 476 Lomita Mall, Stanford, California 94305-4045 Received March 2, 2004. Revised Manuscript Received June 29, 2004.

[55] Krebs, F. C., Alstrup, J., Spanggaard, H., Larsen, K., and Kold, E. (2004). Production of large-area polymer solar cells by industrial silk screen printing, lifetime considerations and lamination with polyethyleneterephthalate. Solar Energy Materials ans Solar Cells.

[56] Krebs, F. C., Carl´e, J. E., Cruys-Bagger, N., Andersen, M., Lilliedal, M. R., and ans Soren Hvidt, M. A. H. (2005). Lifetime of organic photovoltaics: photochemistry, atmosphere effects and barrier layer in ito-mehppv:pcbm-aluminium devices. Solar Energy Materials ans Solar Cells.

[57] Kung-Hwa Wei. (2013). *Development and Characterization of New Donor-Acceptor Conjugated Polymers and Fullerene Nanoparticles for High Performance Bulk Heterojunction Solar Cells*. Journal of National Chiao Tung University, Department of Materials Science & Eng.**106**:34-44.

[58] Levy MY, Honsberg CB. Rapid and precise calculations of energy and particle flux for detailed balance photovoltaic applications. Solid-State Electronics. 2006;50:1400-1405.

[59] Light sensitive device- U.S. Patent 2,402,662 Issue date: June 1946

[60] Lindholm FA, Fossum JG, Burgess EL. Application of the superposition principle to solar-cell analysis. IEEE Transactions on Electron Devices. 1979;26:165–171.

[61] Liyuan Han "Dye-Sensitized Solar Cells with Nanotechnologies" Advanced Photovoltaics Center NIMS) [2009].

[62] Mark Z. Jacobson (2009). Review of Solutions to Global Warming, Air Pollution, and Energy Security p. 4.

[63] M. Dreesa! R. M. Davis J. R. Heflinb! "Improved morphology of polymer-fullerene photovoltaic devices with thermally induced concentration gradients" Department of Physics, Virginia Tech, Blacksburg, Virginia 24061- Received 22 July 2004; accepted 9 November 2004; published online 11 January 2005.

[64] M. K. Nazeeruddin, P. Réchy, T. Renouard, S. M. Zakeeruddin, R. Humphry-Baker, P. Comte, P. Liska, L. Vevey, E. Costa, V. Shklover, L. Spicca, G. B. Deacon, C. A. Bignozzi, M. Grätzel, J. Am. Chem. Soc. 2001, 123, 1613.

[65] M. M. Wienk, J. M. Kroon, W. J. H. Verhees, J. Knol, J. C. Hummelen, P. A. van Hal, R.A. J. Janssen, Angew. Chem. Int. Ed. 2003, 42, 3371.

[66] Moon, Soo-Jin; Itzhaik, Yafit; Yum, Jun-Ho; Zakeeruddin, Shaik M.; Hodes, Gary; GräTzel, Michael (2010). "Sb2S3-Based Mesoscopic Solar Cell using an Organic Hole Conductor". The Journal of Physical Chemistry Letters 1 (10): 1524. doi:10.1021/jz100308q.

[67] M. Svensson, F. Zhang, S. C. Veenstra, W. J. H. Verhees, J. C. Hummelen, J. M. Kroon, O. Inganäs, M. R. Andersson, Adv. Mater. 2003, 15, 988.

[68] N. S. Sariciftci (Ed.), (1998), *Primary photo excitations in conjugated polymers:Molecular Exciton versus Semiconductor Band Model*. World Scientific Publishers, Singapore.

[69] Oleg Mirzov, Licentiate thesis "Single-molecule imaging and spectroscopy of the π conjugated polymer MEH-PPV" .Lund University 2006.

[70] Ozlem Usluer,1,2 Christian K€astner,3 Mamatimin Abbas,1,4 Christoph Ulbricht,1 Vera Cimrova,5 Andreas Wild,6 Eckhard Birckner,7 Nalan Tekin,8 Niyazi Serdar Sariciftci,1 Harald Hoppe,3 Silke Rathgeber,9 Daniel A. M. Egbe1 "Charge Carrier Mobility, Photovoltaic, and Electroluminescent Properties of Anthracene-Based Conjugated Polymers Bearing Randomly Distributed Side Chains" 1Linz Institute for Organic Solar Cells, Physical Chemistry, Johannes Kepler University Linz, Received 28 February 2012; accepted 18 April 2012; published online 25 May 2012.

[71] P. A. van Hal, M. P. T. Christiaans, M. M. Wienk, J. M. Kroon, R. A. J. Janssen, J. Phys. Chem. B 1999, 103, 4352.

[72] Perlin, John (2004). "The Silicon Solar Cell Turns 50". National Renewable Energy Laboratory. http://www.nrel.gov/docs/fy04osti/33947.pdf. Retrieved 5 October 2010.

[73] Peter Gevorkian. (2007). *Sustainable energy systems engineering: the complete green building design resource*. McGraw-Hill Professional. pp. 498. http://books.google.com/books?id=i8rc.

[74] Photovoltaics. Engineering.Com (2007-07-09). Retrieved on 2011-01-19.

[75] Photovoltaic Systems DOE whitepaper August 2010

[76] Pope, M.; Swenberg, C. E. Electronic Processes in Organic Crystals and Polymers; Oxford University Press: New York, 2 ed., 1999.

[77] P. Schilinsky, C. Waldauf, and C. J. Brabec, Appl. Phys. Lett. 2002, 81, 3885.

[78] René Janssen "Introduction to polymer solar cells"- (3Y280) Departments of Chemical Engineering & Chemistry and Applied Physics Eindhoven University of Technology, The Netherlands- 2005.

[79] Renewable Energy Policy Network for the 21st Century. 2006. Renewables – Global Status Report - 2006 Update.

[80] R. H. Friend, R. W. Gymer, A. B. Holmes, J. H. Burroughes, R. N. Marks, C. Taliani, D.
D. C. Bradley, D.A. Dos Santos, J.L. Brédas, M. Löglund, W.R. Salaneck, Nature 1999, 397, 121.

[81] Salima Alem, Remi de Bettignies, and Jean-Michel Nunzia "Efficient polymer-based interpenetrated network photovoltaic cells" Equipe de Recherche Technologique Cellules Solaires Photovoltaı¨ques Plastiques and Proprie´te´s Optiques des Mate´riaux et Applications, Laboratoire Associe´, Universite´ d'Angers, 49045 Angers, France Michel Cariou ~Received 5 September 2003; accepted 15 January 2004.

[82] Sangmoo Jeong, Erik C. Garnett, Shuang Wang, Zongfu Yu, Shanhui Fan, Mark L. Brongersma, Michael D. McGehee,*, and Yi Cui*, "Hybrid Silicon Nanocone−Polymer Solar Cells" Department of Electrical Engineering and -Department of Materials Science and Engineering, Stanford University, Stanford, California 94305, United States ,Stanford Institute for Materials and Energy Sciences, SLAC National Accelerator Laboratory, 2575 Sand Hill Road, Menlo Park, California 94025, United States [2012].

[83] Santra, Pralay K.; Kamat, Prashant V. (2012). "Mn-Doped Quantum Dot Sensitized Solar Cells: A Strategy to Boost Efficiency over 5%". Journal of the American Chemical Society 134 (5): 2508–11. doi:10.1021/ja211224s. PMID 22280479.

[84] Semonin, O. E.; Luther, J. M.; Choi, S.; Chen, H.-Y.; Gao, J.; Nozik, A. J.; Beard, M. C. (2011). "Peak External Photocurrent Quantum Efficiency Exceeding 100% via MEG in a Quantum Dot Solar Cell". Science 334 (6062): 1530–3. doi:10.1126/science.1209845. PMID 22174246.

[85] S. E. Shaheen, C. J. Brabec, N. S. Sariciftci, F. Padinger, T. Fromherz, J. C. Hummelen, Appl. Phys. Lett. 2001, 78, 841.

[86] Sinton RA, Cuevas A. Contactless determination of current–voltage characteristics and minority-carrier lifetimes in semiconductors from quasi-steady-state photoconductance data. Applied Physics Letters [Internet]. 1996;69:2510-2512. Available from: http://link.aip.org/link/?APL/69/2510/1.

[87] Solar Cell Research || The Prashant Kamat lab at the University of Notre Dame. Nd.edu (2007-02-22). Retrieved on 2012-05-17.

[88] Solar Junction Breaks Concentrated Solar World Record with 43.5% Efficiency. Optics.org (2011-04-19). Retrieved on 2011-01-19.

[89] Solar Stocks: Does the Punishment Fit the Crime? (FSLR, SPWRA, STP, JASO, TSL, LDK, TAN) – 24/7 Wall St. 24/7 Wall St. (2011-10-06). Retrieved on 2012-01-03.

[90] Shirakawa, H.; Louis, E. J.;MacDiarmid, A. G.; Chiang, C. K.; Heeger, A. J.
J. Chem. Soc. Chem. Comm. 1977, (16), 578–580.

[91] Spanggaard, H. and Krebs, F. C. (2004). A brief history of the development of organic and polymeric photovoltaics. science direct.

[92] Srinivas Sista, Mi-Hyae Park, Ziruo Hong,* Yue Wu, Jianhui Hou, Wei Lek Kwan, Gang Li, and Yang Yang* Dr. Z. Hong, Prof. Y. Yang, S. Sista, M.-H. Park, Dr. Y. Wu, Dr. J. Hou, W. L. Kwan "Highly Efficient Tandem Polymer Photovoltaic Cells" Department of Materials Science and Engineering University of California Los Angeles Los Angeles, CA 90095 (USA) E-mail: zrhong@ucla.edu; yangy@ucla.edu [2010].

[93] S. Schuller, P. Schilinsky, J. Hauch, C. J. Brabec, Appl. Phys. A 2004, 79, 37.

[94] Swanson, R. M. (2000). "The Promise of Concentrators". Progress in Photovoltaics: Res. Appl. 8 (1): 93–111. doi:10.1002/(SICI)1099-159X(200001/02)8:1<93::AID-PIP303>3.0.CO;2-S.

[95] Tao, M. 2008. Inorganic Photovoltaic Solar Cells: Silicon and Beyond. The Electrochemical Society Interface, Winter, pp.30-35.

[96] T.Bazouni: What is the Fill Factor of a Solar Panel". http://www.solarfreaks.com/what-is-the-fill-factor-of-a-solar-panel-t138.html. Retrieved 2009-02-17.

[97] Tiedje T, Yablonovich E, Cody GD, Brooks BG. **Limiting Efficiency of Silicon Solar Cells**. IEEE TRANSACTIONS ON ELECTRON DEVICES. 1984 ;ED-31.

[98] T. Martens, J. D'Haen, T. Munters, Z. Beelen, L. Goris, J. Manca, M. D'Olieslaeger, D. Vanderzande, L. De Schepper, R. Andriessen, Synth. Met. 2003, 138, 243.

[99] The Nobel Prize in Physics 1921: Albert Einstein, Nobel Prize official page

[100] Thin-Film Cost Reports. pvinsights.com. 2011 [last update]. http://pvinsights.com/Report/ReportPM.php. Retrieved June 19, 2011.

[101] T. Offermans, S. C. J. Meskers, R. A. J. Janssen, J. Chem. Phys. 2003, 119, 10467.

[102] Triple-Junction Terrestrial Concentrator Solar Cells.(PDF). Retrieved on 2012-01-03.

[103] U. Bach, D. Lupo, P. Comte, J. E. Moser, F. Weissörtel, J. Salbeck, H. Speitzer, M. Grätzel, Nature 1998, 395, 583.

[104] Ulrich Brackmann, (2000). *Laser Dyes*. Third Edition, Lambda Physik AG Publishers· Goettingen. Germany.

[105] V. D. Michailetchi, P. W. M. Blom, J. C. Hummelen, M. T. Rispens, J. Appl. Phys. 2003, 94, 6849.

[106] Wayne McMillan, "The Cast Mono Dilemma", BT Imaging

[107] W. U. Huynh, J. J. Dittmer, A. P. Alivisatos, Science 2002, 295, 2425.

[108] X. Yang, J. K. J. Van Duren, R. A. J. Janssen, M. A. J. Michels, and J. Loos, Macromolecules 2004, 37, 2151-2158

[109] Youngkyoo Kim1*, Steffan Cook2, Sachetan M. Tuladhar1, Stelios A. Choulis1, Jenny Nelson1*, James R. Durrant2, Donal D. C. Bradley1*, Mark Giles3, Iain Mcculloch3, Chang-Sikha4 and Moonhor Ree5 "A strong regioregularity effect in self-organizing conjugated polymer films and high-efficiency polythiophene:fullerene solar cells" 1Department of Physics, Blackett Laboratory, Imperial College London, London. Published online: 5 February 2006.

[110] Yu-Han Chang a, Shin-Rong Tseng a, Chun-Yu Chen a, Hsin-Fei Meng a,*, En-Chen Chen b, Sheng-Fu Horng b, Chian-Shu Hsu c "Polymer solar cell by blade coating" Institute of Physics, National Chiao Tung University, Hsinchu 300, Taiwan, Republic of China Department of Electrical Engineering, National Tsing Hua University, Hsinchu 300, Taiwan, Republic of China Department of Applied Chemistry, National Chiao Tung University, Hsinchu 300, Taiwan, Republic of China [2009].

APPENDIX

The calculations of the current density, Fill Factor and the conversion efficiency for the samples.

Group A:

(1) A3

I_{mp},V_{mp}(26, 1.08) ; I_{sc},V_{oc}(29, 1.22) ; J_{sc} =7.733 mA/ cm^2 ; Area=2.5*1.5=3.75 cm^2

$$FF = \frac{I_{mp} \times V_{mp}}{I_{sc} \times V_{oc}} = \frac{26 \times 1.08}{29 \times 1.22} = \frac{28.08}{35.38} = 0.793668$$

$$\mathrm{J_{sc}} = \frac{\mathrm{I_{SC}}}{Area} = 7.733 \mathrm{mA/\ cm^2}$$

$$\eta = \mathrm{FF} \times \mathrm{J_{SC}} \times \mathrm{V_{OC}} = 7.487$$

(2) A6

I_{mp},V_{mp}(8.8, 1.24); I_{sc},V_{oc}(10, 1.32) ; J_{sc} =2.857 mA/ cm^2 ; Area=2.5*1.4=3.5 cm^2

$$FF = \frac{I_{mp} \times V_{mp}}{I_{sc} \times V_{oc}} = \frac{8.8 \times 1.24}{10 \times 1.32} = \frac{10.912}{13.2} = 0.8266$$

$$\mathrm{J_{sc}} = \frac{\mathrm{I_{SC}}}{Area} = 2.857 \mathrm{mA/\ cm^2}$$

$$\eta = \mathrm{FF} \times \mathrm{J_{SC}} \times \mathrm{V_{OC}} = 3.117$$

(3) A9

I_{mp},V_{mp}(43, 1.26); I_{sc},V_{oc}(52, 1.3); J_{sc} =8.32 mA/ cm^2 ; Area=2.5*2.5=6.25 cm^2

$$FF = \frac{I_{mp} \times V_{mp}}{I_{sc} \times V_{oc}} = \frac{43 \times 1.26}{52 \times 1.3} = \frac{54.18}{67.6} = 0.8014$$

$$J_{sc} = \frac{I_{SC}}{Area} = 8.32\,mA/\,cm^2$$

$$\eta = FF \times J_{SC} \times V_{OC} = 8.66$$

(4) A12

I_{mp},V_{mp}(43,0.96) I_{sc},V_{oc}(55, 1.24); J_{sc} =10.47619 mA/ cm^2;Area=2.5*2.1=5.25 cm^2

$$FF = \frac{I_{mp} \times V_{mp}}{I_{sc} \times V_{oc}} = \frac{43 \times 0.96}{55 \times 1.24} = \frac{41.28}{68.2} = 0.60527$$

$$J_{sc} = \frac{I_{SC}}{Area} = 10.47619 mA/\,cm^2$$

$$\eta = FF \times J_{SC} \times V_{OC} = 7.862$$

(5) A15

I_{mp},V_{mp}(42, 0.98) I_{sc},V_{oc}(51, 1.21) ; J_{sc}=12.75 mA/ cm^2 ; Area=2.5*1.6=4 cm^2

$$FF = \frac{I_{mp} \times V_{mp}}{I_{sc} \times V_{oc}} = \frac{42 \times 0.98}{51 \times 1.21} = \frac{41.16}{61.71} = 0.66699$$

$$J_{sc} = \frac{I_{SC}}{Area} = 12.75 mA/\,cm^2$$

$$\eta = FF \times J_{SC} \times V_{OC} = 10.28$$

<u>Group B:</u>

(1) B2

I_{mp},V_{mp}(19.5, 0.82) I_{sc},V_{oc}(23, 1.25) ; J_{sc}=6.133 mA/ cm^2 ;Area=2.5*1.5=3.75 cm^2

$$FF = \frac{I_{mp} \times V_{mp}}{I_{sc} \times V_{oc}} = \frac{19.5 \times 0.82}{23 \times 1.25} = \frac{15.99}{28.75} = 0.5561$$

$$J_{sc} = \frac{I_{SC}}{Area} = 6.133 \text{mA/ cm}^2$$

$$\eta = FF \times J_{SC} \times V_{OC} = 4.263$$

(2) B5

I_{mp},V_{mp}(7.7, 1.04) I_{sc},V_{oc}(9, 1.25) ; J_{sc}=2.25 mA/ cm^2 ;Area=2.5*1.6=4 cm^2

$$FF = \frac{I_{mp} \times V_{mp}}{I_{sc} \times V_{oc}} = \frac{7.7 \times 1.04}{9 \times 1.25} = \frac{8.008}{11.25} = 0.7118$$

$$J_{sc} = \frac{I_{SC}}{Area} = 2.25 \text{mA/ cm}^2$$

$$\eta = FF \times J_{SC} \times V_{OC} = 2.0019$$

(3) B8

I_{mp},V_{mp}(7.4, 1.12) I_{sc},V_{oc}(9, 1.17) ; J_{sc}=1.894 mA/ cm^2 ;Area=2.5*1.9=4.75 cm^2

$$FF = \frac{I_{mp} \times V_{mp}}{I_{sc} \times V_{oc}} = \frac{7.4 \times 1.12}{9 \times 1.17} = \frac{8.288}{10.53} = 0.787$$

$$J_{sc} = \frac{I_{SC}}{Area} = 1.894 \text{mA/ cm}^2$$

$$\eta = FF \times J_{SC} \times V_{OC} = 1.744$$

(4) B14

I_{mp},V_{mp}(41, 1.16) I_{sc},V_{oc}(49, 1.24); J_{sc}=7.84 mA/ cm^2 ;Area=2.5*2.5=6.25 cm^2

$$FF = \frac{I_{mp} \times V_{mp}}{I_{sc} \times V_{oc}} = \frac{41 \times 1.16}{49 \times 1.24} = \frac{47.56}{60.76} = 0.7827$$

$$J_{sc} = \frac{I_{SC}}{Area} = 7.84 \text{mA/ cm}^2$$

$$\eta = FF \times J_{SC} \times V_{OC} = 7.609$$

(5) B11

I_{mp},V_{mp}(51, 0.88) I_{sc},V_{oc}(59, 1.19) ; J_{sc}=9.44 mA/ cm^2 ;Area=2.5*2.5=6.25 cm^2

$$FF = \frac{I_{mp} \times V_{mp}}{I_{sc} \times V_{oc}} = \frac{51 \times 0.88}{59 \times 1.19} = \frac{44.88}{70.21} = 0.639$$

$$\mathrm{J_{sc}} = \frac{\mathrm{I_{SC}}}{Area} = 9.44\,\mathrm{mA/\ cm^2}$$

$$\eta = \mathrm{FF} \times \mathrm{J_{SC}} \times \mathrm{V_{OC}} = 7.178$$

Group C:

(1) C1

I_{mp},V_{mp}(41, 1.2) I_{sc},V_{oc}(47, 1.35) ;J_{sc}=7.52 mA/ cm^2 ;Area=2.5*2.5=6.25 cm^2

$$FF = \frac{I_{mp} \times V_{mp}}{I_{sc} \times V_{oc}} = \frac{40 \times 1.2}{47 \times 1.36} = \frac{48}{63.92} = 0.7509$$

$$\mathrm{J_{sc}} = \frac{\mathrm{I_{SC}}}{Area} = 7.52\,\mathrm{mA/\ cm^2}$$

$$\eta = \mathrm{FF} \times \mathrm{J_{SC}} \times \mathrm{V_{OC}} = 7.62$$

(2) C13

I_{mp},V_{mp}(38, 1.18) I_{sc},V_{oc}(46, 1.31) ; J_{sc}=7.66 mA/ cm^2 ;Area=2.5*2.4=6 cm^2

$$FF = \frac{I_{mp} \times V_{mp}}{I_{sc} \times V_{oc}} = \frac{38 \times 1.18}{46 \times 1.31} = \frac{44.84}{60.26} = 0.7441$$

$$\mathrm{J_{sc}} = \frac{\mathrm{I_{SC}}}{Area} = 7.66\,\mathrm{mA/\ cm^2}$$

$$\eta = \mathrm{FF} \times \mathrm{J_{SC}} \times \mathrm{V_{OC}} = 7.466$$

(3) C7

I_{mp},V_{mp}(8.4, 1.02) I_{sc},V_{oc}(10, 1.25) ;J_{sc}=2.352 mA/ cm^2 ;Area=2.5*1.7=4.24 cm^2

$$FF = \frac{I_{mp} \times V_{mp}}{I_{sc} \times V_{oc}} = \frac{8.4 \times 1.02}{10 \times 1.25} = \frac{8.568}{12.5} = 0.68544$$

$$\mathrm{J_{sc}} = \frac{\mathrm{I_{SC}}}{Area} = 2.352\,\mathrm{mA/\ cm^2}$$

$$\eta = \mathrm{FF} \times \mathrm{J_{SC}} \times \mathrm{V_{OC}} = 2.015$$

(4) C4

I_{mp},V_{mp}(9.8, 0.88) ; I_{sc},V_{oc}(12, 1.26); J_{sc}=3 mA/ cm^2 ;Area=2.5*1.6=4 cm^2

$$FF = \frac{I_{mp} \times V_{mp}}{I_{sc} \times V_{oc}} = \frac{9.8 \times 0.88}{12 \times 1.26} = \frac{8.624}{15.12} = 0.5703$$

$$\mathrm{J_{sc}} = \frac{\mathrm{I_{SC}}}{Area} = 3\,\mathrm{mA/\ cm^2}$$

$$\eta = \mathrm{FF} \times \mathrm{J_{SC}} \times \mathrm{V_{OC}} = 2.155$$

(5) C10

I_{mp},V_{mp}(12.8, 0.94) I_{sc},V_{oc}(15, 1.21) ;J_{sc}=2.857 mA/ cm^2 ;Area=2.5*2.1=5.25 cm^2

$$FF = \frac{I_{mp} \times V_{mp}}{I_{sc} \times V_{oc}} = \frac{12.8 \times 0.94}{15 \times 1.21} = \frac{12.032}{18.15} = 0.6629$$

$$\mathrm{J_{sc}} = \frac{\mathrm{I_{SC}}}{Area} = 2.857\,\mathrm{mA/\ cm^2}$$

$$\eta = \mathrm{FF} \times \mathrm{J_{SC}} \times \mathrm{V_{OC}} = 2.291$$